



UNIVERSITÉ
DE LORRAINE



Fusion research: challenges, news and examples of academic involvement

Prof. Dr. Gérard BONHOMME, and co-workers
*Institut Jean Lamour, UMR 7198 CNRS – University of Lorraine,
Dpt P2M, team 107 (hot plasmas)
Gerard.Bonhomme@univ-lorraine.fr*

***Last News
from GOLEM and COMPASS!***



The GOLEM tokamak
arrived into its new location in this building
on 12th December 2007

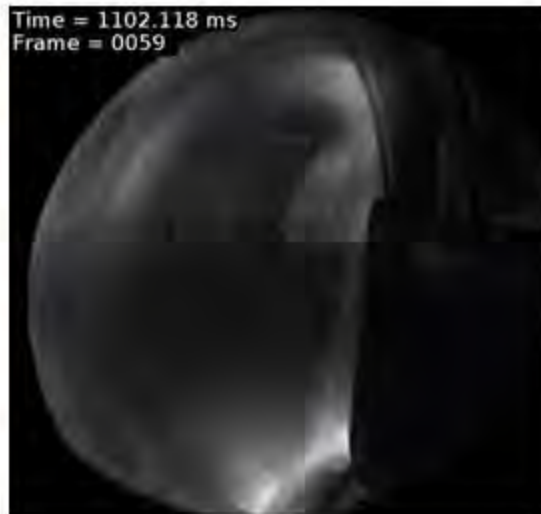


NBI and Ohmic H-mode achieved at COMPASS tokamak on 29th November 2012

- **Ohmic H-mode** – gradual decrease of D_{α} signal and its fluctuation observed during plasma current ramp-down => transition to Type III ELMs and ELM free period
- **NBI H-mode** – 10 ms after start of NBI (210 kW) rapid decrease of D_{α} signal and increase of stored energy observed



The COMPASS tokamak



L-mode



H-mode

Fusion Research

- Overview and news
 - Do we need fusion?
 - ITER current status
- Challenges
- Academic involvement: some examples
 - Development and validation of diagnostic tools for turbulent fluctuations and transport (probes, fast imaging,...)
 - Dust tracking
 - Plasma-wall interaction (lab studies)
 - Participation in experimental campaigns on large devices
 - Education
- The ESTELL project

Energy: a major challenge for the 21st century

China 2006: + 105 GW, 90% coal!

More than the total French electricity per year (80 GW)

Today: > 80 % of primary energy comes from fossil resources

Gaz & petrol consumption exceeds new discoveries

EU highly dependant for its energy (> 50 %)

Energy = 4000 billions euros per year

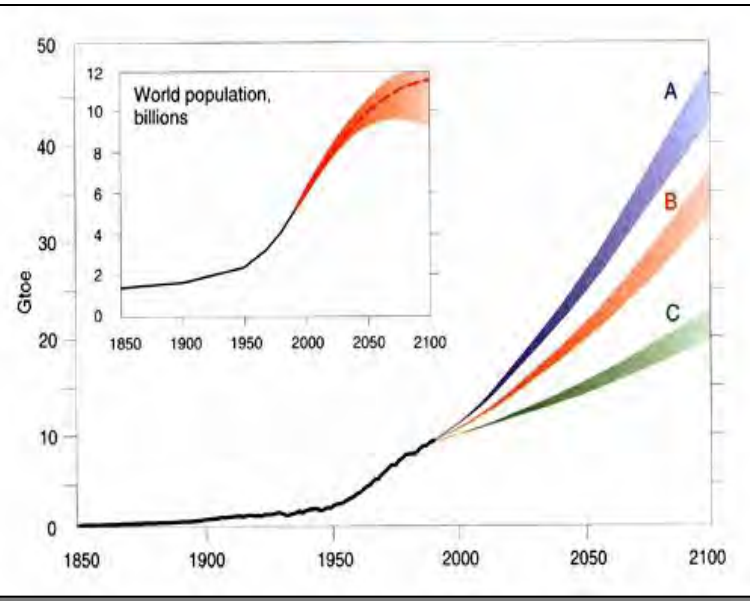
Back to coal or do better ?

Moderate consumption, renewable energy, fission, fusion

Fusion presents major advantages

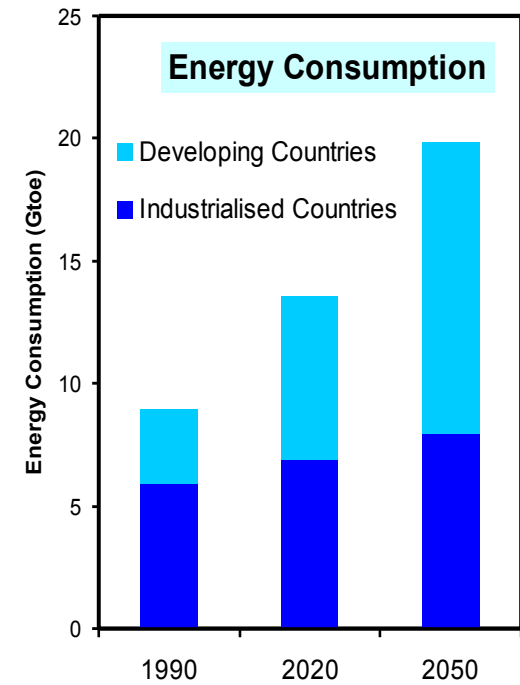
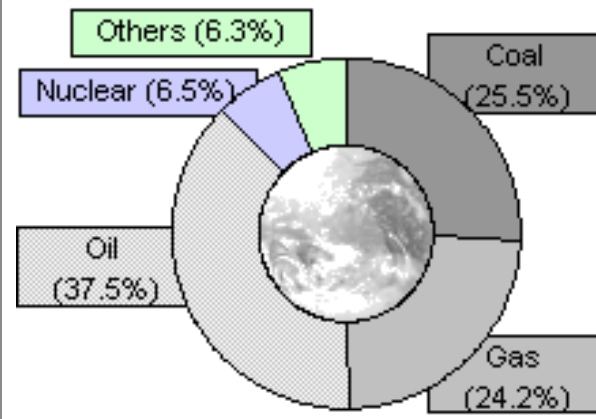
but requires advances in physics and technologies

Trends in global energy consumption

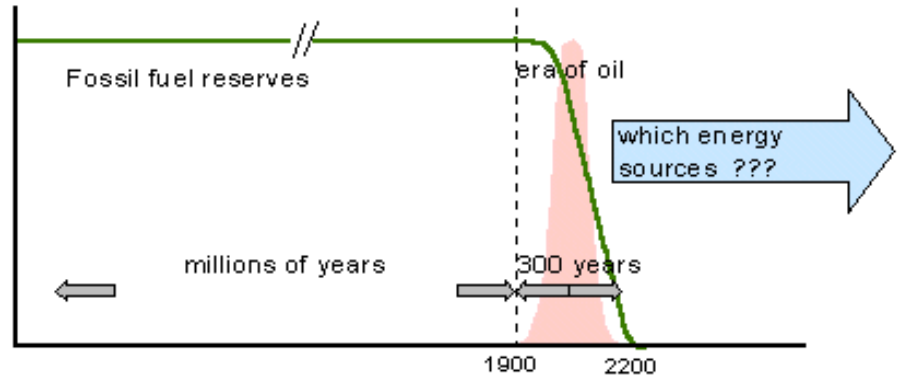


A : strong growth
B : moderate growth
C : green scenario

3 scenarios

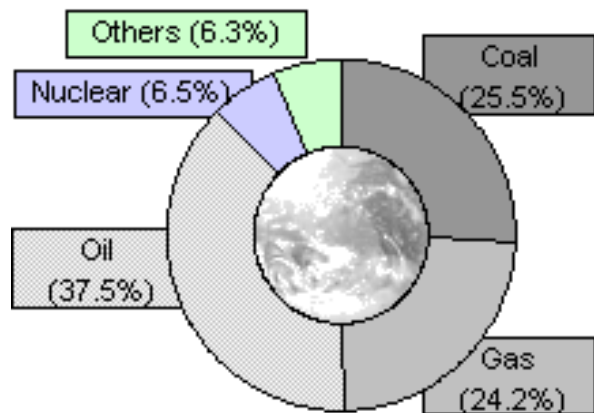


- Energy consumption forecasts:
- between 20 and 40 Gtoe in 2100
 - much more higher growth in electricity demand



Primary energy and electricity production

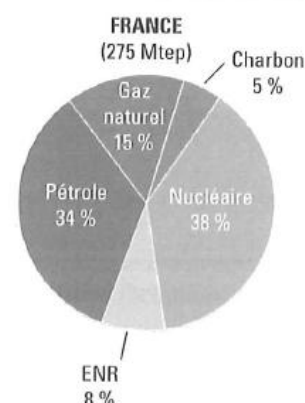
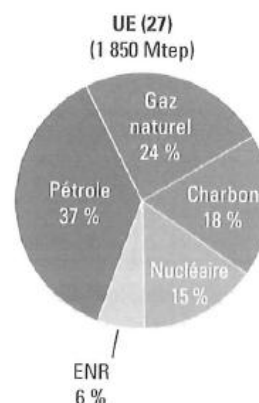
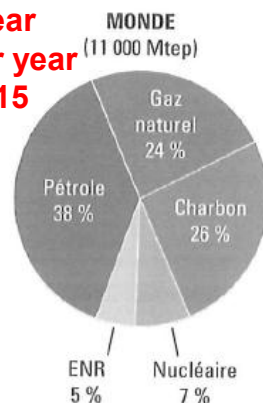
Structure of the primary global energy consumption (2007)



Structure of Electricity production (2007)

1 Mtep = 10^6 tonne oil equivalent , and
 1 tep or toe corresponds to ~ 12 000 kWh
 1 TW = $24 \times 365 = 8760$ TWh/year

11 000 Mtep per year
~132 000 TWh per year
corresponds to ~ 15 TW



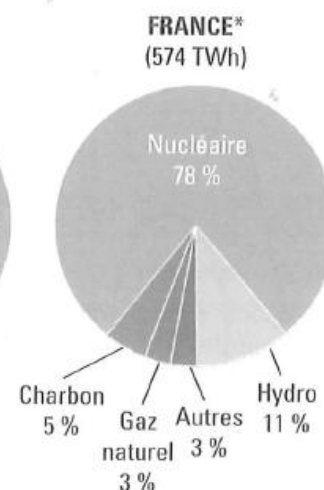
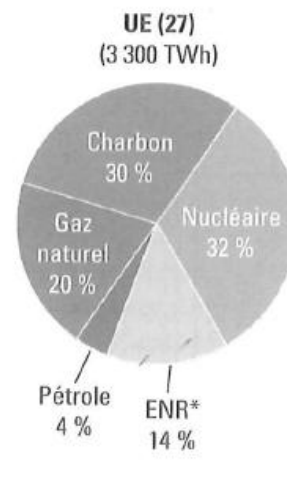
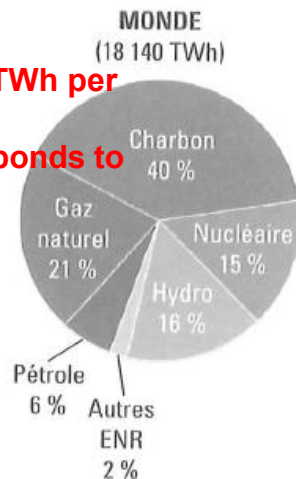
TAUX DE DÉPENDANCE : 56 %

- Pétrole : 75 % importé
- Gaz naturel : 60 % importé
- Charbon : 40 % importé

TAUX DE DÉPENDANCE : 51 %

- Pétrole : 99 % importé
- Gaz naturel : 95 % importé
- Charbon : 100 % importé

18140 TWh per year
corresponds to ~ 2 TW



* Y compris l'hydraulique

* EDF assure 90 % de la production suivie de la CNR et d'ENDESA

Energy and Power: Useful numbers

- The joule (J) and the watt (W), one joule per second (J/s), are the standard international units of energy and power, respectively.

But these units are far too small and the following are preferred:

Energy → **1 kWh** = 3.6 million joules (**3.6 MJ = 3.6×10^6 J**)

Power → **1 kWh/d** (1 kWh per day) ~ **40 W**, with 1 kW ~ 24 kWh/d

- Useful relations:
 - 1 oil barrel (159 l, ~ 0.136 tonne) → 1632 kWh
 - 1 tonne oil (tonne oil equivalent or **1 toe**) → **12 000 kWh**
 - 1 TW (terawatt) = 10^3 GW (gigawatt) = 10^6 MW (megawatt) = 10^9 kW (kilowatt) = 10^{12} W
- Needs:



Current consumption per person in “cartoon Britain 2008”. [From MacKay, <http://www.withouthotair.com/>, UIT Cambridge, 2008]

The challenges of energy supply

- Global energy production is expected to increase by around 60% between 1999 and 2020.
- If production rates remain at present levels, the fossil fuels will be exhausted in about 40 years (oil), 70 years (gas), and 250 years (coal). The actual lifetimes will depend on the rate of production and new discoveries.
- The greenhouse effect is a natural phenomenon due to absorption of infrared radiation by the Earth's atmosphere.

The main greenhouse gas is water vapor. Carbon dioxide, methane, CFCs, and other greenhouse gases enhance the effect of water vapor by increasing its amount.

- Carbon dioxide concentrations have risen from about 280 parts per million in 1750 to about 380 parts per million today, mainly due to human activity, and there has been an associated marked rise in temperature, called global warming, since the 1970s.

Energy plans for Europe

Renewables:

- Wind ($\sim 2\text{W}/\text{m}^2$):
 - 10% of the available space filled with wind farms $\Rightarrow 360\text{ W}$
 $\Rightarrow 9\text{ kWh/d}$ per person
- Hydroelectricity: current power 590 TWh/y (67 GW) $\Rightarrow 3.2\text{ kWh/d}$ (500 millions inhabitants). If doubling $\Rightarrow 6.4\text{ kWh/d}$ per person
- Wave: 4000 km coastline with $10\text{ kW}/\text{m}$ $\Rightarrow 2\text{ kWh/d}$ per person
- Tide: 2.6 kWh/d per person
- Solar photovoltaics and thermal panel on roofs:
 - 10 m^2 of roof mounted PV panels $\Rightarrow 7\text{ kWh/d}$ (high-grade energy)
 - 2 m^2 of water-heating panels $\Rightarrow 3.6\text{ kWh/d}$ (low-grade energy)

\Rightarrow Total **30.6 kWh/d per person**

Solar farming required: 5% of Europe area (450 m^2 per person)

$\Rightarrow 54\text{ kWh/d}$ per person

Problems = (i) cost; (ii) getting power in the winter

- Crops (plants capture $0.5\text{ W}/\text{m}^2$ or $5\text{ kW}/\text{ha}$) $\Rightarrow 12\text{ kWh/d}$ per person

\Rightarrow Total **96.6 kWh/d per person < 125**

The bottom line: Europe cannot live on its own renewable. If the aim is to get off fossil fuels, Europe needs nuclear or solar power in other people's desert, or both.

Energy scenarios for the future

Two main approaches:

- one dominant energy source (historically: wood, coal, oil, gas, ...)
- simultaneous use of a whole range of energy sources
- **Energy sources must fulfil the following criteria:**
 - **Acceptable environmental constraints (CO₂, waste)**
 - **Economically viable & socially acceptable**
 - **Safety in regards to major accidents**
 - **Large scale Production**
 - **Secure providing (limited importations)**
- **Development of existing and new sources:**

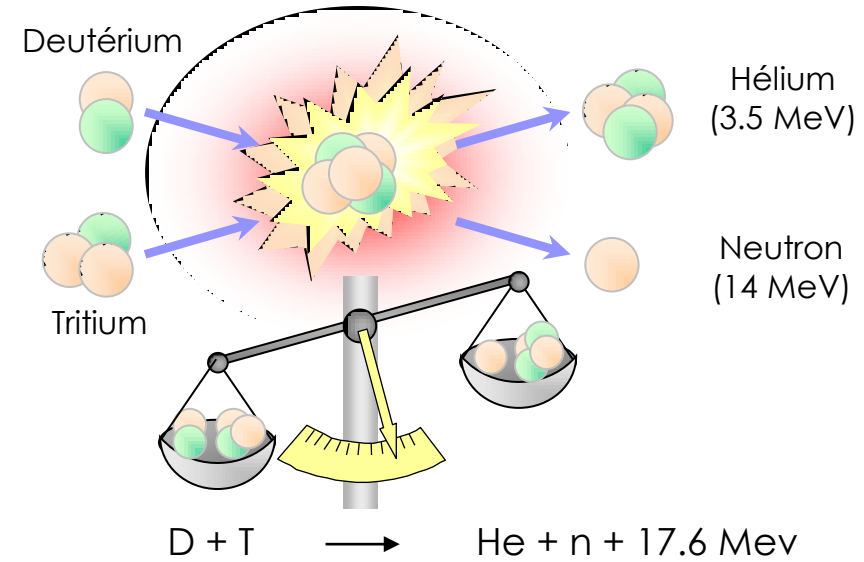
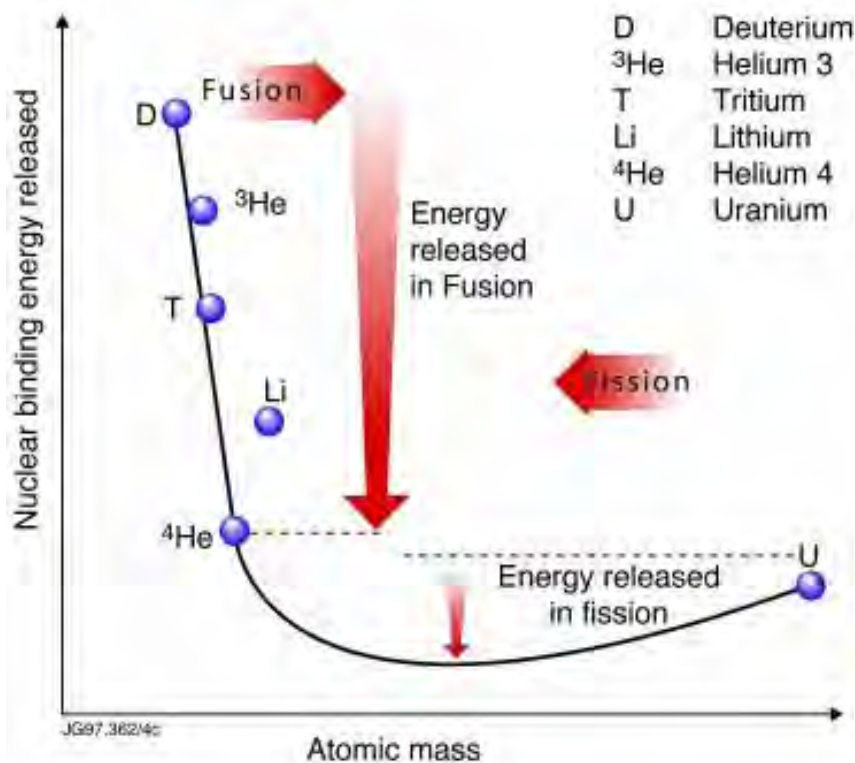
Fossil fuels	Renewable energies
Fission	Fusion

- **All options must be developed**

Thermonuclear Fusion: General Principles

Thermonuclear fusion: general principles

Fusion and Fission



The fusion of two light nuclei releases energy: it is the energy source of our Sun and other stars

Because of the natural electrostatic repulsion of nuclei, fusion reactions require an energy supply

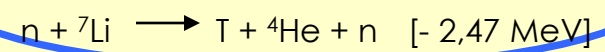
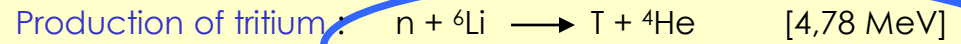
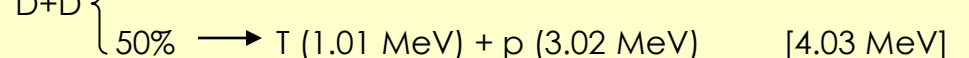
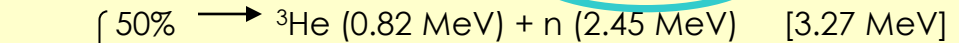
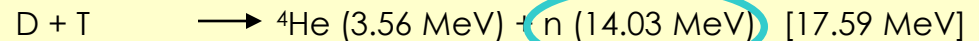
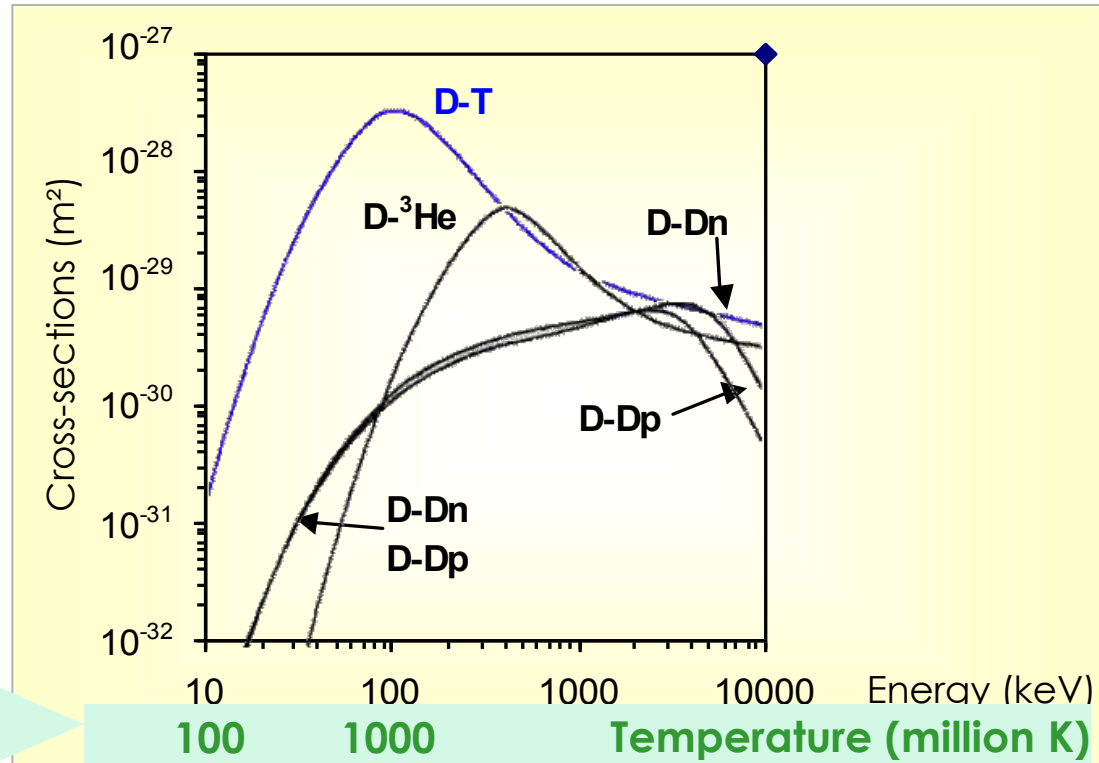
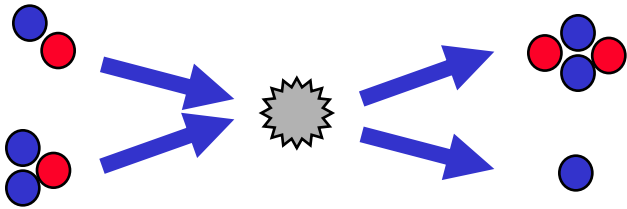
The released energy per unit of mass is 1 to 10 millions greater than in a chemical combustion reaction

Fusion reactions – cross sections

➤ Fusion reactions cross-sections are ~600 smaller than fission cross-sections

➤ The $D + T \rightarrow He + n$ reaction is the most accessible one.

➤ Very high temperatures are required (> 100 millions degrees) to overcome the Coulomb barrier



Power balance

Fusion Power

- P_{fus} = number of reactions per second
× energy released by one reaction
- $P_{\text{fus}} = n_D n_T \langle \sigma \cdot V \rangle_{DT} Q_{DT} = P_{\text{neut}} + P_{\alpha}$
- $Q_{DT} = 17,6 \text{ MeV} = 2,8 \cdot 10^{-12} \text{ J}$
- $P_{\text{neut}} = 0,8 P_{\text{fus}} \quad P_{\alpha} = 0,2 P_{\text{fus}}$

In one year, a 1 GW_e power plant would need
100 kg (D) + 150 kg (T) instead of
~ 700 000 tonnes of oil or
~ 30 t of uranium enriched to 3% of ^{235}U

Power released in the plasma

- $P_{DT} (\text{W/m}^3) = P_{\alpha} = 5.6 \times 10^{-13} n_D n_T \langle \sigma \cdot V \rangle_{DT}$
- **D-T Mixture 50/50** : $n_D = n_T = n_i / 2$

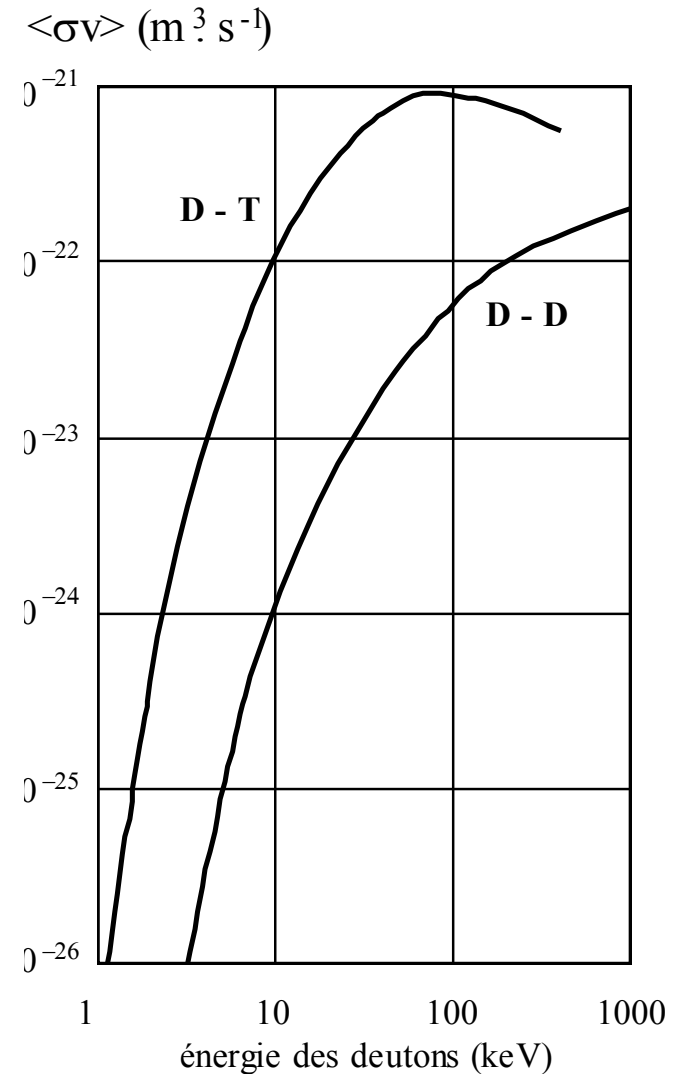
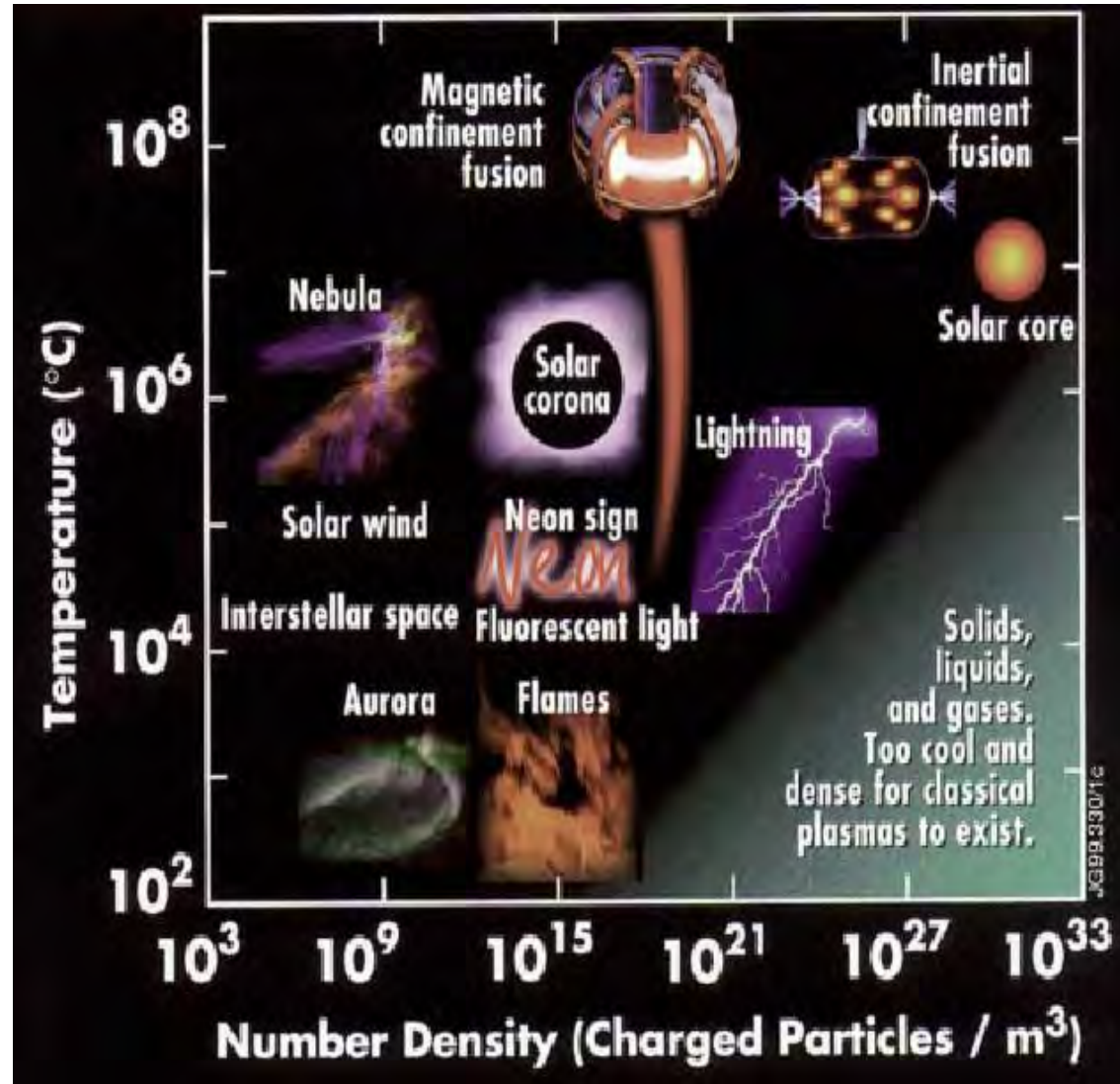
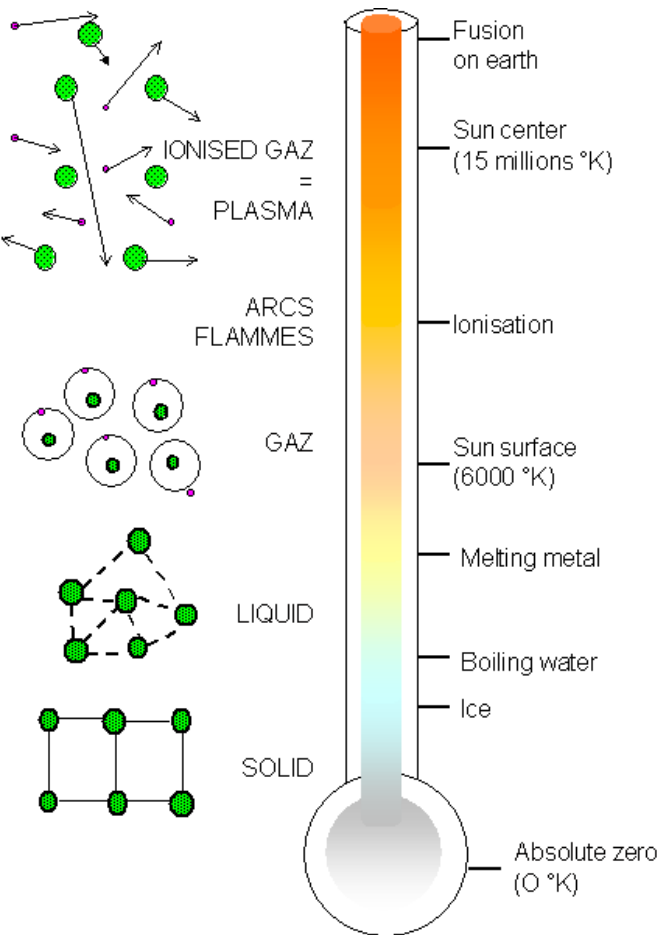


Fig. 7.2 : Moyenne du produit $\langle \sigma v \rangle$ obtenue pour une distribution maxwellienne sur v .

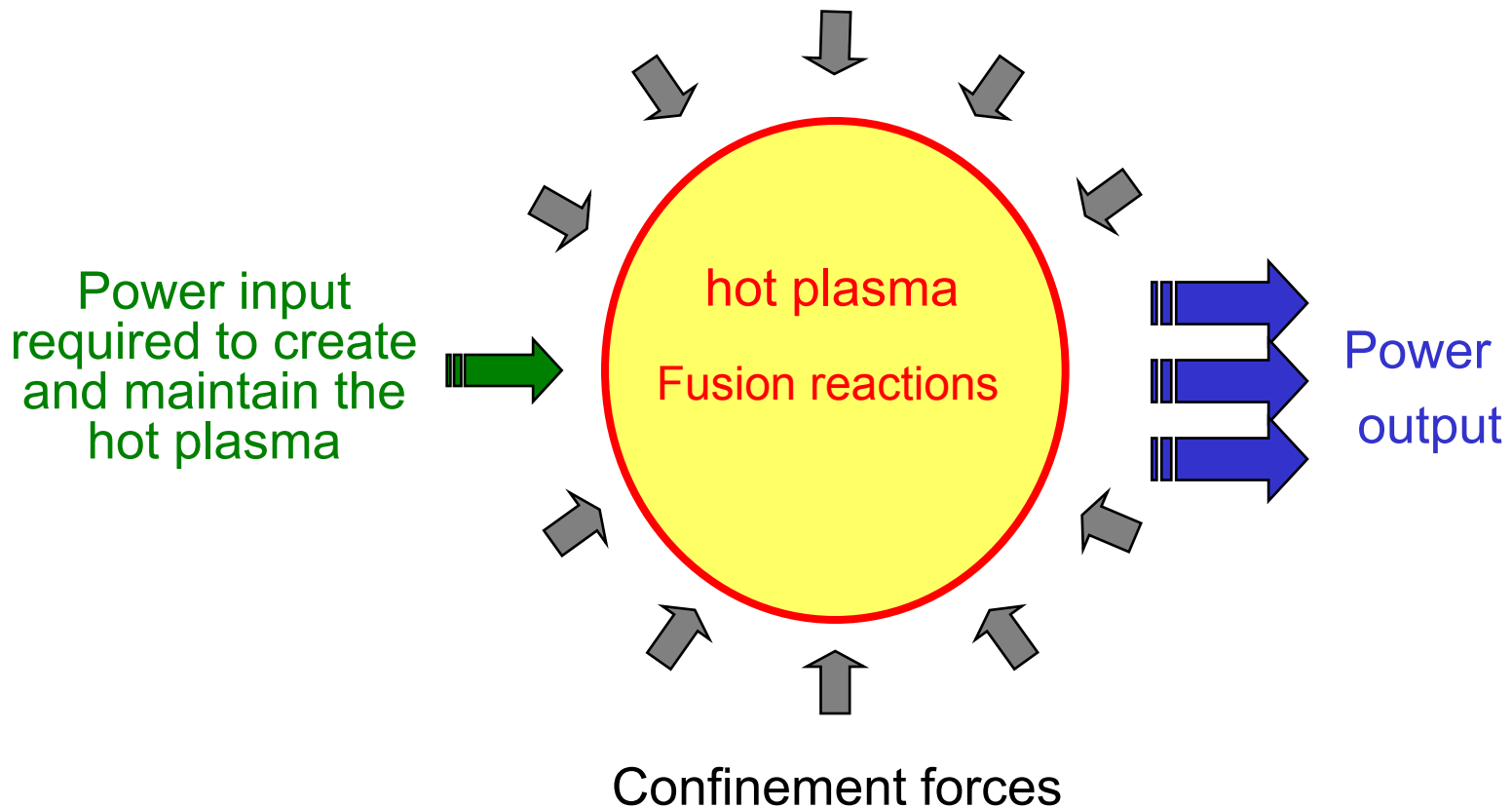
Plasma: the fourth state of matter



- a plasma is an electrically neutral ionized gas
- Plasma is the most widespread form of matter in the universe (~99%)

1 electron-Volt (eV) ~ 11600° K

"The mixture D-T must be maintained at
 $T_i \sim 2 \times 10^8$ degrés
in order to have a sufficient reactivity"



The Lawson criterion

$$P_{\text{losses}} = W/\tau_E, \text{ where } W = (3/2)(n_i T_i + n_e T_e) = 3n_i T_i$$

where τ_E Energy confinement time

$$(n_i^2 \langle \sigma V \rangle_{DT} Q_{DT} / 4)(0,2 + 1 / Q) \geq 3n_i T_i / \tau_E$$

$$\Rightarrow n_i \tau_E \geq 3 T_i / (\langle \sigma V \rangle_{DT} Q_{DT} / 4)(0,2 + 1 / Q) \quad \text{or}$$

$$n_i \tau_E \geq g(T_i)$$

$g(T_i)$ minimum for $T_i \approx 26 \text{ keV}$

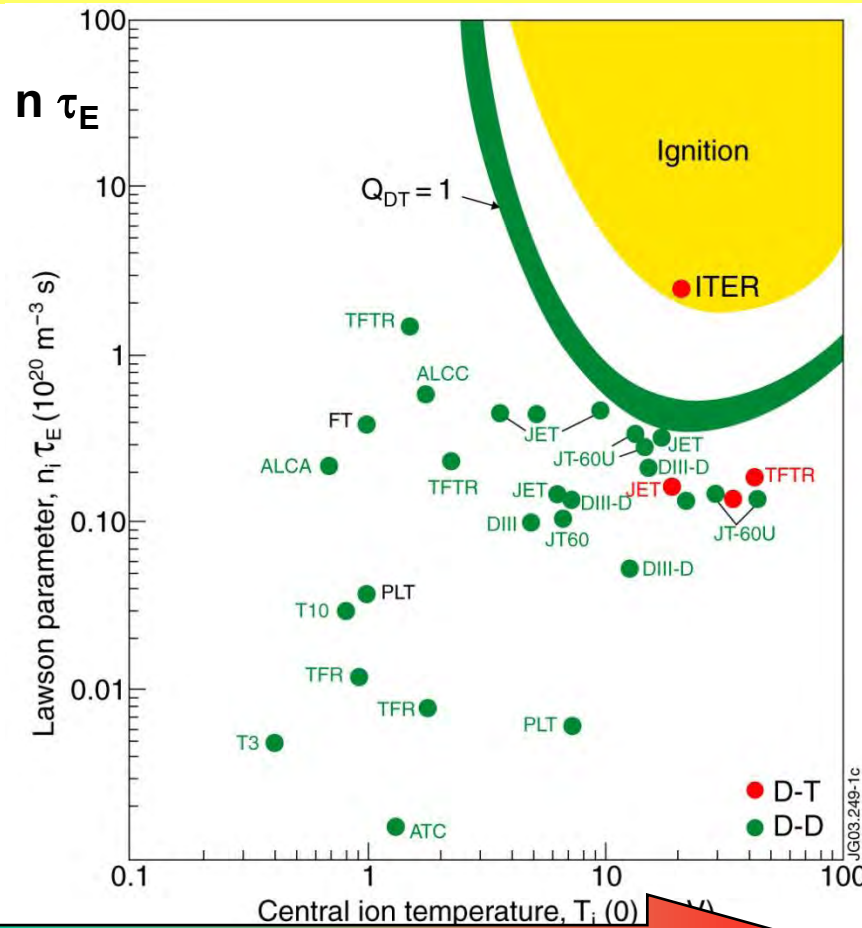
with $Q_{DT} = 17,6 \cdot 10^3 \text{ keV}$, $Q \rightarrow \infty$

$\langle \sigma V \rangle_{DT} \approx 1.1 \times 10^{-24} (T_i)^2 \text{ [MKS]}$

if $10 \leq T_i \leq 30 \text{ keV}$

$$n_i T_i \tau_E > 3 \times 10^{+21} \text{ (keV} \cdot \text{m}^{-3} \cdot \text{s)}$$

Pressure

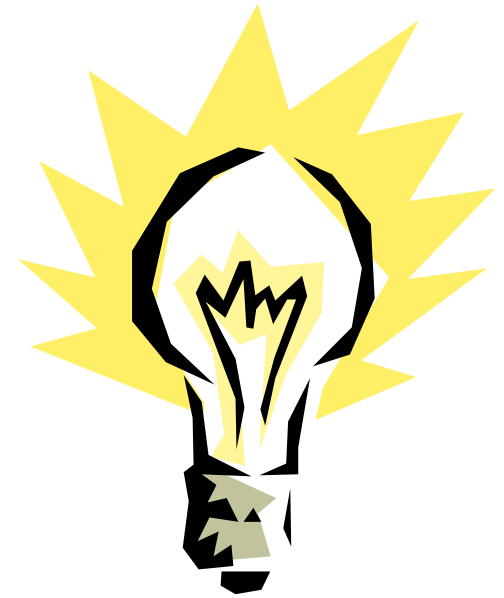


Ignition: If pressure and energy confinement time τ_E are such that the Lawson criterion is satisfied, then α (He^{++}) particles alone are sufficient to maintain the temperature.

The power balance

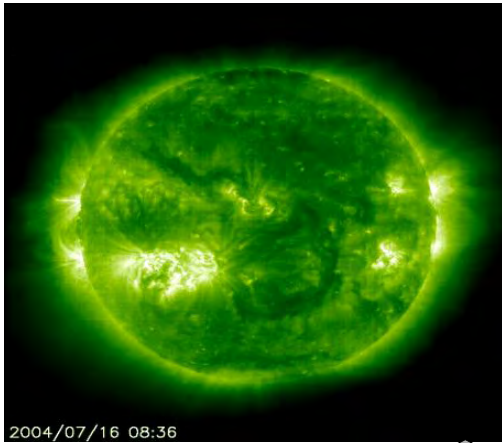
- $P_{\text{fus}} = P_{\text{neut}} + P_{\alpha} \approx 5 P_{\alpha} \approx 5(n_i^2 \langle \sigma V \rangle_{\text{DT}} / 4) E_{\alpha}$ (D-T 50/50)
- $dW_P / dt = P_{\text{inj}} + P_{\alpha} - P_{\text{losses}} = 0$
- $Q = P_{\text{fus}} / P_{\text{inj}}$ (Power amplification)

Break-even	$Q = 1$	$P_{\text{fus}} \geq P_{\text{inj}}$
Ignition	$Q = \infty$	$P_{\alpha} \geq P_{\text{losses}}$ $P_{\text{inj}} = 0$

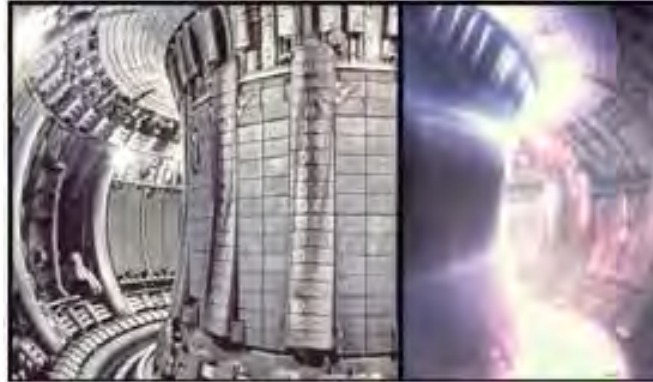


Three methods to achieve fusion

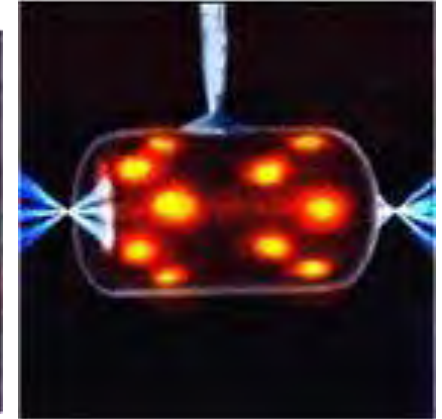
Sun



Tokamak
JET/ITER



Lasers on target



Confinement:

Size:

Duration:

Pressure:

gravitational:

1.3×10^8 m

3×10^{16} s

10^9 atm

magnetic:

10 m

400 s

2 atm

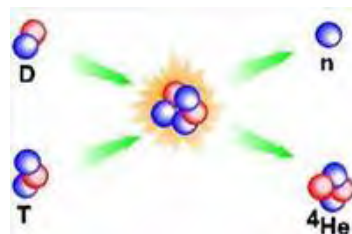
inertial :

10^{-2} m

10^{-8} s

10^9 atm

Temperature: ~ 100 million deg \Leftrightarrow thermal energy ~ 10 keV



Ignition condition:

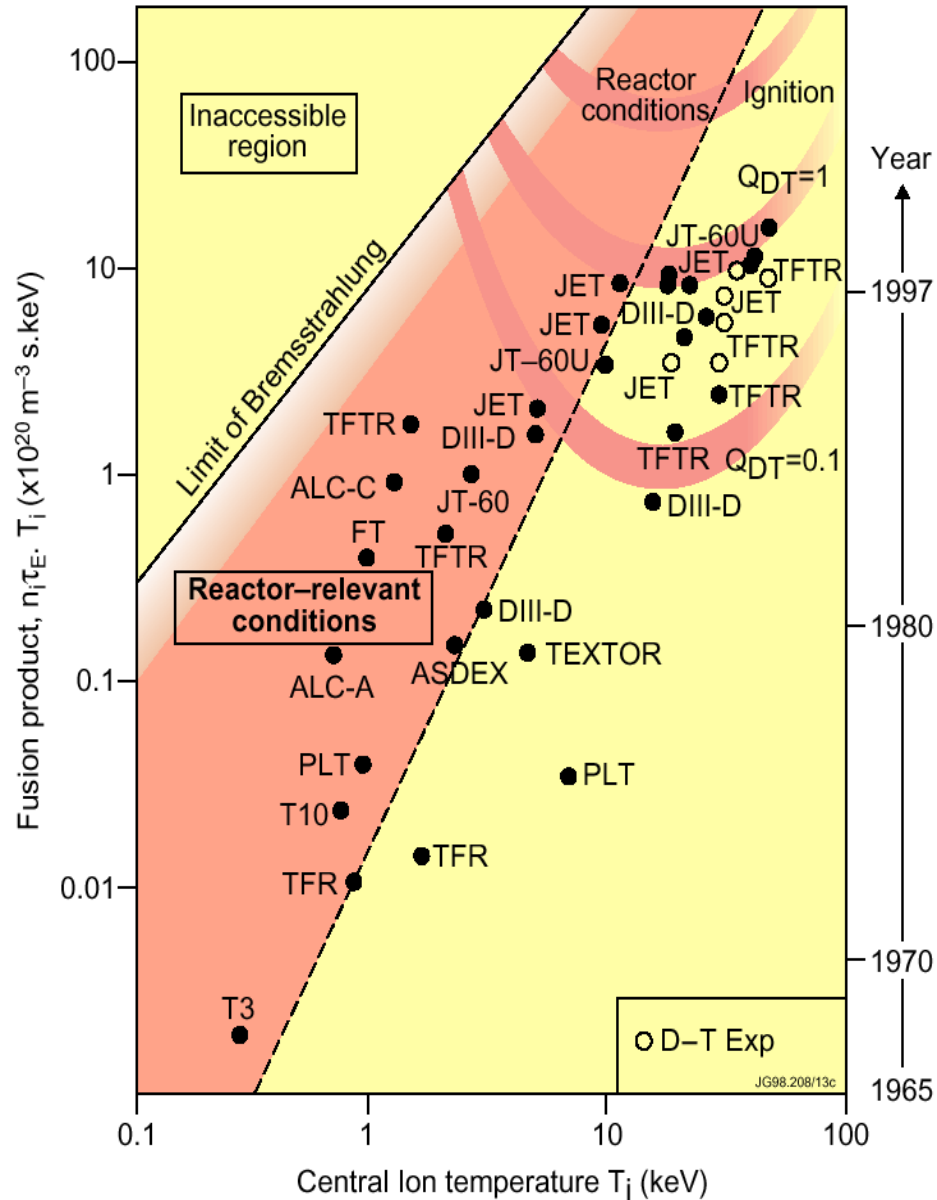
$nT_i \tau_E \sim 10^{21} \text{ m}^{-3} \cdot \text{keV} \cdot \text{s} \sim 1 \text{ bar} \cdot \text{second}$

$\tau_E =$ Energy confinement time

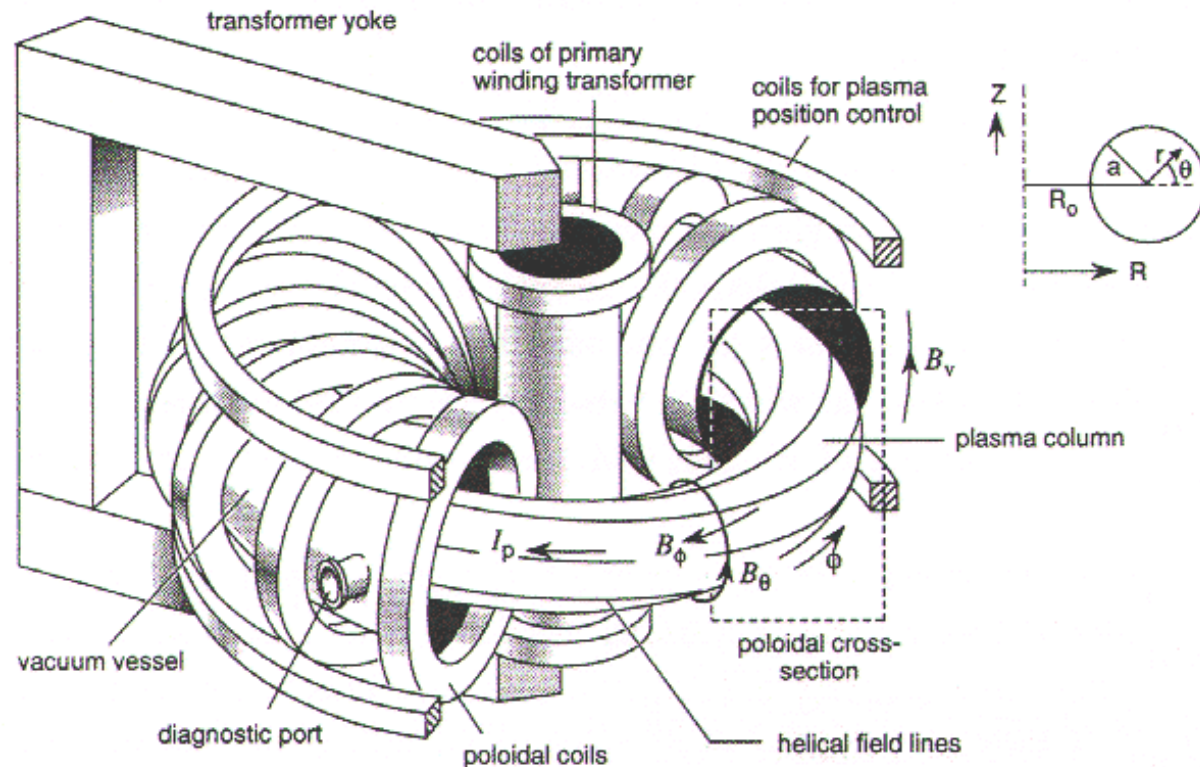
Past achievements

Performances are measured with respect to the Lawson criterion

- From every new machine a big progress has been made.
- With JET the break-even ($Q=1$) has been reached
- A factor of 6 in $nT\tau$ is still required
- *This will be possible from ITER*



Castor alias GOLEM



major radius: $R = 0.4 \text{ m}$

minor radius:

$a = 0.085 \text{ or } 0.060 \text{ m}$

toroidal magnetic field:

$B_t < 1.5 \text{ T}$

plasma current $I < 25 \text{ kA}$

pulse length $t < 50 \text{ ms}$

plasma density:

$n_e = 0.2\text{-}3.0 \cdot 10^{19} \text{ m}^{-3}$

electron temperature:

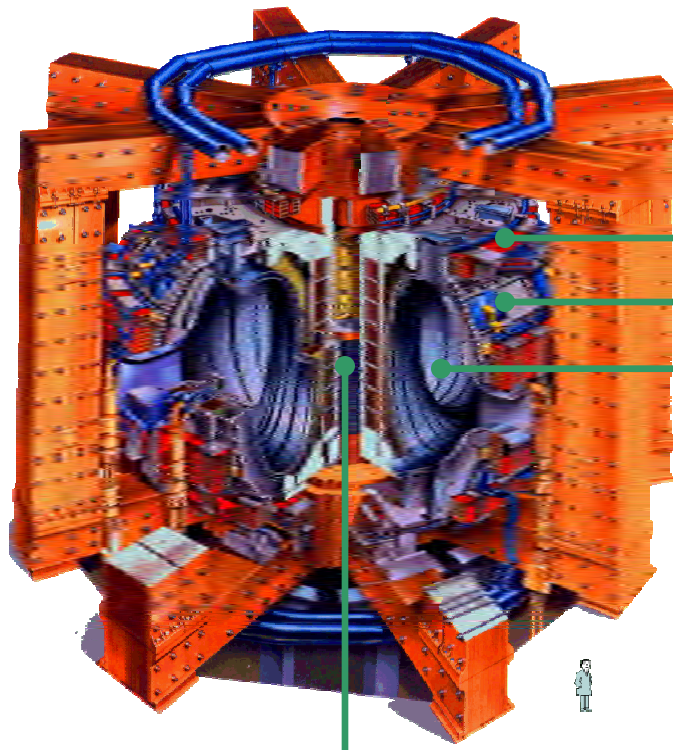
$T_e(0) < 200 \text{ eV}$

ion temperature:

$T_i(0) < 100 \text{ eV}$

The CASTOR (Czech Academy of Sciences TORus) device is a tokamak with a circular cross section. The last closed magnetic surface is defined by a poloidal limiter made of molybdenum. Hydrogen is used as a working gas. As a source of energy for the toroidal magnetic field, 1 MJ condenser bank is used. A delay LC line with the energy of several tens of kJ generates and heats the plasma. The plasma position is stabilized by a feedback system.

The European JET Tokamak

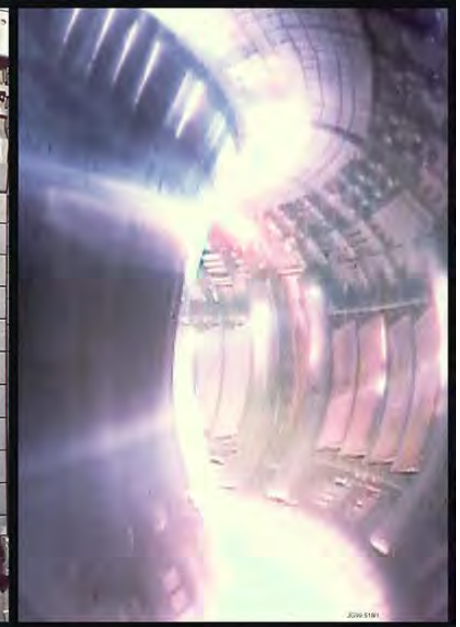
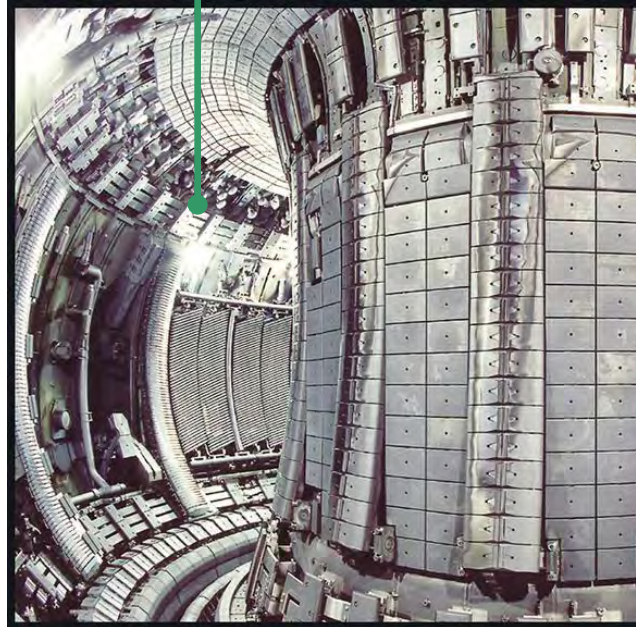
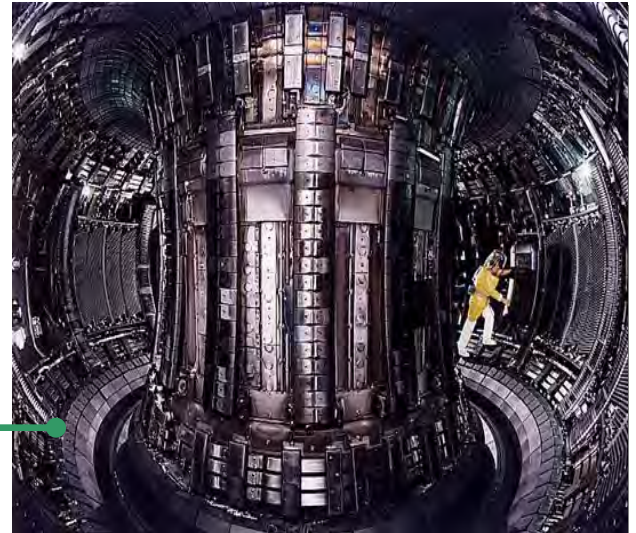


poloidal coil

toroidal coil

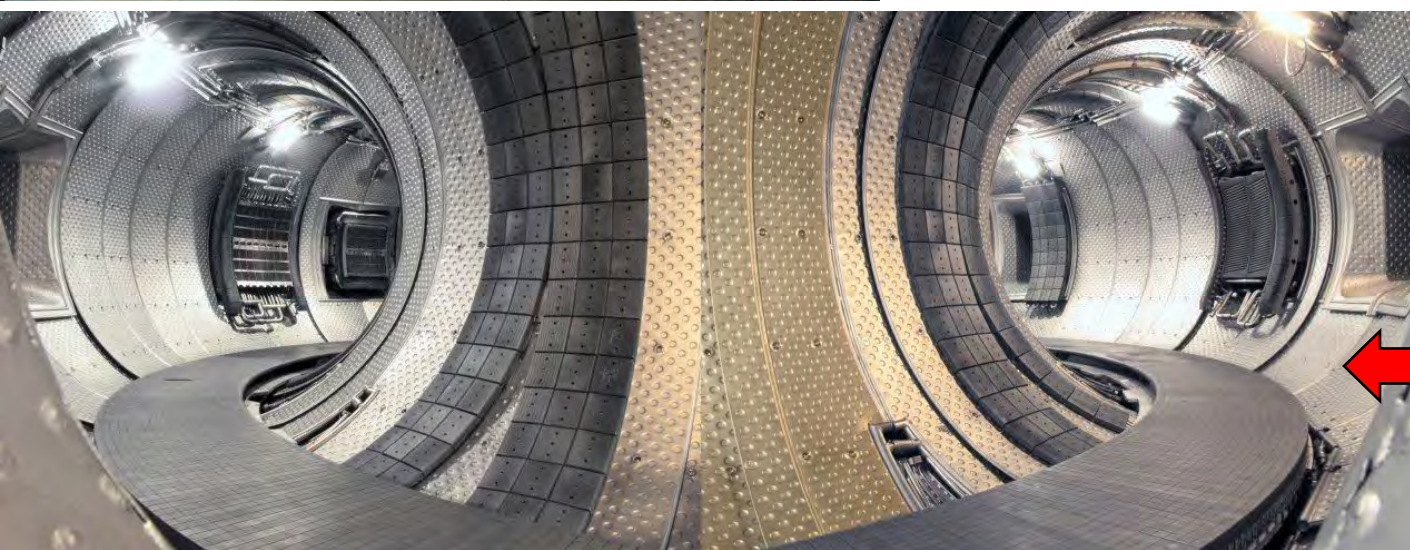
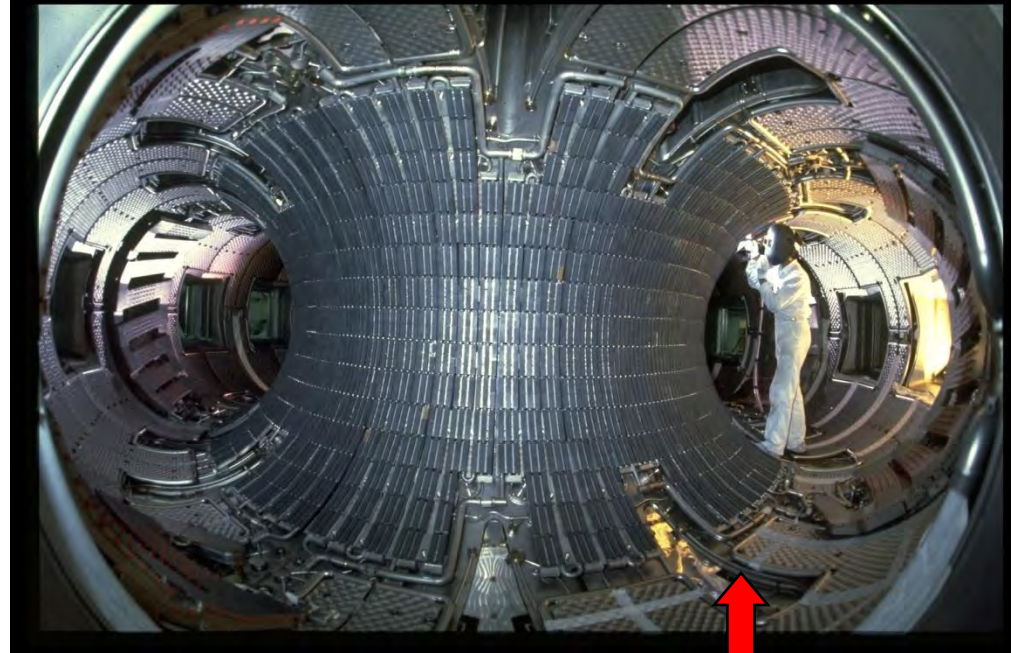
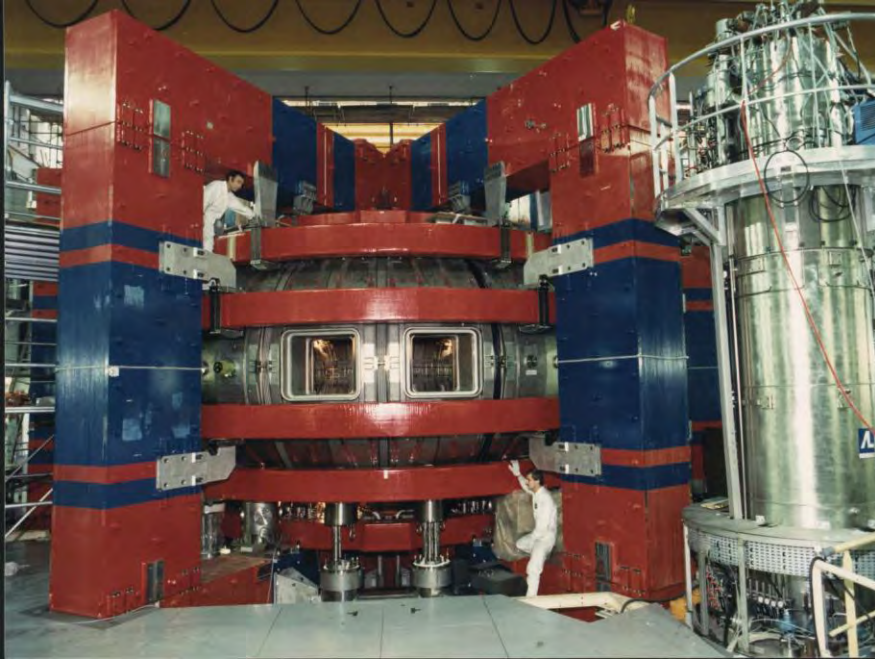
Vacuum vessel

Central solenoid



Tore Supra

World record for extracted energy in steady state (>1000 MJ for 6mn30s)

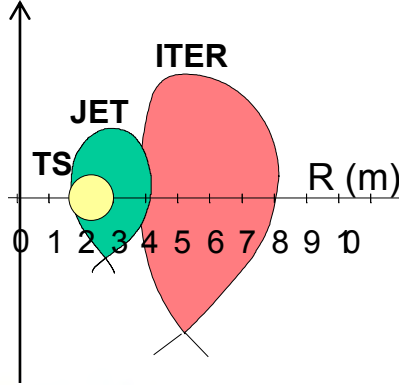


until 1999

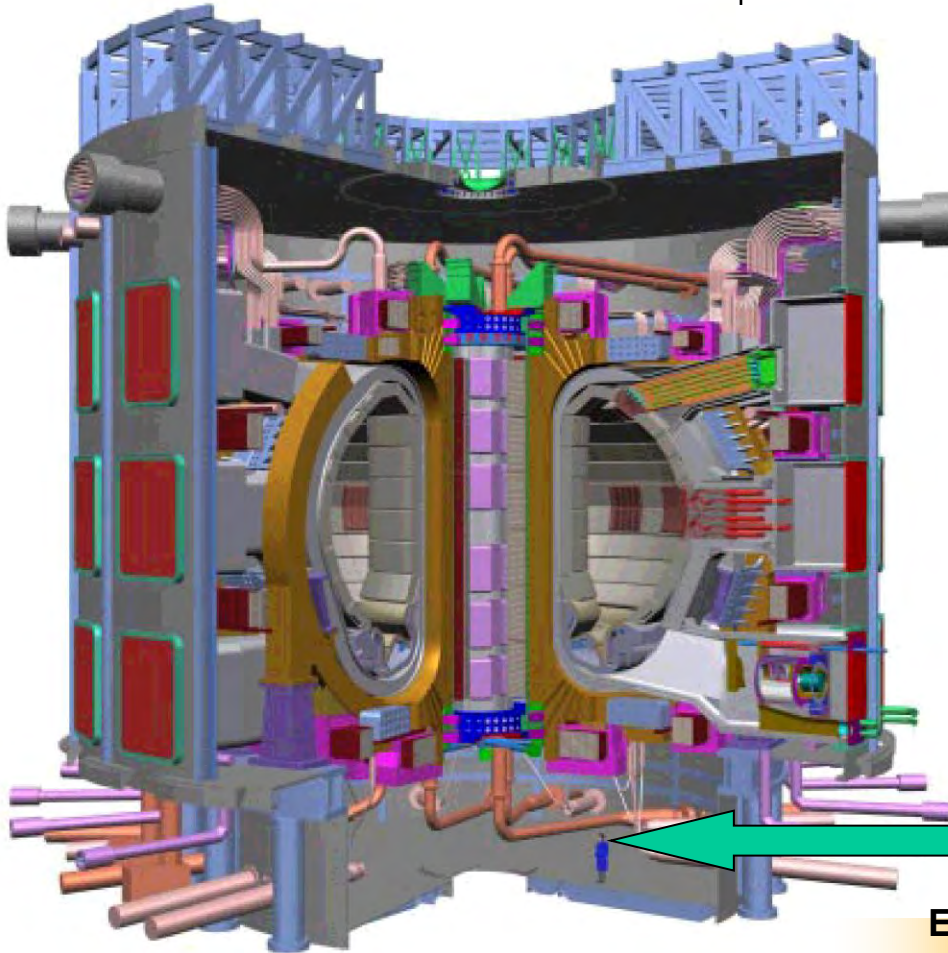
*CIEL Components
(2002)*

ITER

Size: 2 x JET



Main Parameters	ITER
R : major radius (m)	6.2
a : minor radius (m)	2.0
Magnetic field (T)	5.3
Plasma current (MA)	15
Fusion Power (MW)	500
Pulse duration (s)	400
Amplification factor (Q)	10 (ignition possibly)
Construction costs	~ 2×4.6 G€



Fusion Power: 500 MW

Power Gain : 10

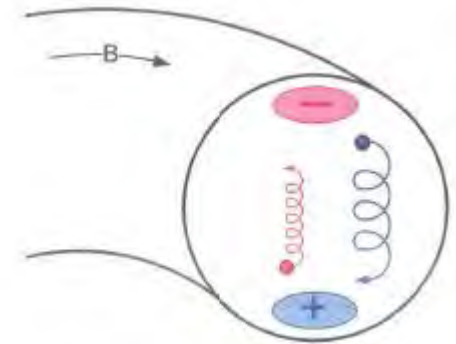
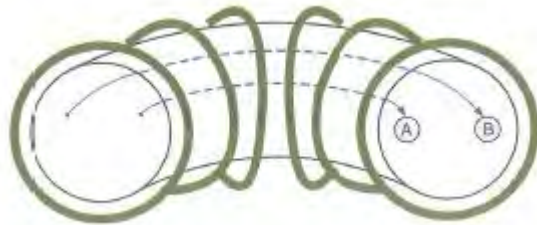
- demonstrate D/T burning
- Tritium breeding blanket
- Flexibility → optimize DEMO parameters

Homo sapiens sapiens

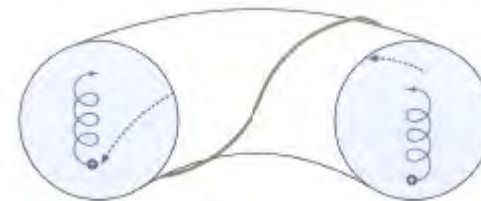


The magnetic bottle

- 3 ways to achieve magnetic confinement in a closed volume
 1. Driving a toroidal current \rightarrow tokamaks, RFPs
 2. Elongating the flux surfaces and making them rotating poloidally as one moves around the torus
 3. Making the magnetic axis non planar

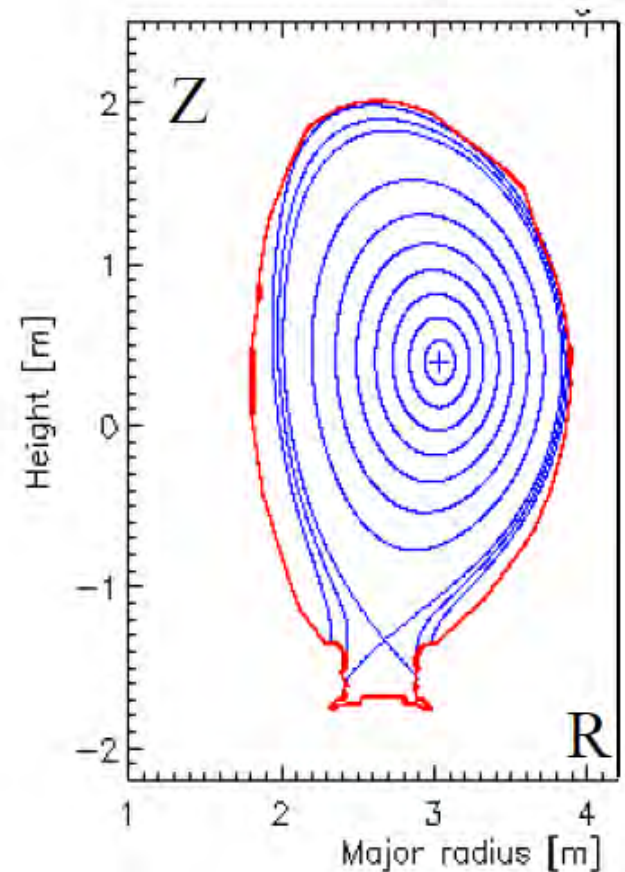
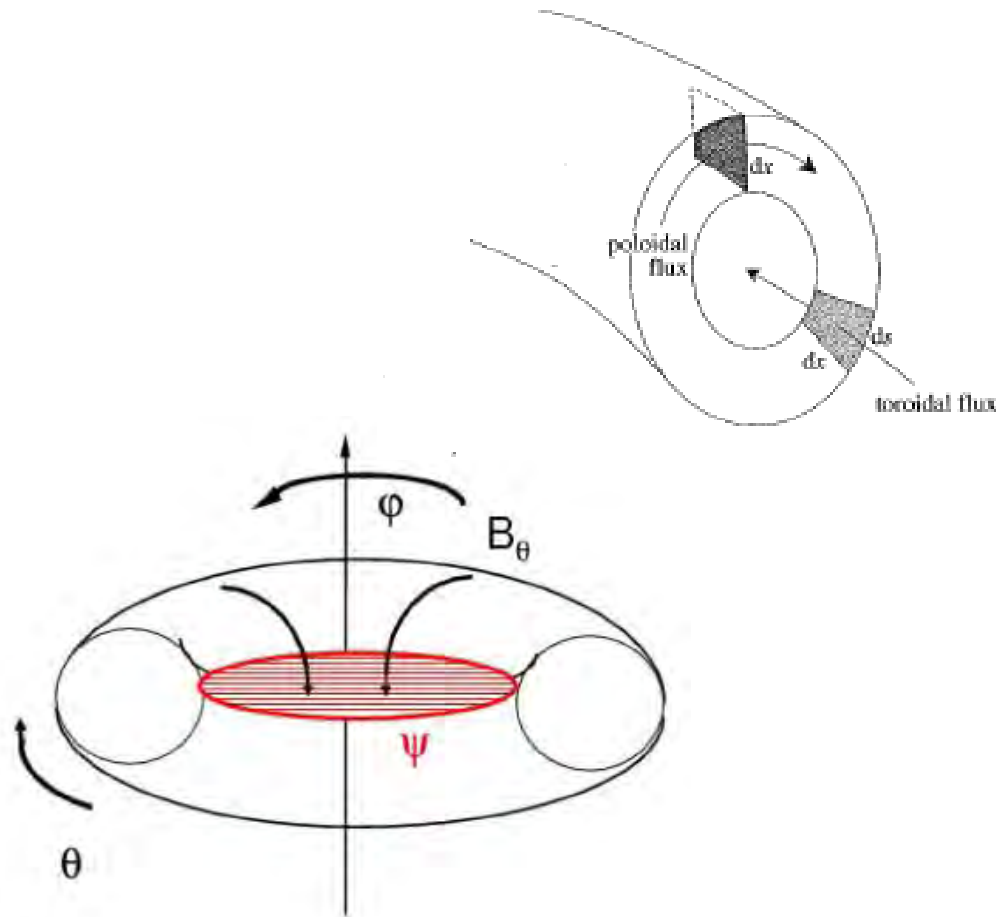


- Tokamaks and Stellarators



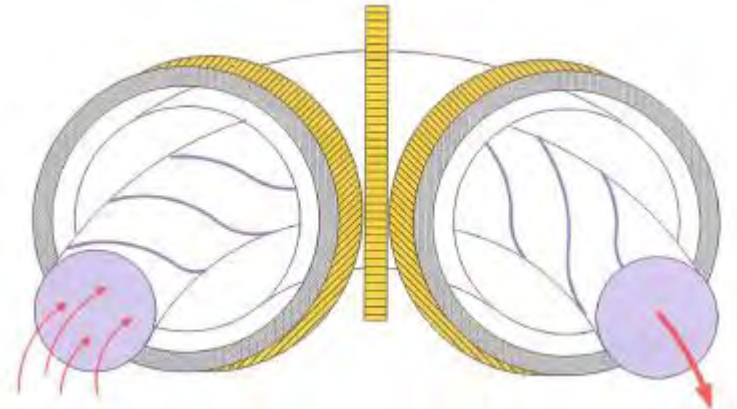
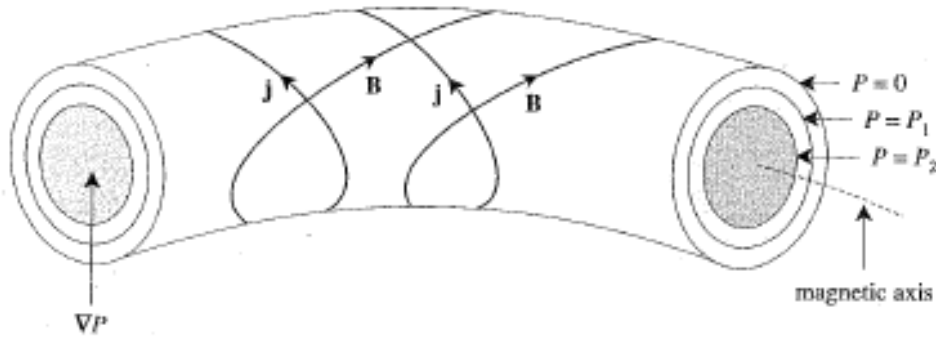
Magnetic surfaces

- Field lines are winded on torii called magnetic surfaces.
- Each magnetic surface is labelled by its poloidal flux ψ



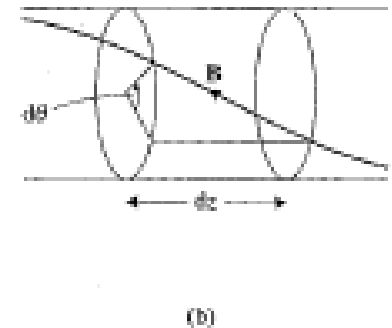
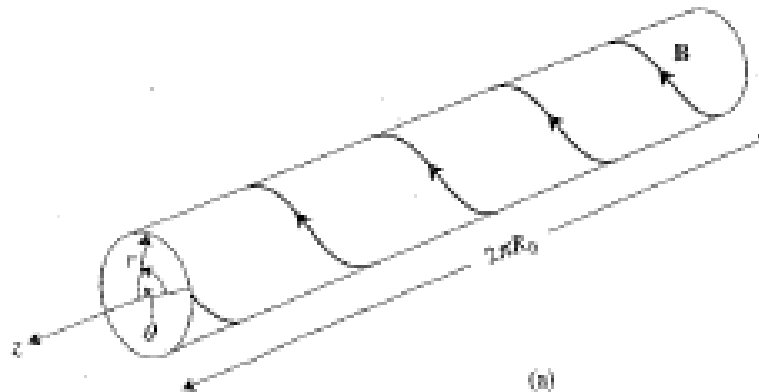
MHD Equilibrium and stability

- Nested isobaric surfaces



- Screw pinch definitions

- Rotational transform and/or Winding number (safety factor q)



The Tokamak: how does it work?

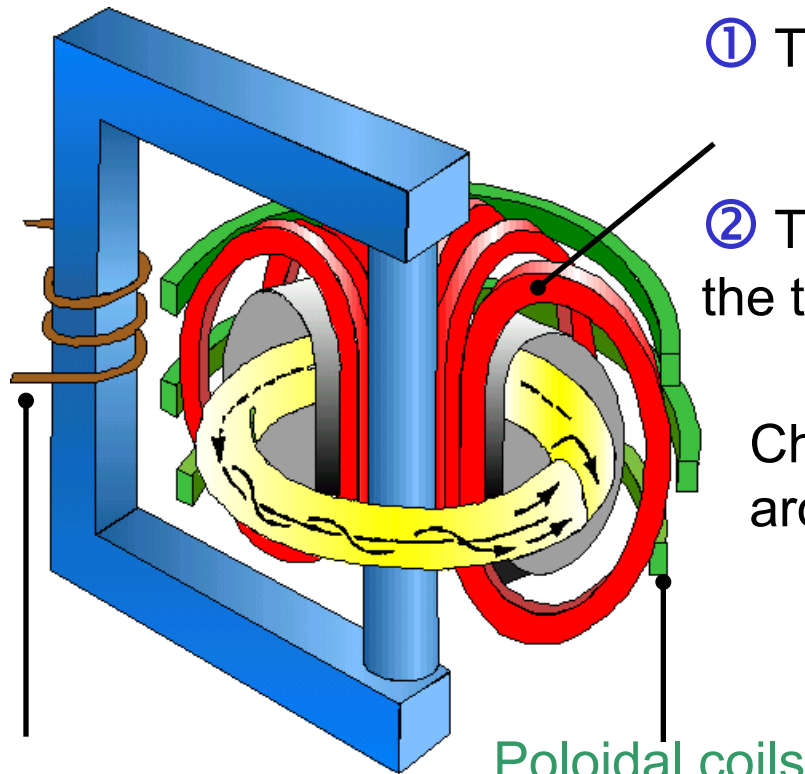
*tokamak (contraction of Russian words, *toroidalnaya* , *kamera*, *magnitnaya*)

- ➔ Tokamak = transformer whose secondary is the plasma
- ➔ The confinement is performed by the combination of **two** magnetic fields:

① The **toroidal** field generated by **toroidal coils**

② The **poloidal** field created by the toroidal plasma current

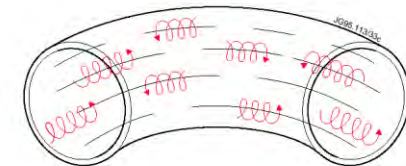
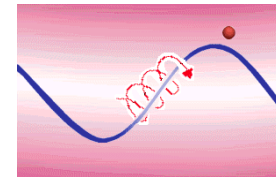
Charged particles trajectories roll around the resulting field lines



+



=



$$\langle \beta \rangle = \frac{\langle p \rangle}{B_0^2 / 2\mu_0} : 3 - 5\%$$

Heating the plasma

- The ohmic regime:

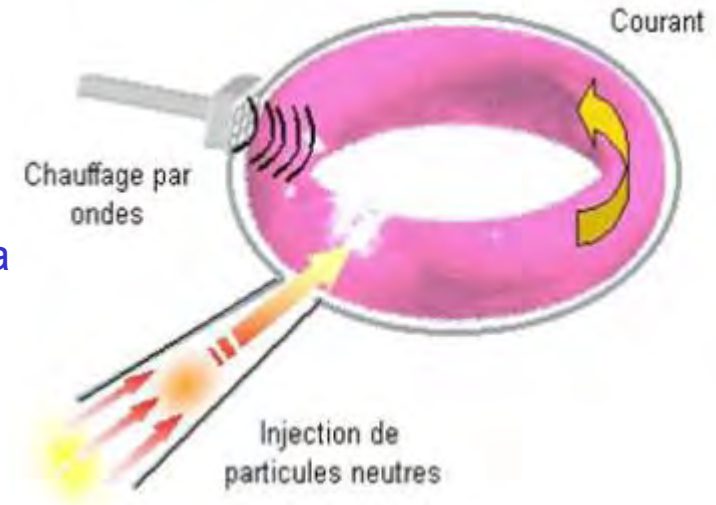
A first mechanism is the natural Joule heating due to the current flowing in the plasma, (and used to create **the tokamak magnetic configuration**). Just like the filament of a light bulb heats up when current passes through, the plasma temperature will rise as a result of intense current (of the order of MA) passing through it. Unfortunately, this effect is proportional to the resistance of the plasma which tends to collapse when the temperature increases, saturates and achieves only limited temperatures (of the order of 10 million degrees). This heating regime is called ohmic regime.

- Additional heating

To achieve the required temperatures, we therefore use additional heating systems. They are classified into two families:

- heating by injection of **neutral particles** of high energy, e.i., the plasma is heated through the collisions between the high energy particles injected and the plasma particles.

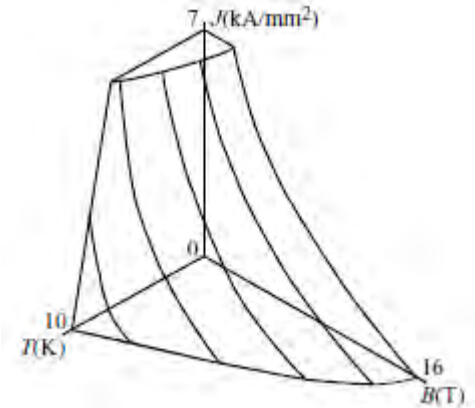
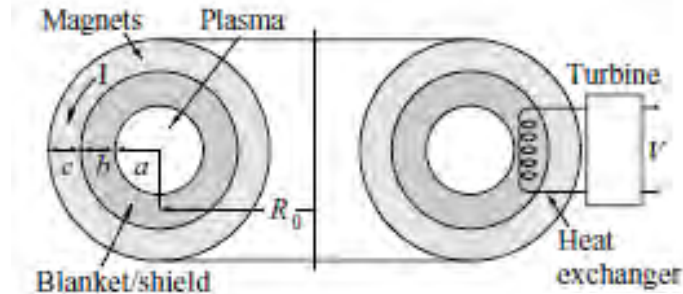
- **the RF heating**, which is to couple to the plasma a wave a resonance with a class of particles in the plasma, (i.e. at the same frequency → **LH, ICRH, ECRH**) and communicate their energy, like a microwave oven which heats a meal by waving water molecules



Design of a generic fusion reactor

- Design parameters

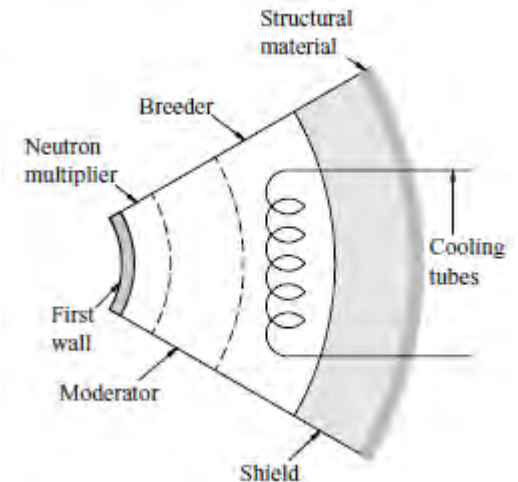
Quantity	Symbol
Minor radius of the plasma	a
Major radius of the plasma	R_0
Thickness of the blanket-and-shield	b
Thickness of the magnets	c
Plasma temperature	T
Plasma density	n
Plasma pressure	p
Fusion power density	S_f
Energy confinement time	τ_E
Magnetic field	B
Normalized plasma pressure	β



- Design goals, engineering and nuclear constraints

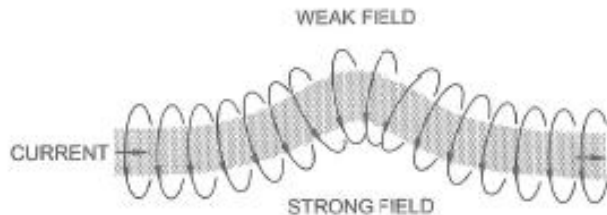
- Electric power $P_E = 1000$ MW
- Wall loading limit $P_w = 4$ MW/m²
- Superconductors, $B_{max} = 13$ T
- Structural material, $\sigma_{max} = 300$ MPa
- D-T fusion cross-section
- Blanket: neutron moderation and tritium breeding

- Design of the reactor

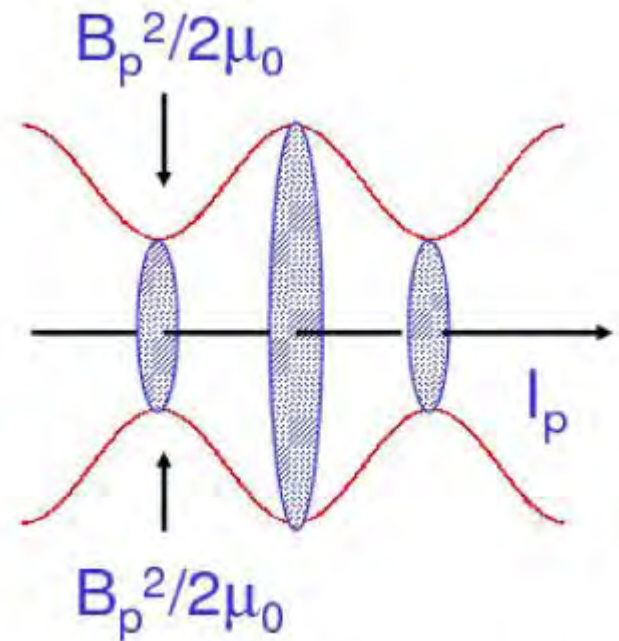
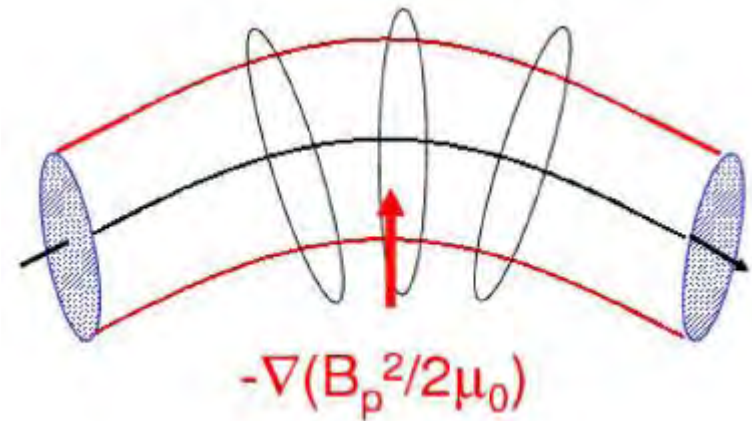


Kink and sausage instabilities

- Kink instability
 - A flexible wire plunged into a Magnetic field is unstable
 - In a z-pinch bending tends to amplify



- Sausage instability
 - In a z-pinch compression zones (intense poloidal field) tend to amplify

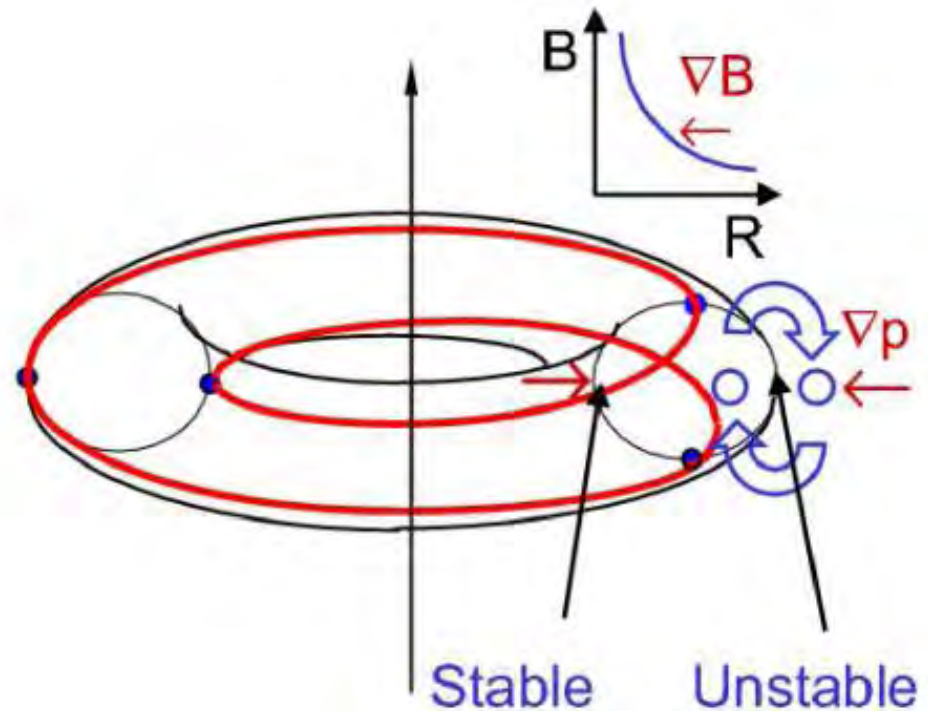
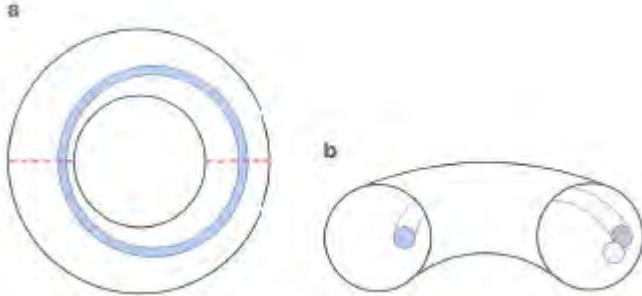


Interchange stability in a tokamak

- Low (high) field side is locally unstable (stable) connected via field lines (ballooning modes)
- Set a β (or pressure) limit

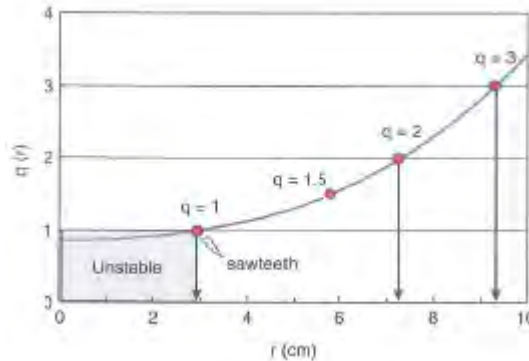
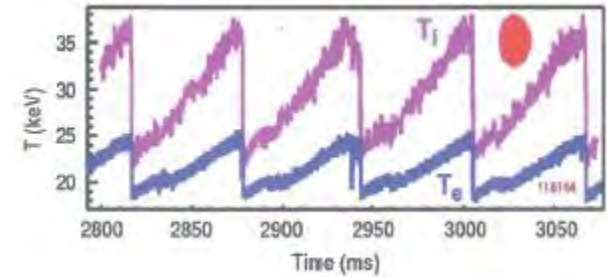
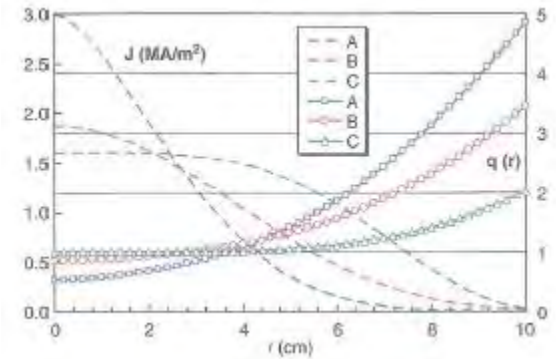
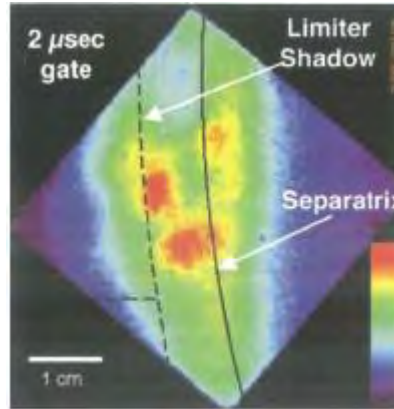
Troyon limit β_N

$$\beta_N \equiv \beta (\%) \frac{aB}{I} \sim 3.5$$



Magnetic islands and sawtooth

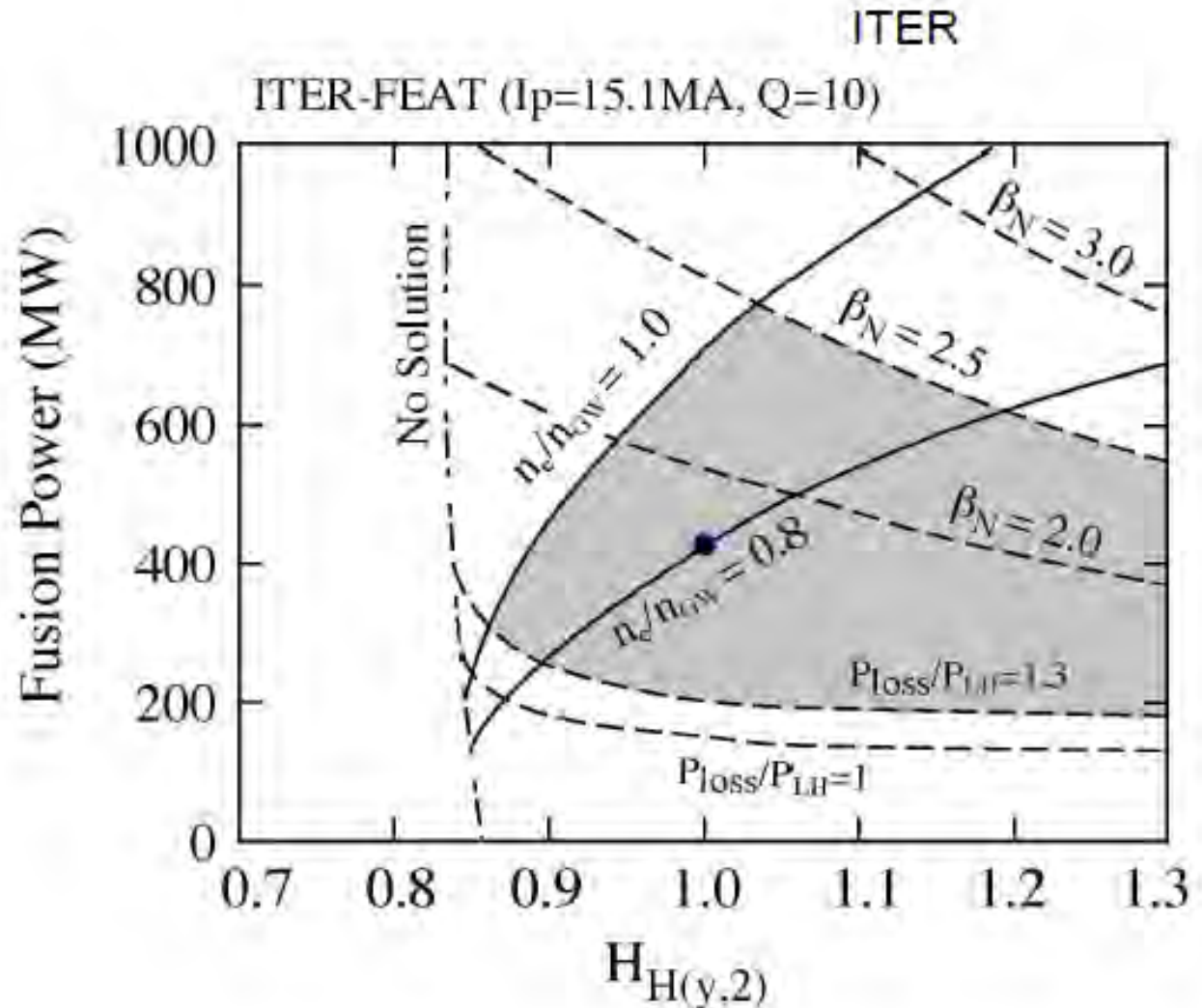
- Kruskal-Shafranov limit



Stability diagram for ITER

Compromise
between
various
constraints:

- density limit
 $n/n_{GW} = 1$
- β limit
- Confinement

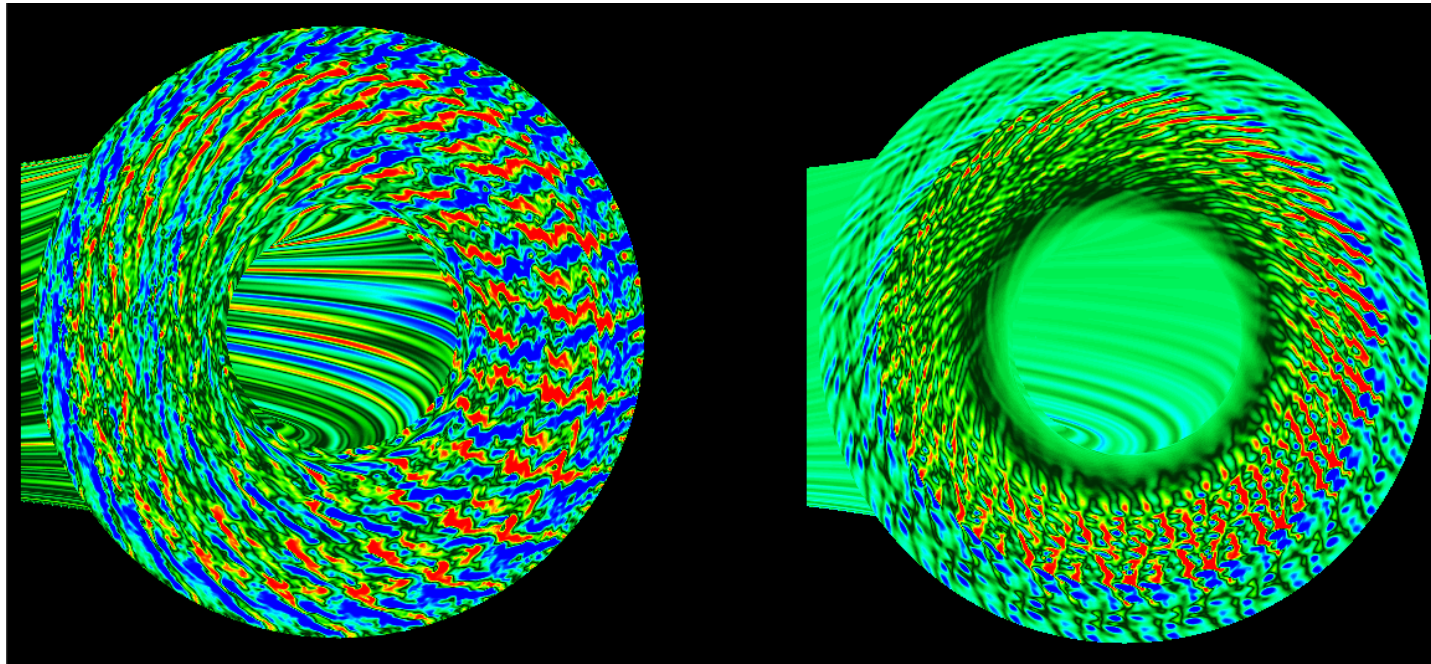


MHD Stability. Conclusions

- Equilibrium is essentially a balance between the pressure gradient and the Lorentz force →
Grad-Shafranov equation
- Two main instabilities:
 - interchange (pressure driven),
 - kink (current driven).
- ITER target plasmas are stable with respect to the main MHD instabilities.

Turbulence, transport and confinement

A shear flow (right) tears the swirls and thus decreases the convective cross-field turbulent transport



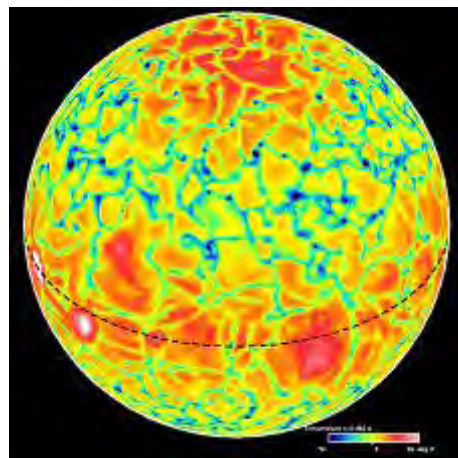
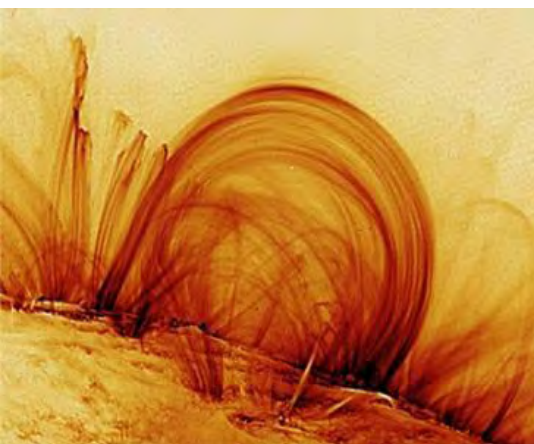
Example of very demanding numerical simulations to study methods to suppress turbulence

- Nonlinear Physics: theoretical predictions are difficult
- Turbulent transport.
- Degradation of the confinement.

Scientific aspects: comparison between sun and tokamak

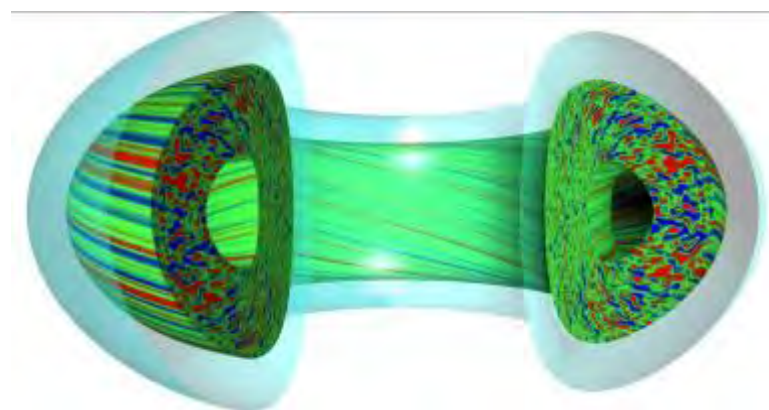
Sun

- Thermoconvection
- Magnetic field generation (dynamo)
- Solar eruptions



Tokamak

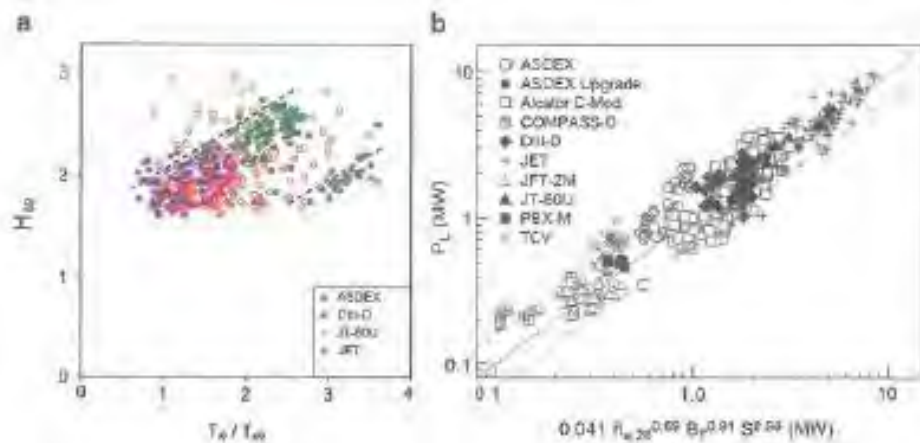
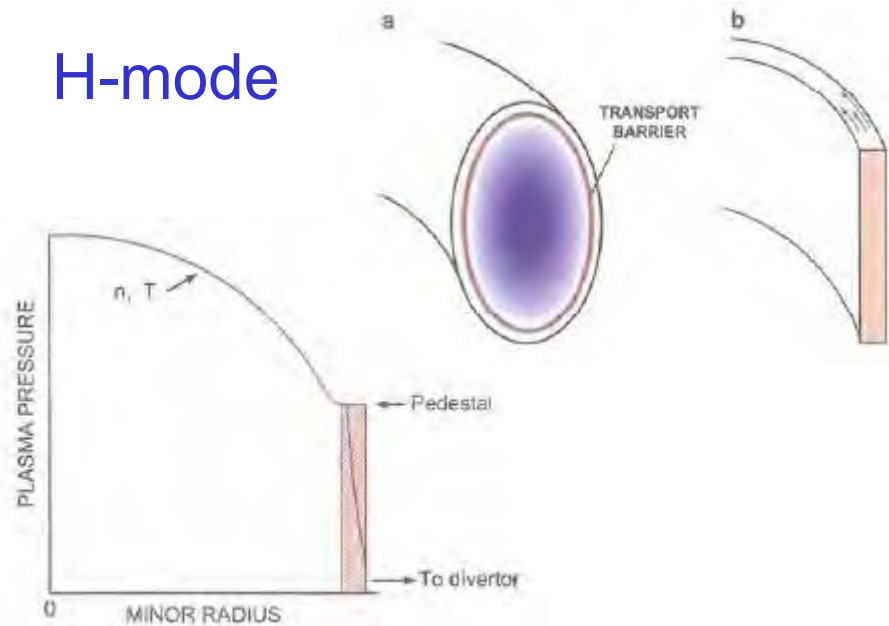
- Turbulent transport
- Mean velocity flow generation
- Relaxations (disruptions)



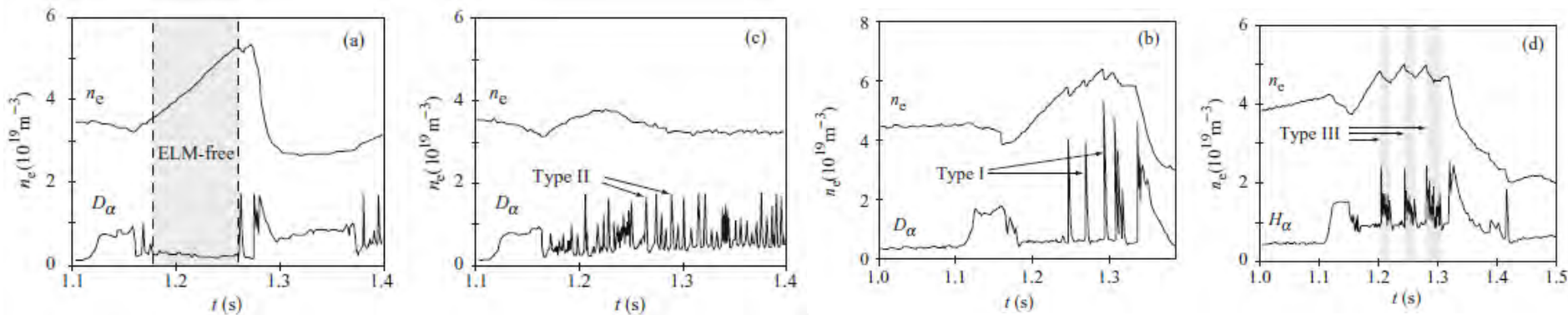
- Large number of similarities between fusion plasmas on earth and stars.
- The main problems in solar physics are thermoconvection, dynamo effect, and solar eruptions.
- Similar research topics exist in tokamak plasmas.
- The main objective in building Tokamaks is to produce energy. They are also very interesting from the point of view of fundamental physics.

L- vs. H-mode, Edge Localized Modes

- H-mode

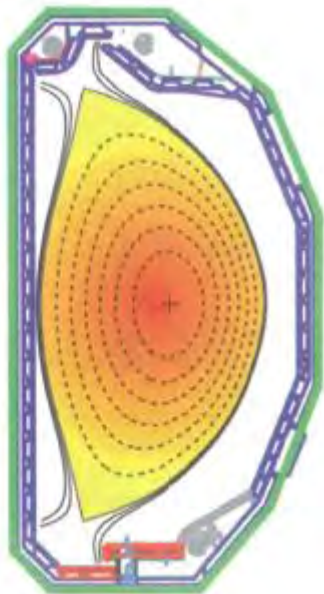


- ELMs



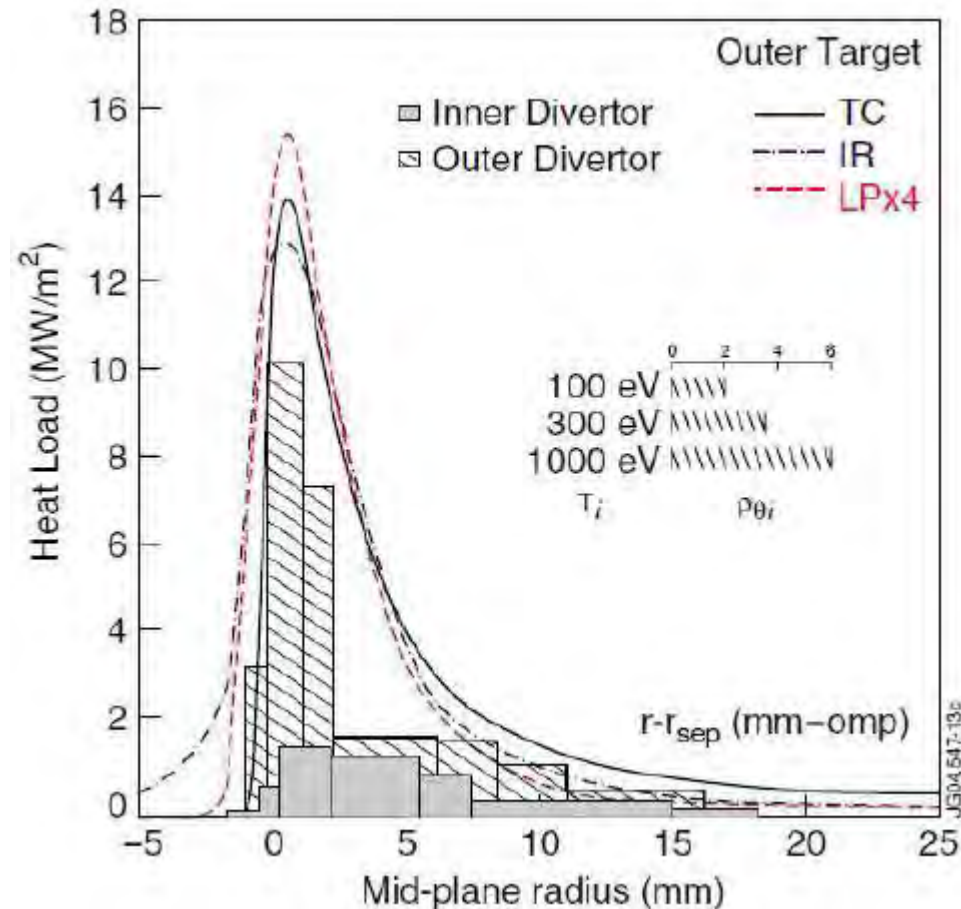
Scrape-off layer

- In the edge : field lines are intercepted by plasma facing components
 - Charged particles follow field lines
- a thin boundary layer develops at the edge:
the Scrape-Off Layer
- The width of the the SOL is small: most of the heat is deposited in a layer whose width is $\sim 1\text{cm}$



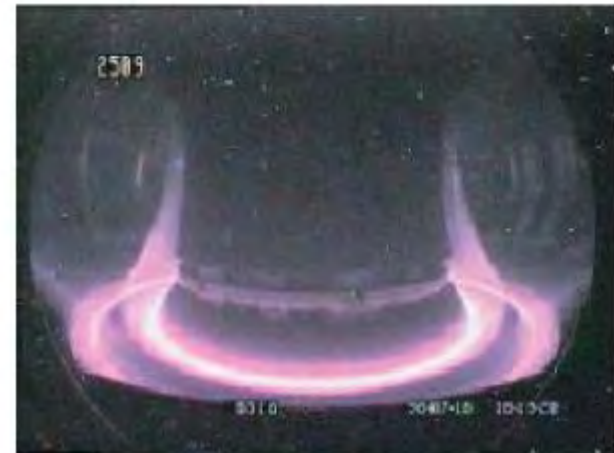
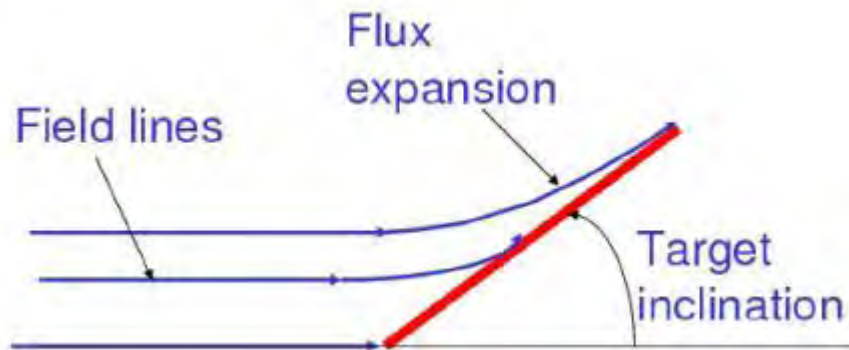
Heat exhaust: a challenge

- ITER : 120 MW must be extracted by plasma facing components.
- Heat flux across the separatrix
 $q_{\perp} = 0.2 \text{ MW/m}^2$
- Parallel heat flux
 $q_{\parallel} \approx q_{\perp} qR/\lambda \approx 1 \text{ GW/m}^2$
- If incidence is normal: well beyond technology capabilities ($\approx 10 \text{ MW/m}^2$)

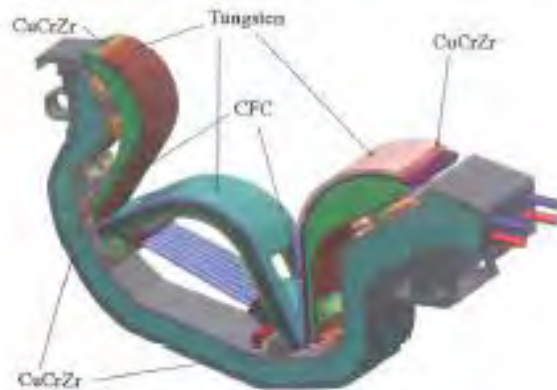


Solutions

- Geometry (field line inclination, flux expansion, ...)
- Radiation: photons do not follow field lines!



An appropriate device: **the divertor**

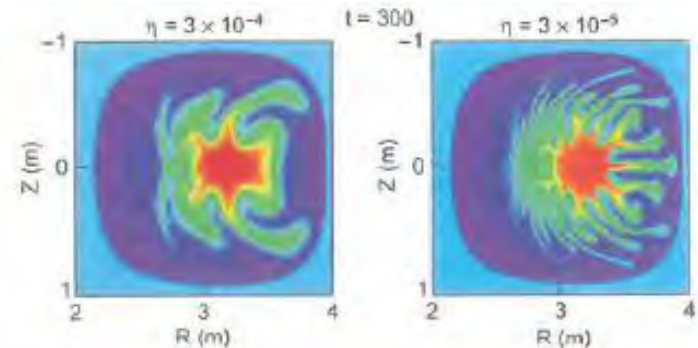
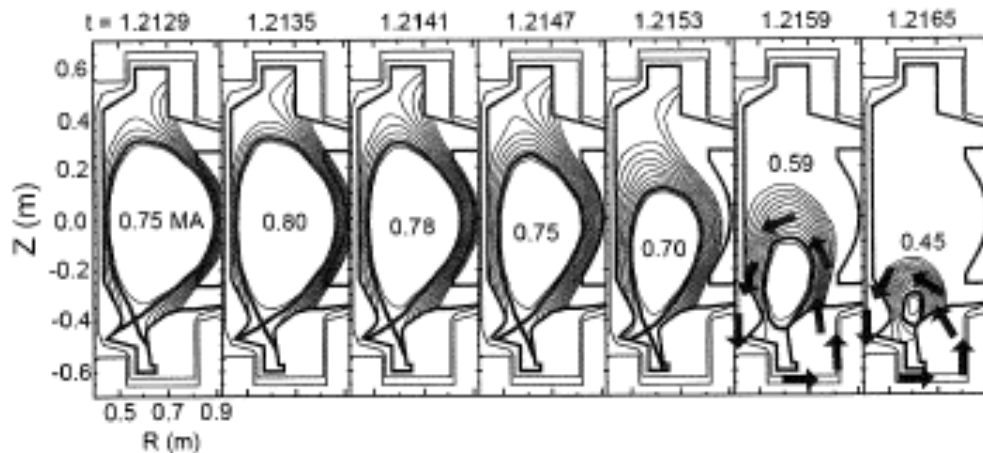


Edge plasma: Summary and Conclusions

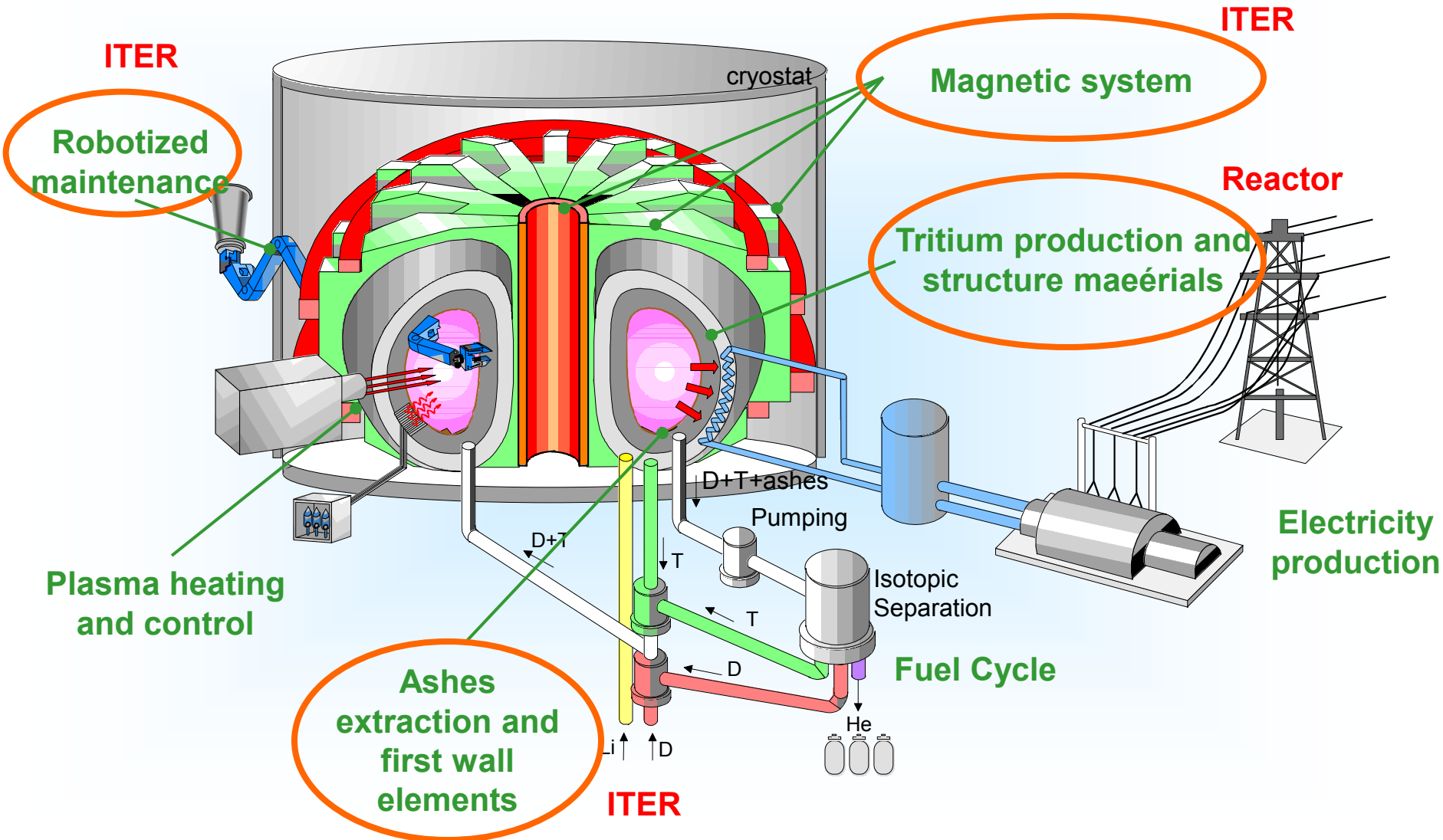
- It is essential to reduce the particle and heat fluxes on the divertor plate
- Sheath potential is not sufficient to reduce enough the fluxes
- An optimum regime is reached by producing a neutral “cushion” in the divertor: detachment
- However detachment may lead to a disruption

Disruptions

- Strong cooling may lead to a local decrease of temperature
- Because of Ohm's law $\sigma(T) J = E$, this may lead to a peaked current density $J \rightarrow$ kink instability
- In usual conditions, this defines a density limit
 $n_G (10^{20} \text{ m}^{-3}) = I_p (\text{MA}) / \pi \kappa a^2$ (Greenwald limit)
- Massive impurity injection also leads to a disruption

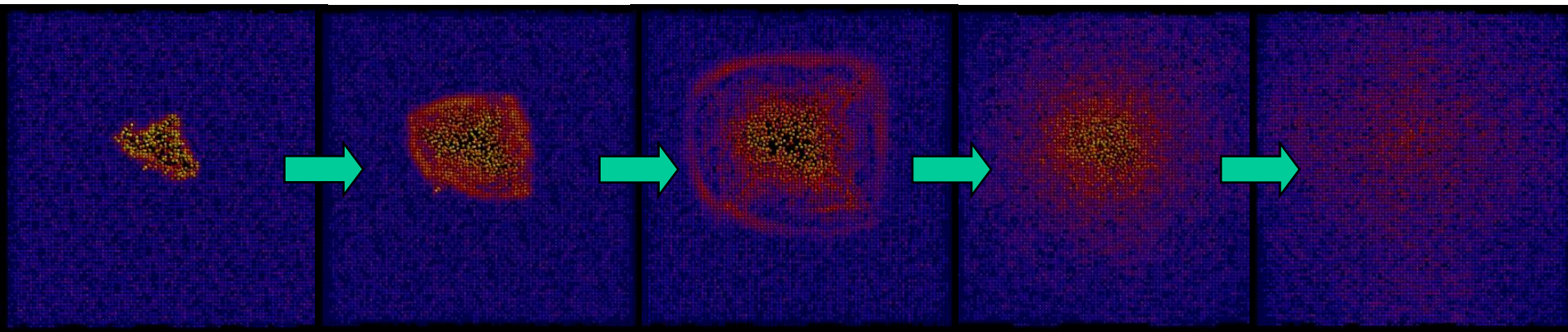
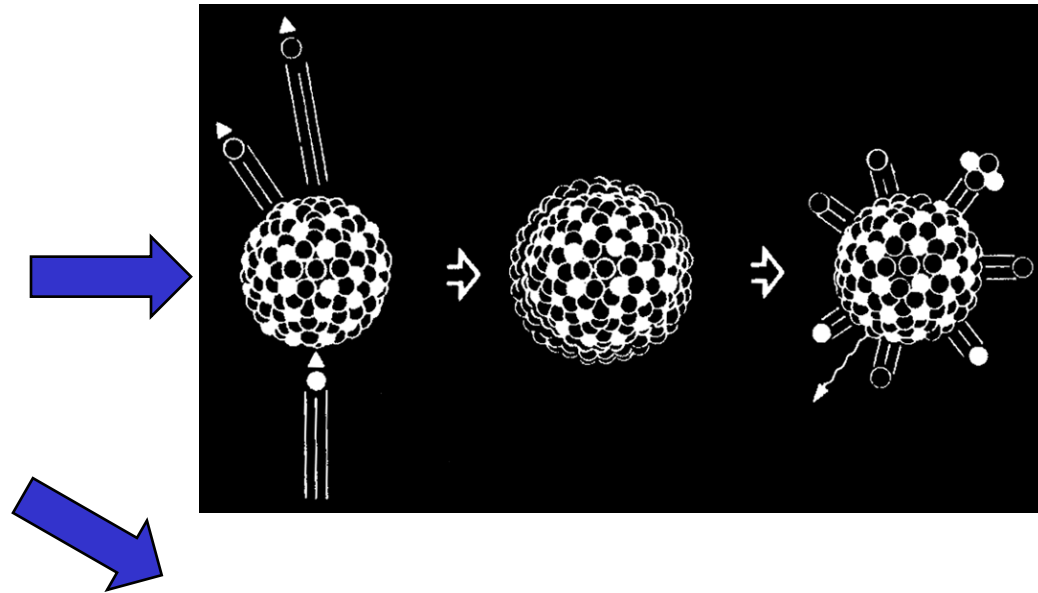


Four technological challenges faced by fusion



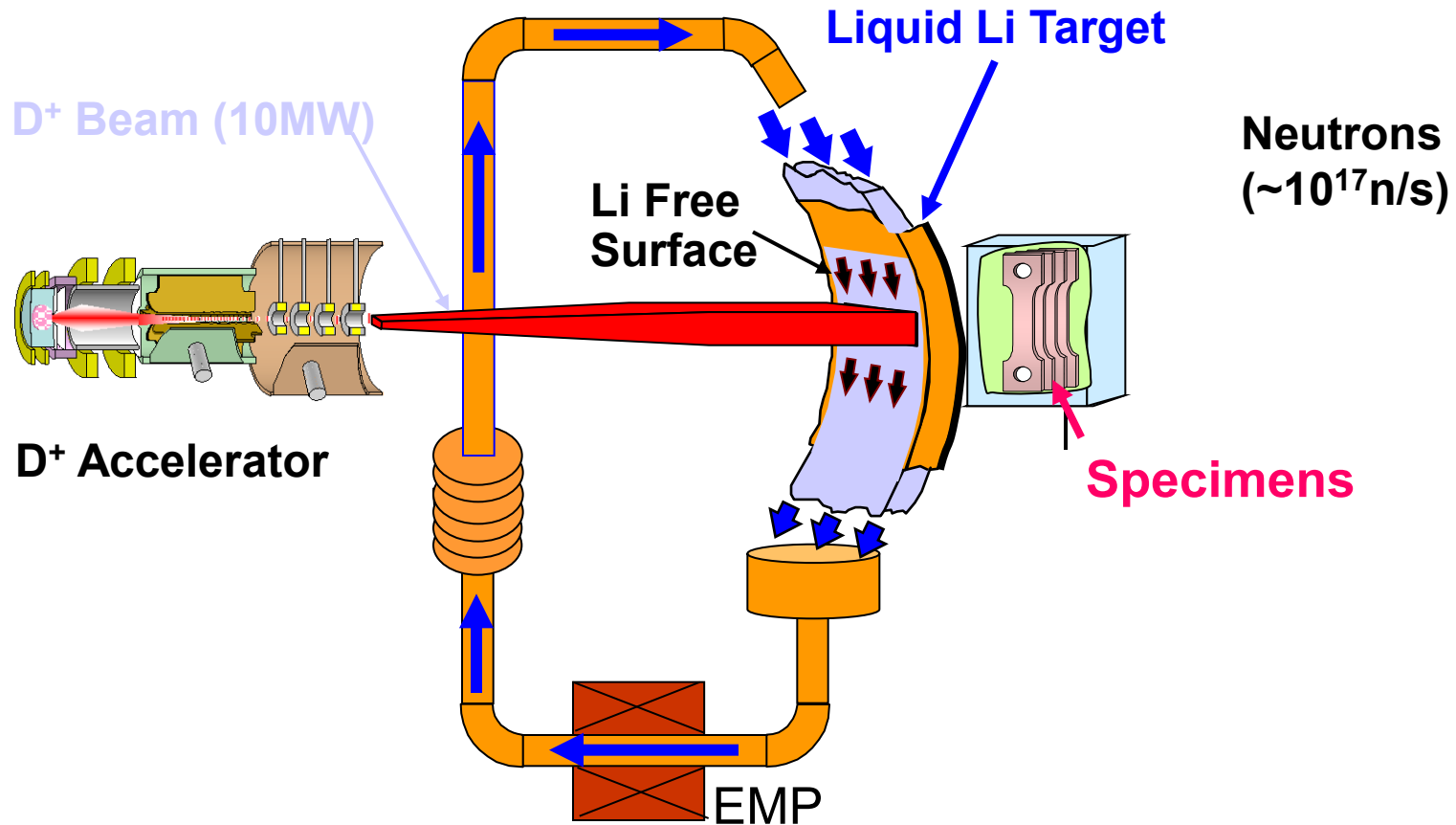
Effects of 14 MeV Neutrons on materials

- The 14 MeV neutrons will produce **transmutation, nuclear reactions and atomic displacement cascades** inside the materials.



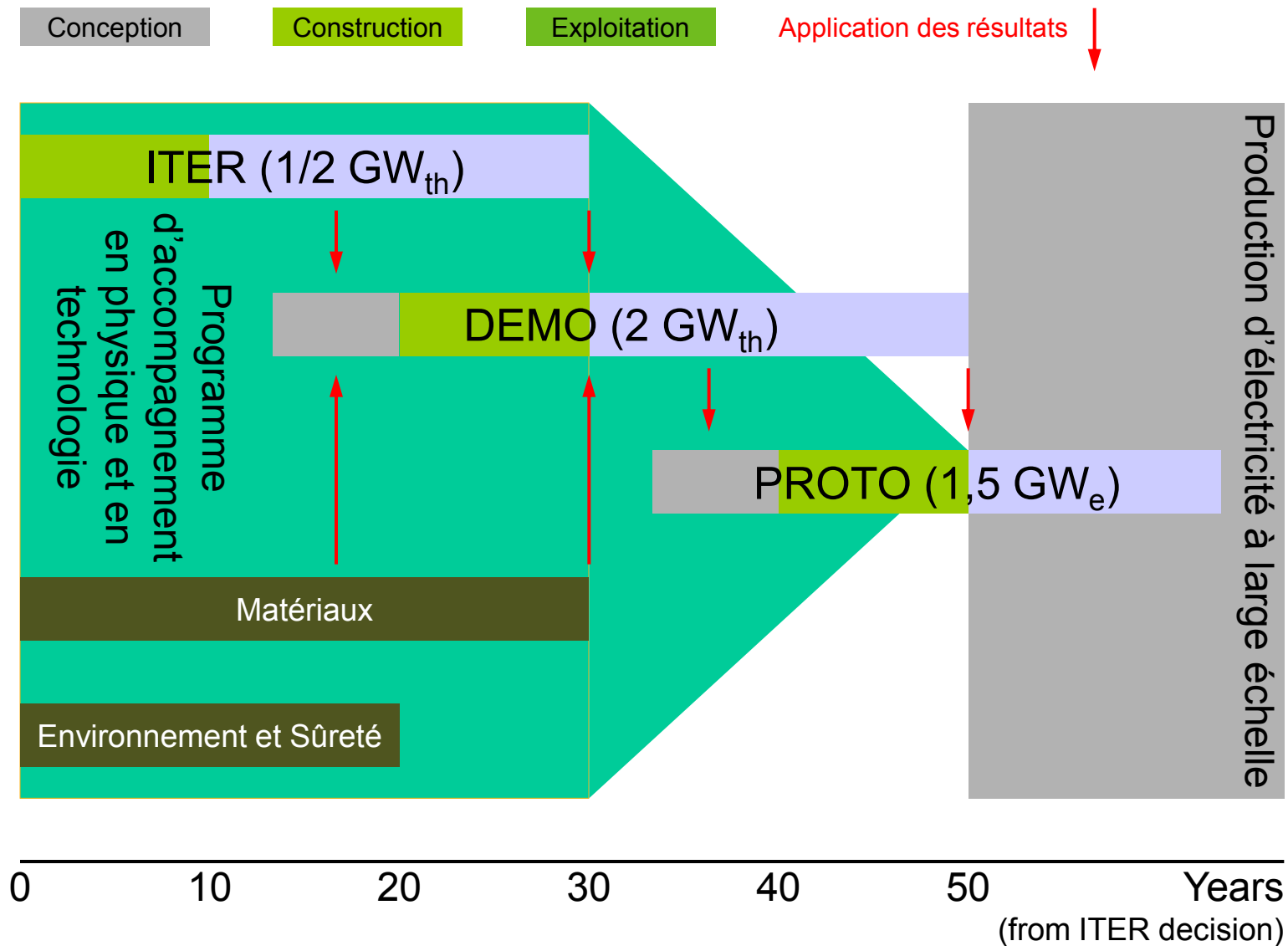
Irradiation facility: IFMIF

Schematic View



EVDA phase in progress in Aomori
Within EU/Japan broader approach

Perspectives for fusion energy



A commercial fusion reactor: when ?

History

~ 100 years



1900-1940 : explanation of solar energy origin

1952 : H -bomb

1958 : 1st theory of magnetic confinement, Sakharov & Tamm

1969 : validation of Tokamak configuration, Lev Artsimovitch

1997 : 16 MW of fusion power in JET

.....

Middle of 21st century : prototype of a fusion reactor

A delay of 100 years between the concept and the applications not unusual

Ex : fuel cell

- Principle : William R. Grove (1839)
- 1 kW prototype F.T. Bacon (1953)
- 1^{er} vehicle equipped with fuel cells (1990)

Ex: Solar Cells

- Principle : Antoine Becquerel (1839)
- 1st Si solar cells (satellites) (1958)

ITER: status and challenges

- The ITER project is a huge undertaking!
- ITER is primarily an experiment
but also a major technology test bed
- An essential step towards a DEMO reactor
(or equally a demonstration that one may not work)

21 November 2006, historical date



ITER Objectives 1/3

Performance and Testing Requirements

- Achieve inductive plasma burn with power amplification, Q (ratio of fusion power to auxiliary heating power), of at least 10, under stationary conditions on the timescales of plasma processes;
- Aim at demonstrating steady-state operation with $Q > 5$;
- Do not preclude the possibility of controlled ignition.
- Integrate the technologies essential for a fusion reactor (e.g. superconducting magnets, remote maintenance);
- Test components for a future reactor (e.g. divertor and torus vacuum pumps);
- Test tritium breeding module concepts for DEMO.

ITER Objectives 2/3

Design Requirements

- Engineering choices and design solutions make maximum use of existing R&D ;
- Machine parameters give confidence in achieving the required plasma and engineering performance.
- The design permits advanced modes of plasma operation and a wide operating range.
- Inductive flat top capability ~ 300-500 s
- Operation limited to a few 10s of thousands of pulses
- Able to support equilibria with high bootstrap current fraction and plasma heating dominated by alpha particles.
- Average neutron flux $> 0.5 \text{ MW/m}^2$
- Average fluence $> 0.3 \text{ MWa/m}^2$
- Later installation of tritium breeding blanket should not be precluded.

ITER Objectives 3/3

Operation Requirements

- Burning plasma experiments should address confinement, stability, exhaust of helium ash, and impurity control.
- Steady state experiments should address issues of non-inductive current drive and other means for profile and burn control and for achieving improved modes of confinement and stability.
- Operating modes should have sufficient reliability for nuclear testing.
- The device is anticipated to operate for ~ 20 years, using externally supplied tritium.

ITER site: Cadarache (Provence)

ITER: 2000 pers (construction)
1000 pers (exploitation)

CEA Centre : 4500 pers



2010

Vinon-sur-Verdon

ITER
autonomous site

CEA boundary



Tore Supra

CEA

400 kV line



ITER site: Cadarache (Provence) 2012



Site construction complete (2019)

39 buildings and technical areas, 180 hectares

TOKAMAK BUILDING

POWER SUPPLIES

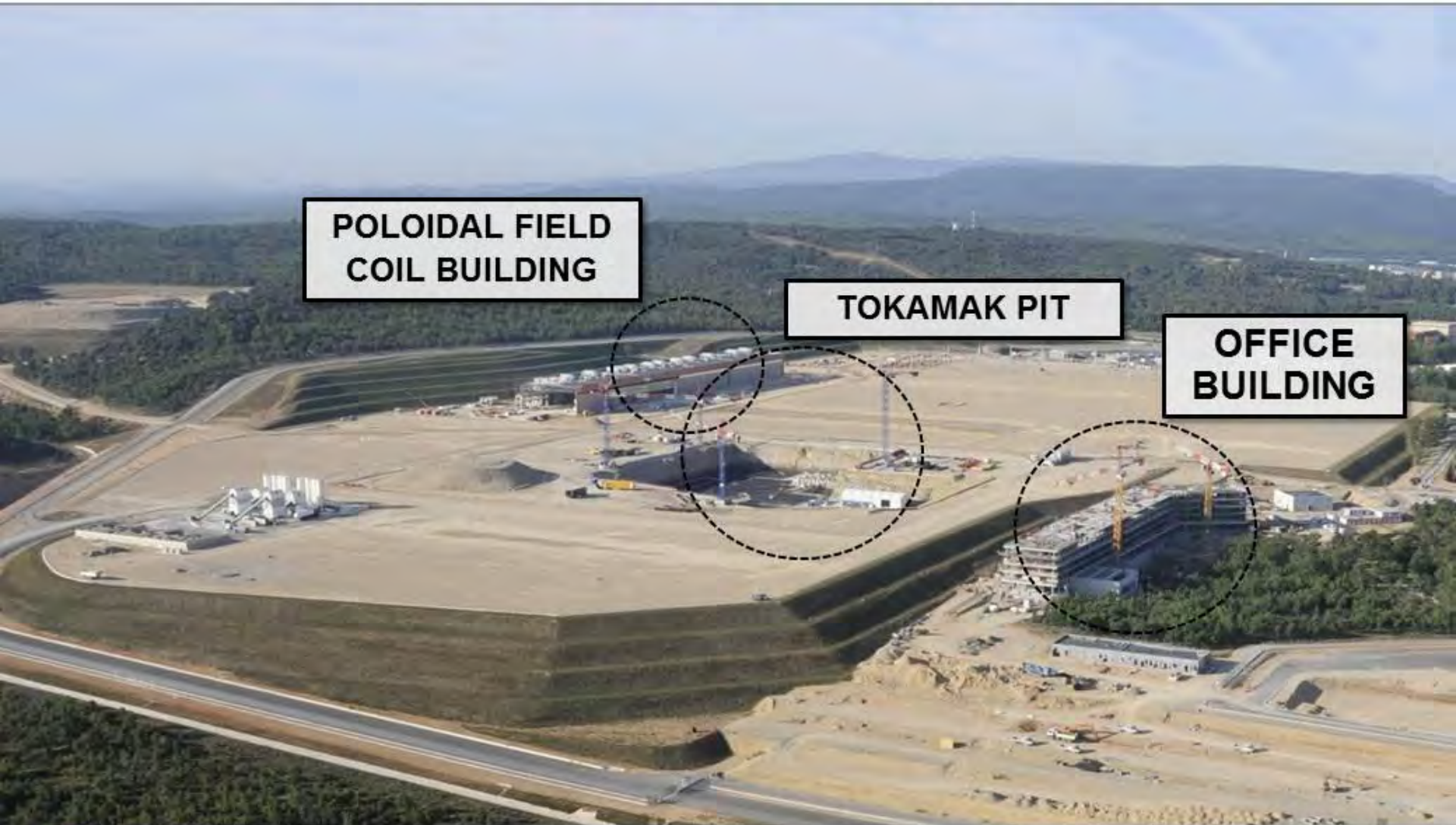
OFFICE BUILDING

Site platform is ready (2009), after 4 years of work

40 ha platform, 2.5 million m³ of earth moved, good bedrock (100 t m⁻²)



Platform status - Sept 2011



**POLOIDAL FIELD
COIL BUILDING**

TOKAMAK PIT

**OFFICE
BUILDING**

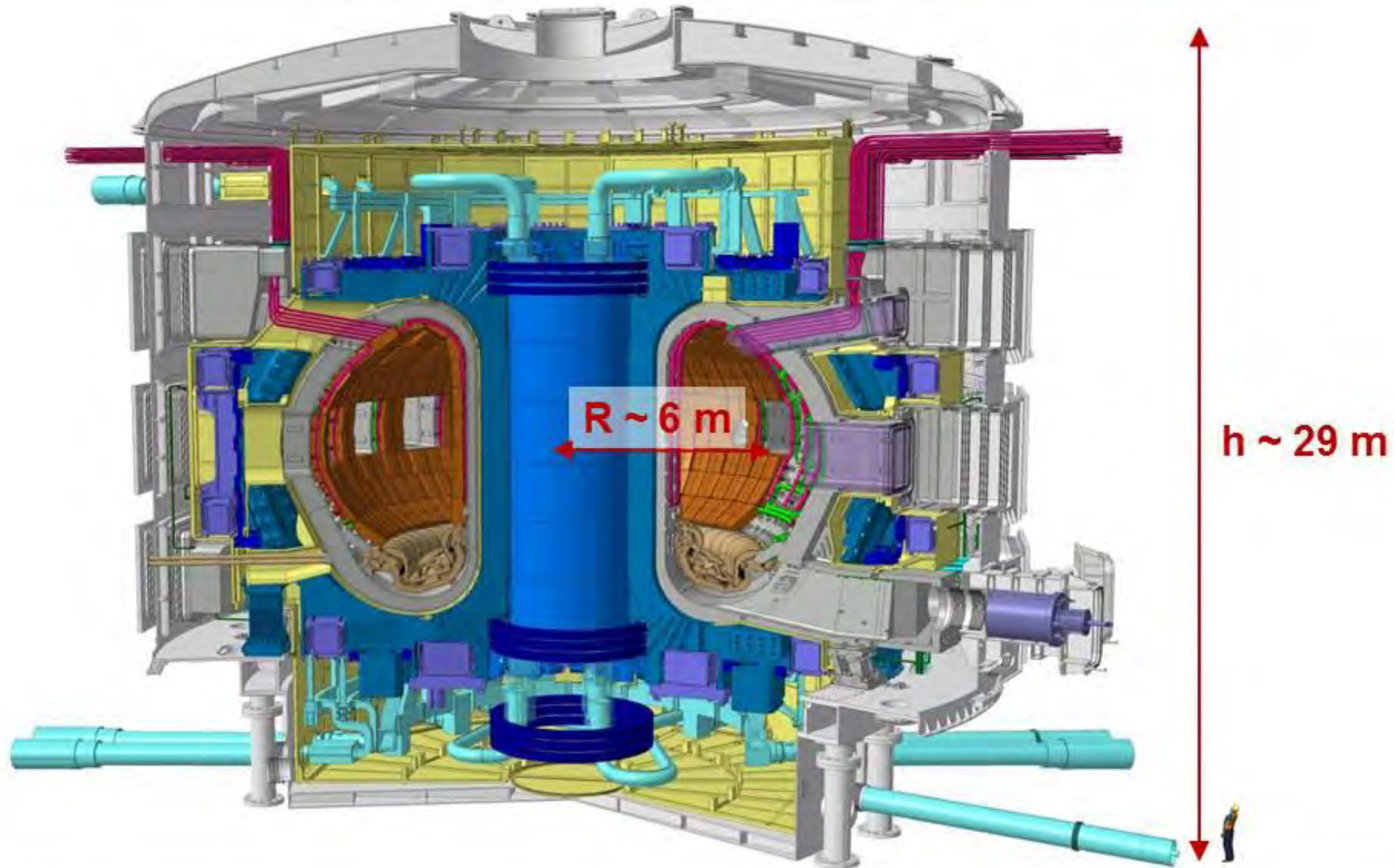
Status of the tokamak complex construction

Tokamak sits on an array of seismic plinths



July 2012

The ITER device



Design goals

1 Physics

- Produce a significant fusion power amplification factor ($Q \geq 10$) in long-pulse operation
- Aim to achieve steady-state operation of a tokamak ($Q = 5$) and retain the possibility of exploring 'controlled ignition' ($Q \geq 30$)

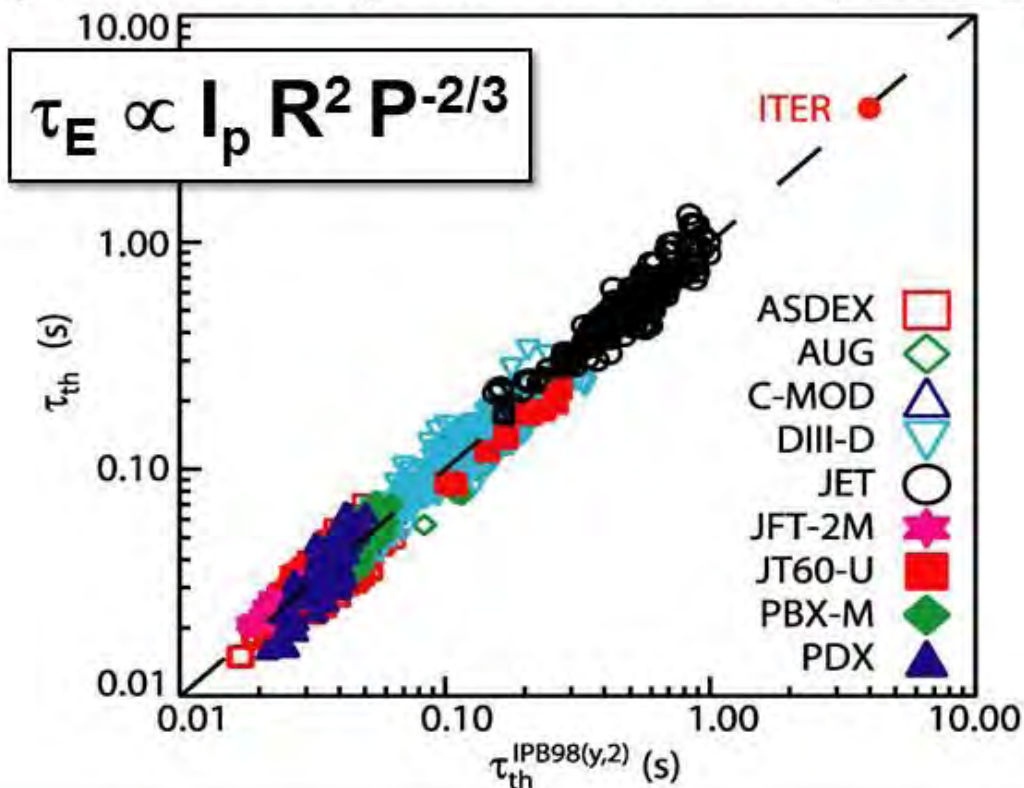
2 Technology

- Demonstrate integrated operation of technologies for a fusion power plant
- Test components required for a fusion power plant
- Test concepts for a tritium breeding module

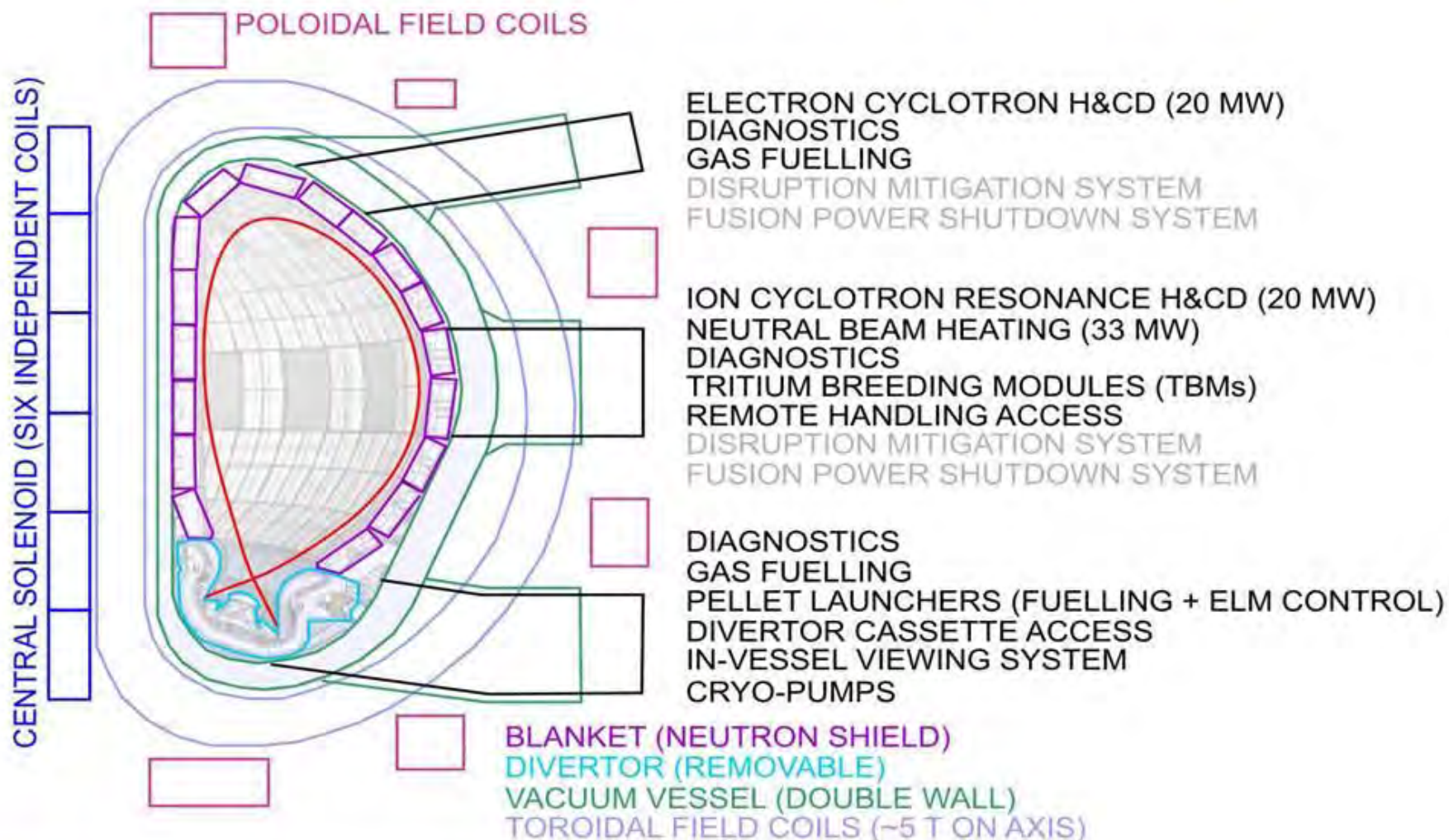
ITER reference scenario for Q =10

- Type I ELMing H-mode: robust mode of operation in today's tokamaks
- L-mode confinement is $\sim 2\times$ less than H-mode (Type-I), generally speaking \rightarrow in the current ITER design, Q=10 in L-mode is "highly unlikely"

IPB98(y,2) TYPE-I ELMing H-MODE SCALING FROM EXPERIMENT



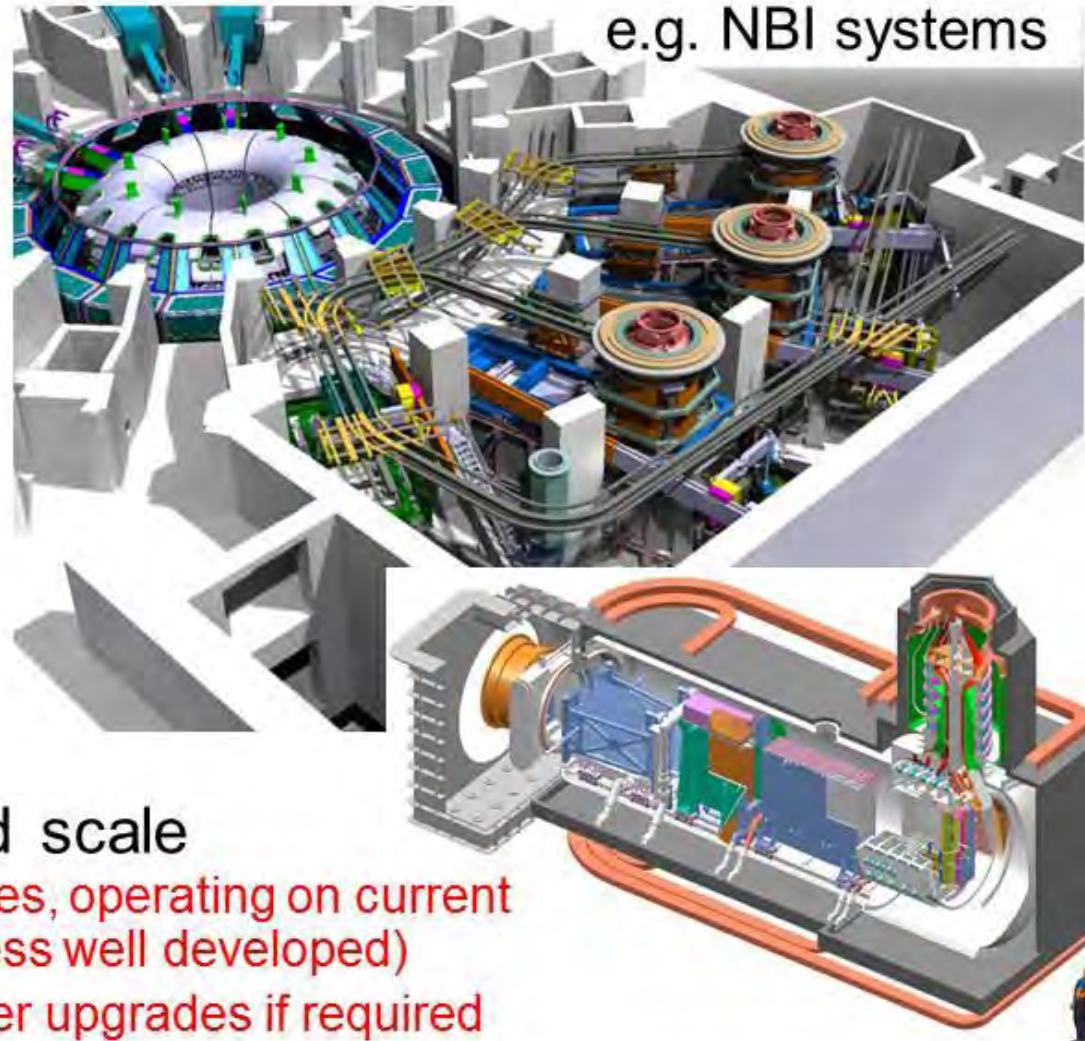
Overview of major systems



Heating the Plasma

System	Power
NBI -ve ion, 1 MeV	33 MW
ECH & CD 170 GHz	20 MW
ICRH & CD 40 – 55 MHz	20 MW

P_{aux} for $Q_{\text{DT}} = 10$ nominal
scenario: 40 – 50 MW



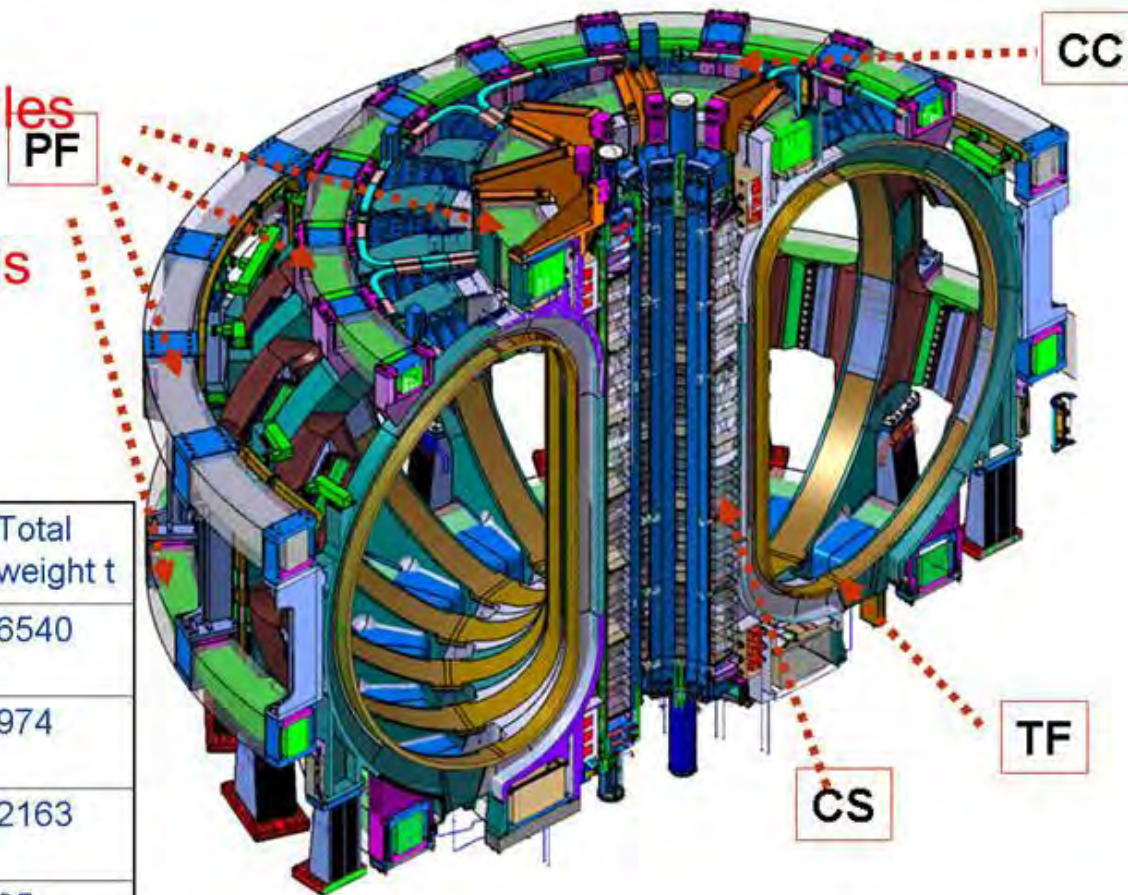
All are on an unprecedented scale

- Upscale from known technologies, operating on current tokamaks (-ve ion NBI source less well developed)
- Systems have flexibility for power upgrades if required

ITER - Magnet Systems

48 superconducting coils

- 18 Toroidal Field coils
- 6 Central Solenoid modules
- 6 Poloidal Field coils
- 9 pairs of Correction Coils



System	Energy GJ	Peak Field	Total MAT	Cond length km	Total weight t
Toroidal Field TF	41	11.8	164	82.2	6540
Central Solenoid	6.4	13.0	147	35.6	974
Poloidal Field PF	4	6.0	58.2	61.4	2163
Correction Coils CC	-	4.2	3.6	8.2	85

Toroidal field conductor procurement

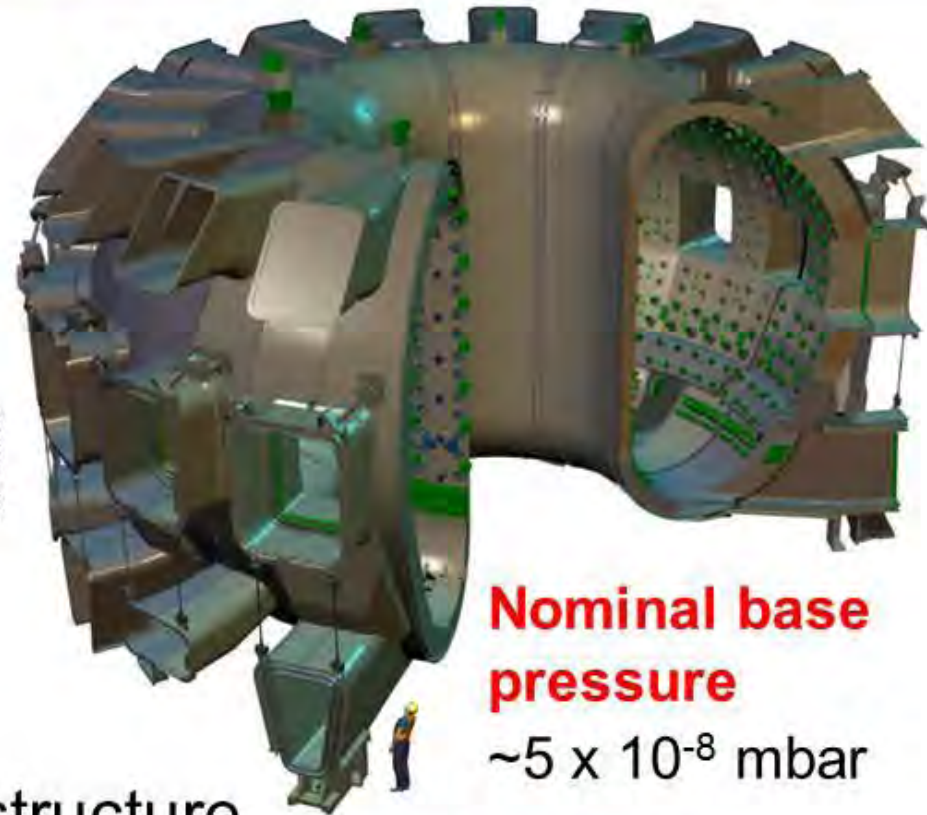
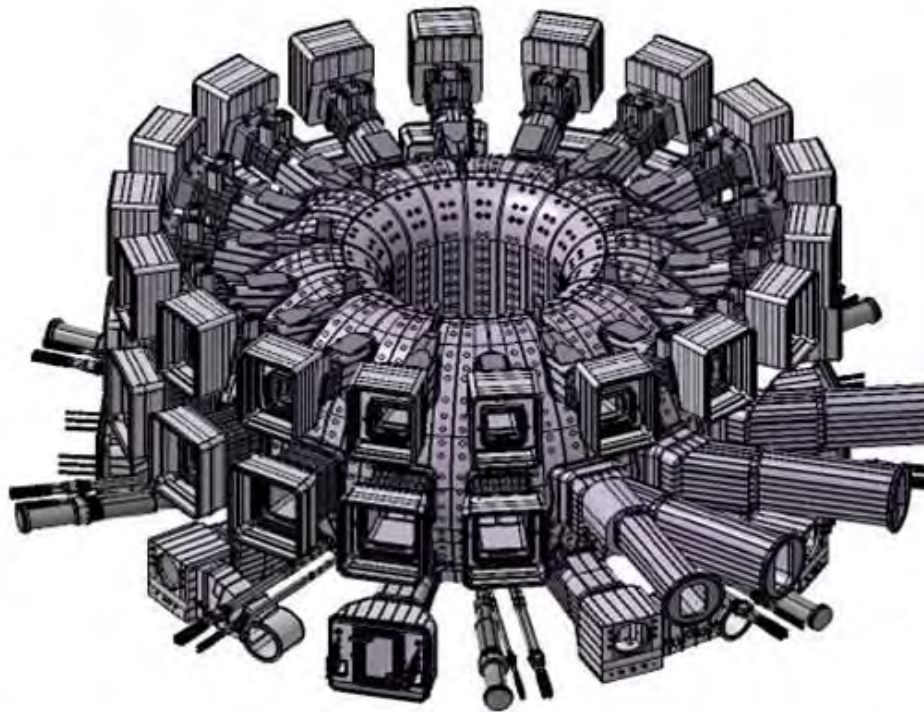


Facts

- ~90 km / 450 tonnes of Nb₃Sn conductor (largest such superconductor procurement in history)
- ~150,000 km of strand
- Operates at ~5 Kelvin
- 11.8 T peak field
- 68 kA peak current in coils

Manufactured by EU, JA, RF, CN, KO & US

Vacuum Vessel

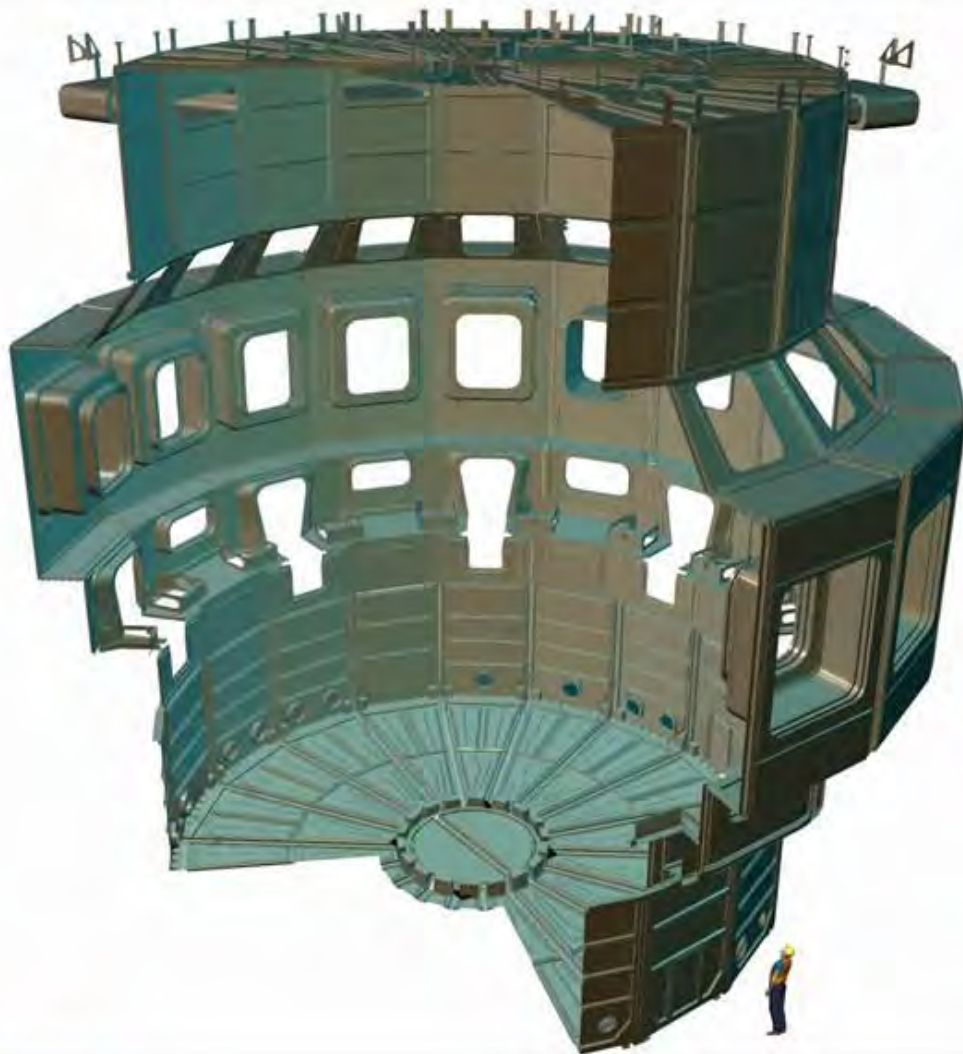


Nominal base pressure
 $\sim 5 \times 10^{-8}$ mbar

Double-walled, stainless steel structure

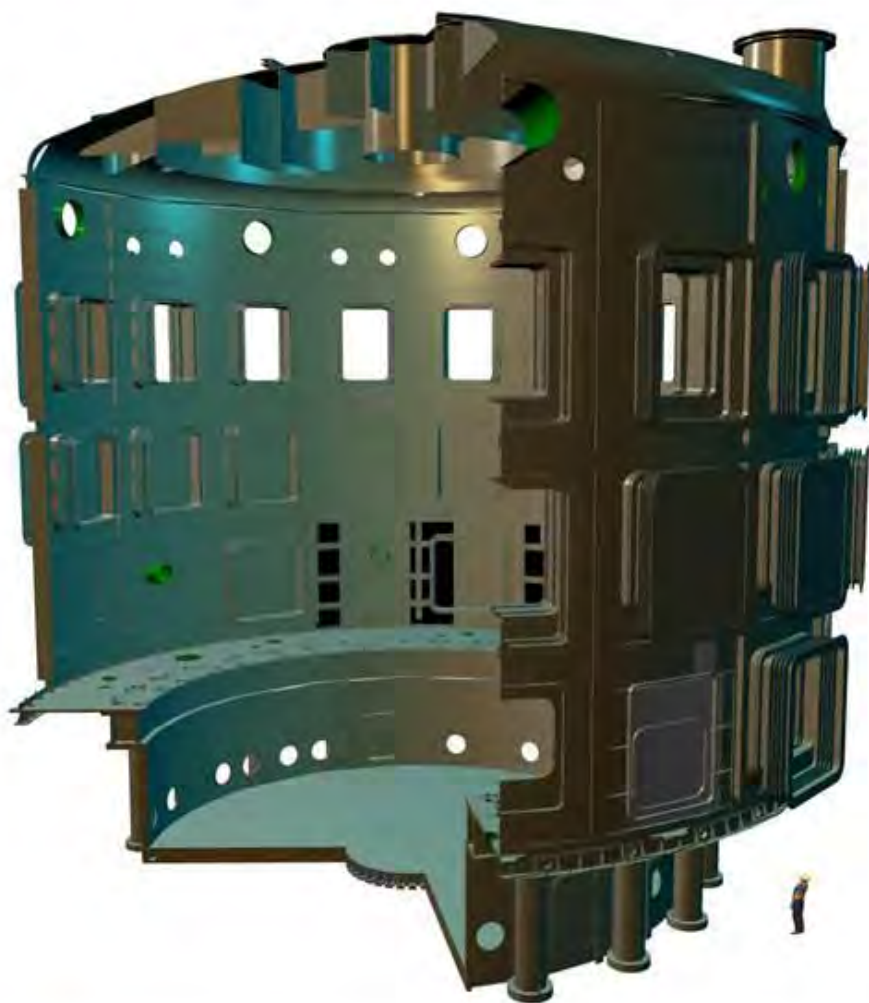
- 19.4m outer diameter, 11.3 m height, SS 316 L(N)-IG, 5300 t
- Primary tritium containment barrier, bakeable to 200°C
- Must withstand enormous vertical forces during disruptions

Main inner heat shield



- Provides barrier for thermal loads from warm components to the superconducting coils (4.5K)
- Operates at 80 K (gaseous He in cooling pipes)
- Stainless steel panels are silver coated to reduce emissivity
- Mass: ~1000 t
- A smaller shield isolates the TF coils from the vacuum vessel

ITER Cryostat: vacuum insulation for SC coils



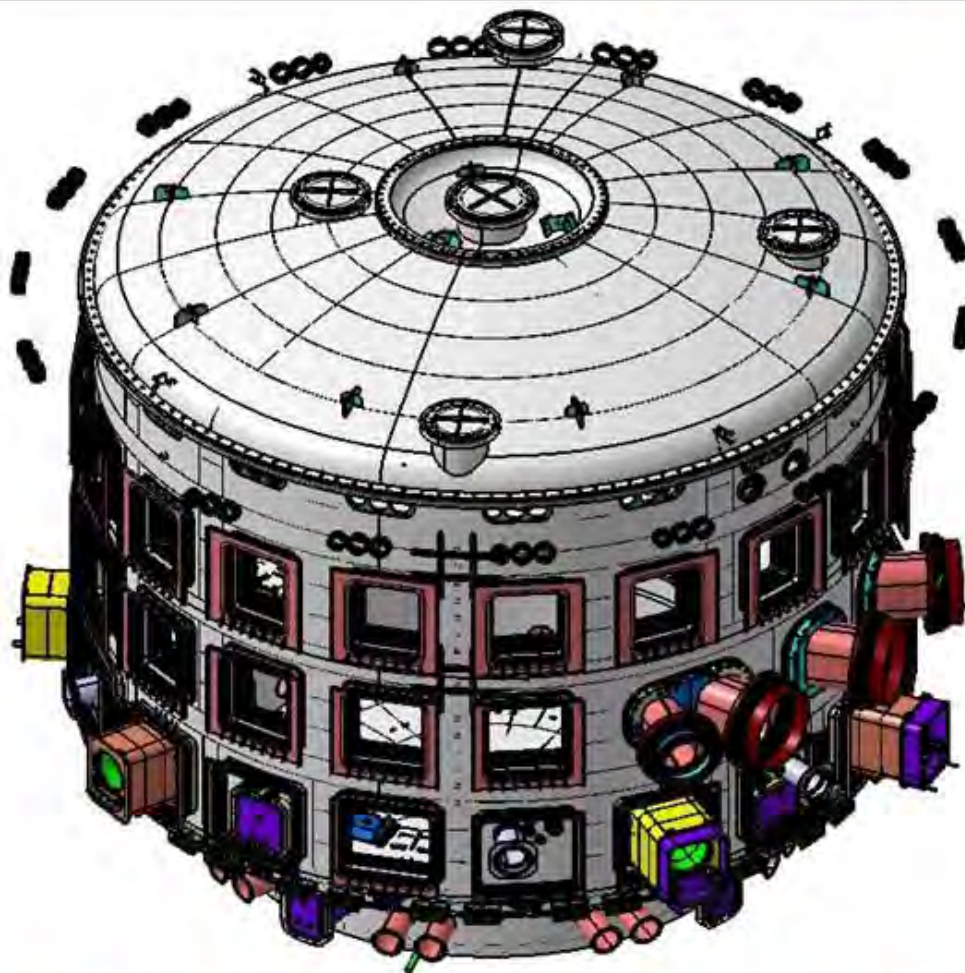
Outer thermal shield

- Diameter: 29.4 m
- Height: ~29 m
- Mass: ~3500 t
- Base pressure $<10^{-4}$ mbar

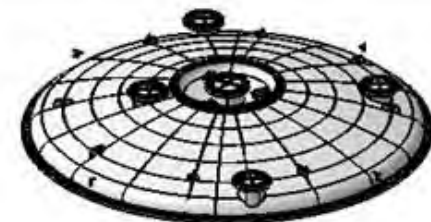
IN-DA will manufacture

- Contract signed with L&T Ltd on 17 August 2012
- Will be dispatched in 54 modules to ITER
- Largest high vacuum pressure chamber ever built

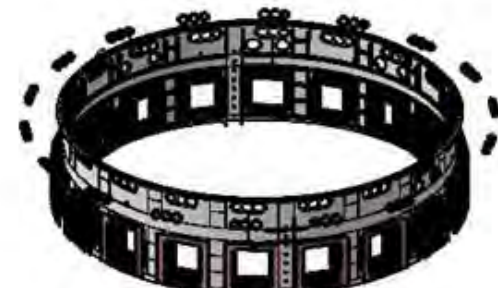
ITER Cryostat



Top lid



Upper cylinder



Lower cylinder



Base section



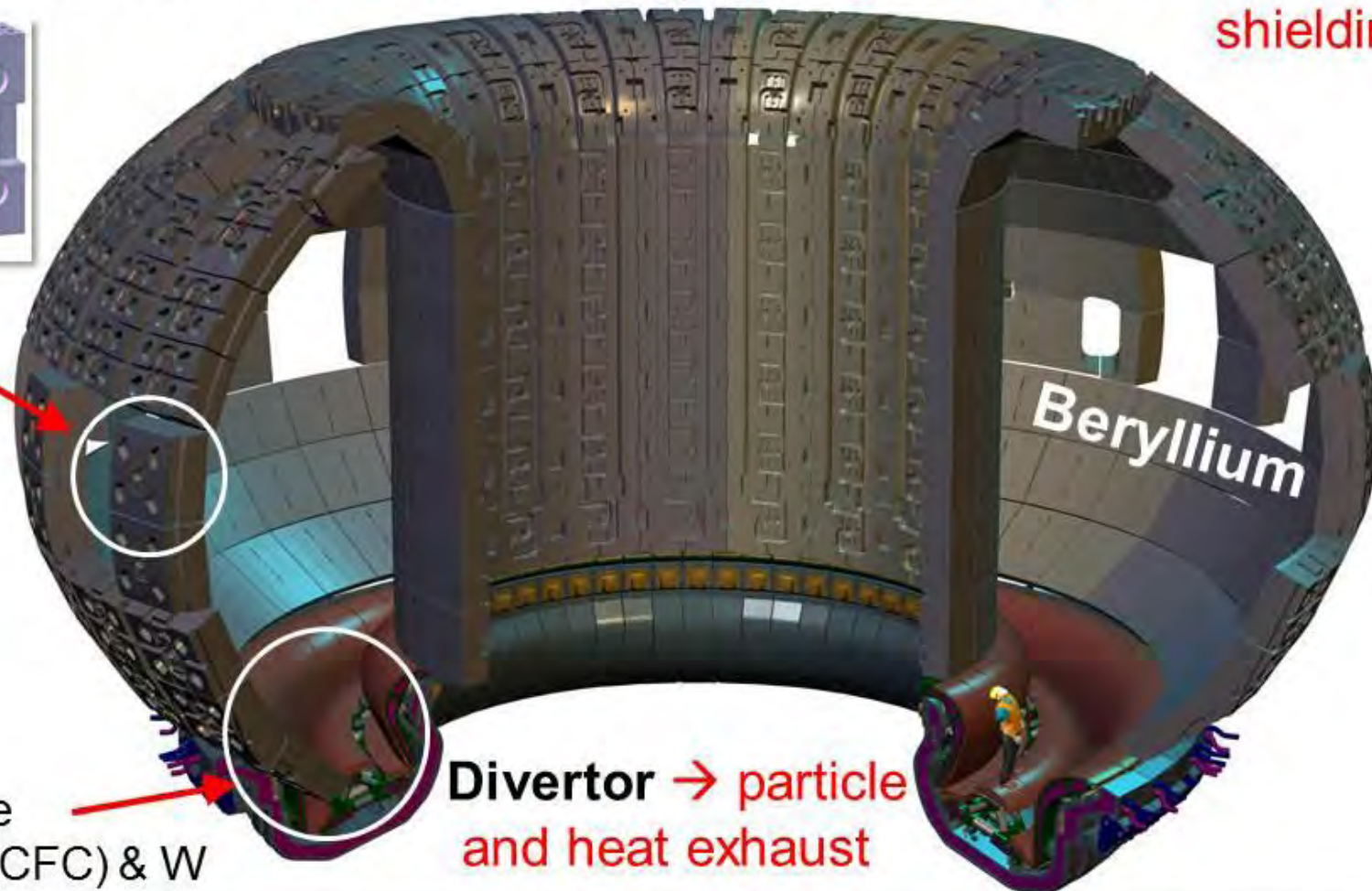
Transfers loads to tokamak floor

Principal plasma-facing components (PFC)

First wall/blanket → heat exhaust, impurity management, nuclear shielding



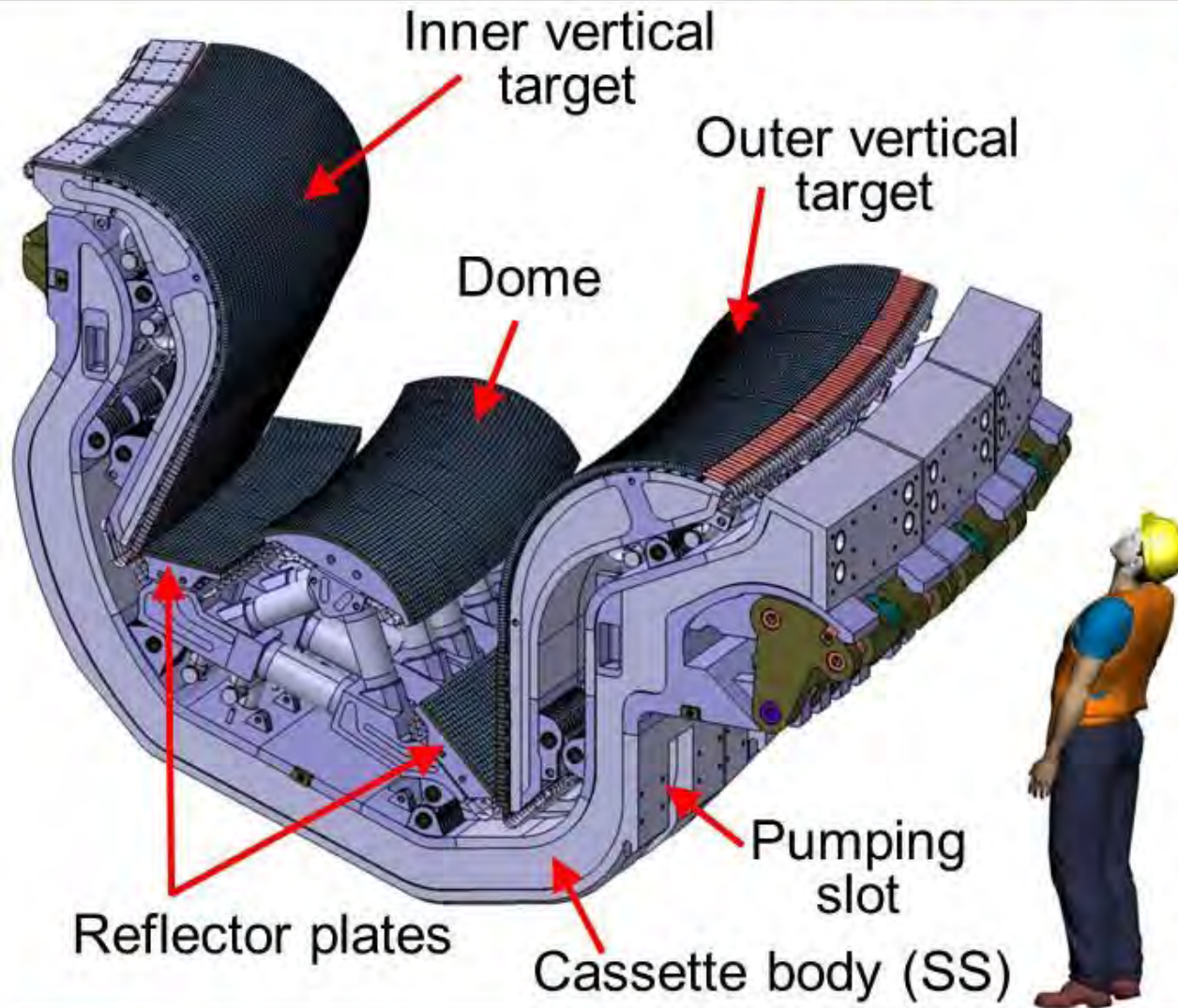
SS shield block
~3.5 t
(1800 t in total)



Carbon fibre composite (CFC) & W

Divertor → particle and heat exhaust

Divertor



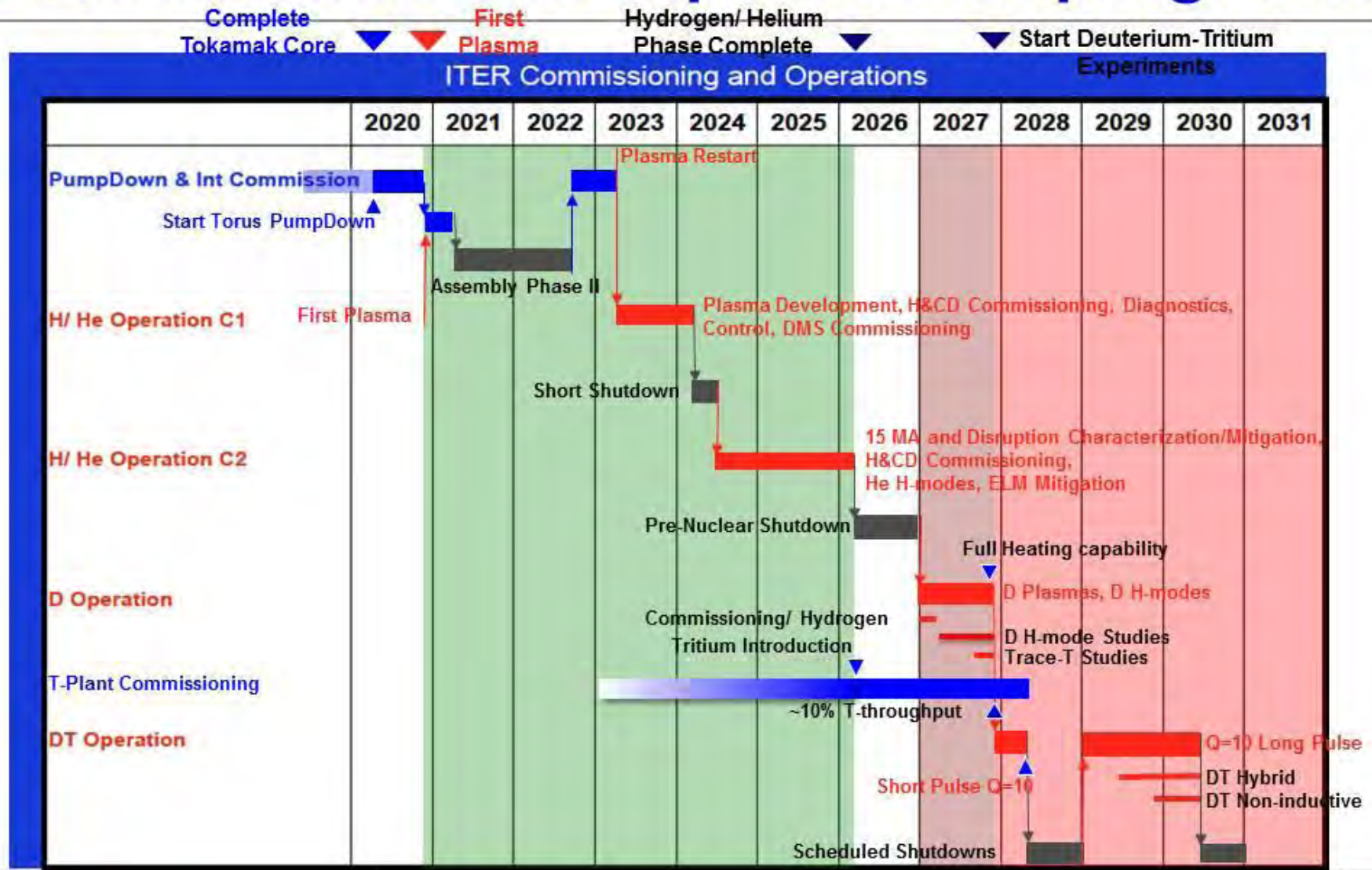
54 divertor assemblies
(~8.7 tonnes each)

4320 actively cooled
heat flux elements

Bakeable to 350°C

All plasma-facing
components will be
in tungsten for the
nuclear phase and
possibly now right
from the start of
operations

ITER schedule and experimental programme



Some key operational/physics challenges

How is ITER different for physics & tokamak operation?

Burning plasma: self-heated by α -particles

- non-linearity in total heating power due to dependence on plasma profiles
- MHD: sawtooth suppression by α -particles, fast particle modes

Plasma control (position, shape, fuelling, heating, stability, exhaust)

- time constant for position control is $>1s \rightarrow$ very easy to damage plasma-facing components (e.g. on inner wall of vacuum chamber)
- very complex control matrix

Very high stored energy

- disruptions, ELMs, melting of metallic PFCs

High plasma current (15 MA for Baseline $Q = 10$ scenario)

- runaway electron damage of PFCs, huge disruption forces

High ion fluence (integrated plasma flux) to PFCs

- erosion of PFCs and migration of wall material, dust formation

Stored energy: disruptions and heat loads to the wall

Disruption → total loss of stored energy in < 100 ms

EXPECTED DISRUPTION HEAT LOADS

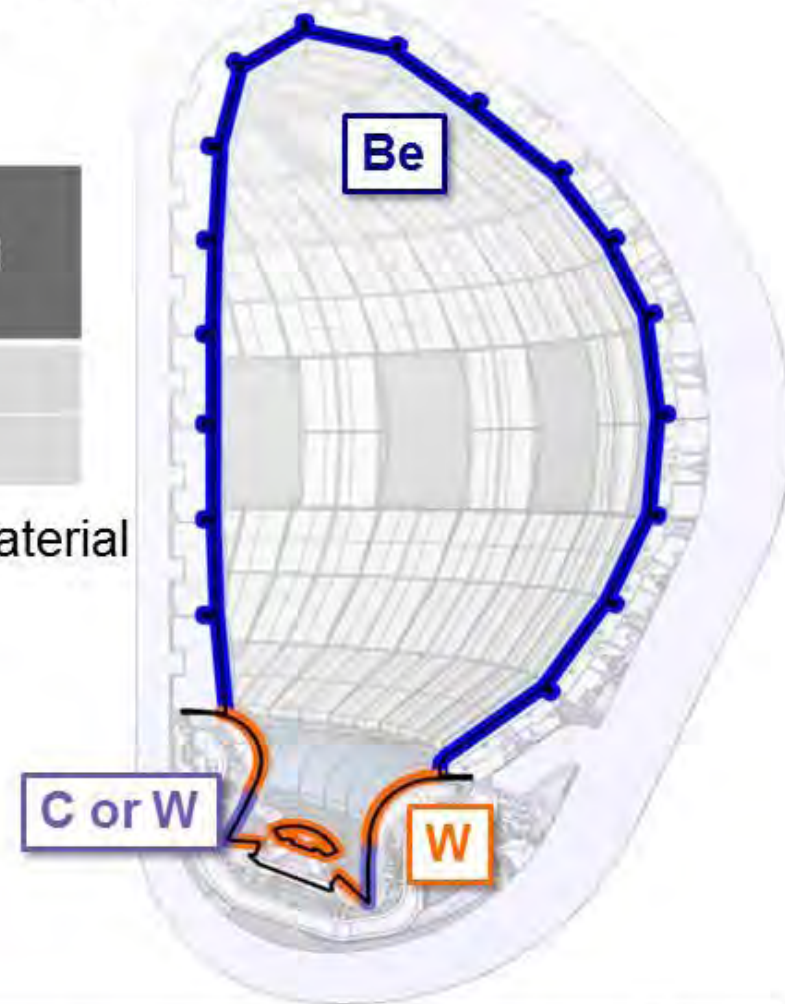
Material	Melt Parameter (MJ m ⁻² s ^{-1/2})	Worst Case Disruption Load (MJ m ⁻² s ^{-1/2})
W (divertor)	50	388
Be	28	570

NB: These numbers don't tell you the amount of material melted, just that some melting will occur

- (and perhaps some protection from “vapour shielding”)

Disruption mitigation is required (and also careful operation) to minimise PFC melting

- NB: 10-15 MA L-mode @ 40 MW also a risk, not just Q=10



Stored energy: disruption mitigation

“Massive gas injection” (MGI) → leading candidate for ITER

- fast valves to introduce strongly radiating gas (Ar, Ne) → spread energy over a large area

JET MGI, Ne injection, 2 MA, 3 T [A. Alonso, M. Lehnen, EFDA-JET]



Major ITER system → not yet fully specified

But it will be soon!

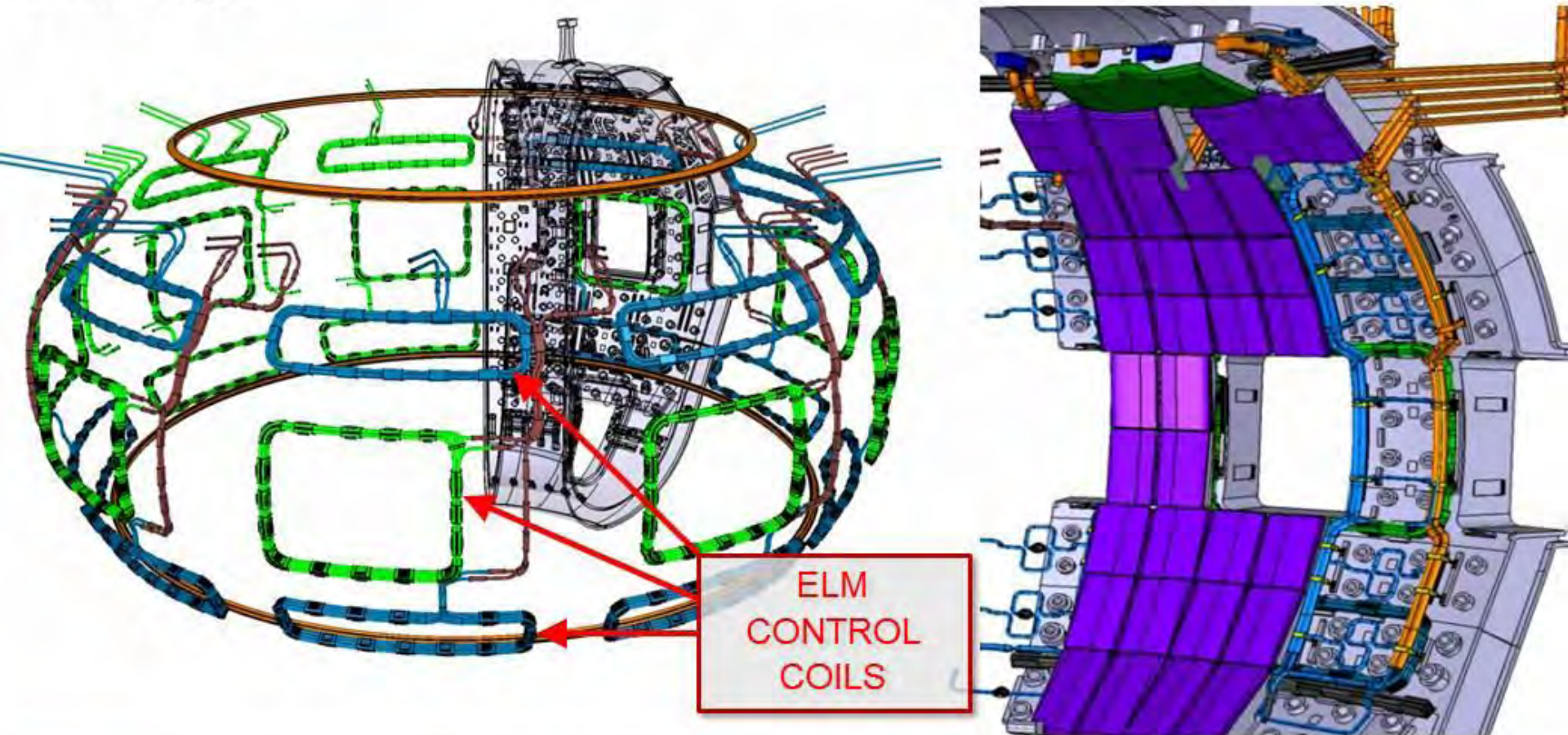
- intense area of study: experiment and modeling

Triggering also a challenge, i.e. accurately predicting a disruption at some $-\Delta t$, not too many false positives

- algorithms under development on existing machines
- want very fast gas valves that are close to the plasma (can tolerate neutrons)

Stored energy: ELM control coils

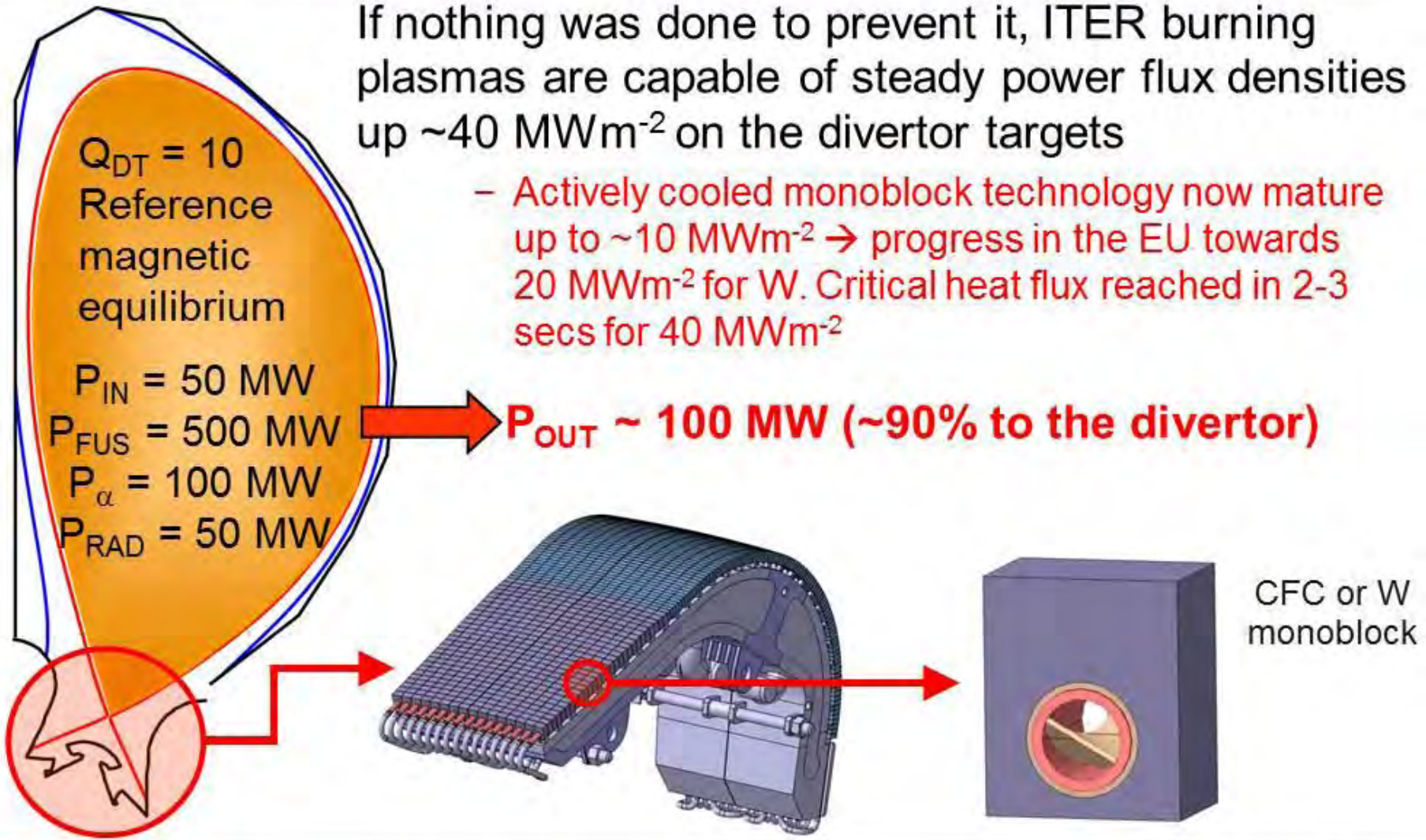
Design activity underway with good progress → integration challenge



Power exhaust: stationary energy flux

If nothing was done to prevent it, ITER burning plasmas are capable of steady power flux densities up to $\sim 40 \text{ MWm}^{-2}$ on the divertor targets

- Actively cooled monoblock technology now mature up to $\sim 10 \text{ MWm}^{-2}$ \rightarrow progress in the EU towards 20 MWm^{-2} for W. Critical heat flux reached in 2-3 secs for 40 MWm^{-2}



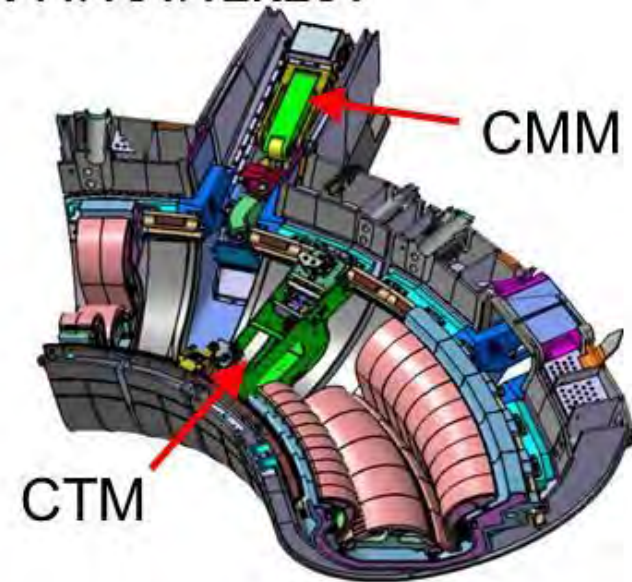
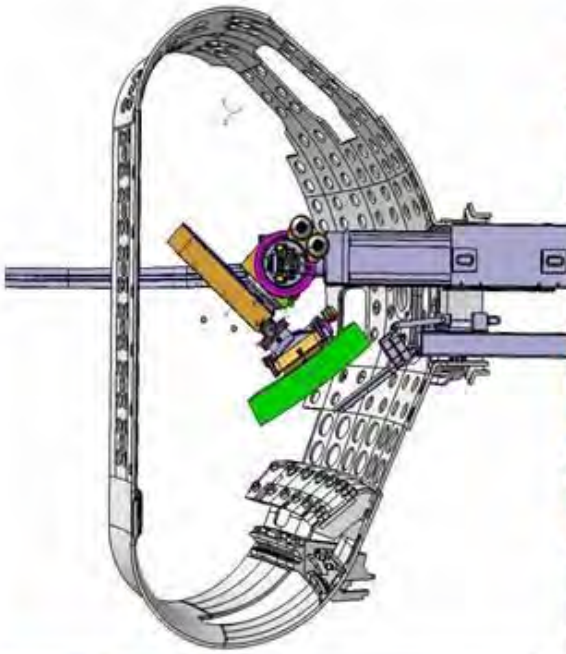
Remote handling

A major part of the ITER effort → extremely challenging to repair and replace complex and heavy components in a nuclear environment

- Dedicated, state-of-the-art systems for both Blanket and Divertor
- Divertor replacement 3-4 x in the machine lifetime (~6 months to exchange)
- First wall panels at least once

Divertor RH procured by EU → major role played by Finland VTT/TUT/TEKES!

On-rail module transporter
- procured by JA



How is ITER different for physics & tokamak operation?

Routine operation at $Q = 10$ (hopefully!) → means operating near design limits

- ITER is the first tokamak that can regularly exceed the technological limits of actively cooled PFCs
- Extremely robust machine protection system mandatory

Nuclear operation (tritium and neutrons)

- retention of tritium on PFCs
- tritium reprocessing
- tritium breeding test modules (TBMs)
- remote handling is required for 100% of in-vessel work during the nuclear phase
- dust inventory
- (diagnostic design)
- (TF coil heating)
- LICENSING

Nuclear operation: tritium reprocessing – the T-Plant

Of the ~ max 100 g of tritium fuel per Q=10 pulse, only ~0.3% will be burned by fusion reactions → T reprocessing is required

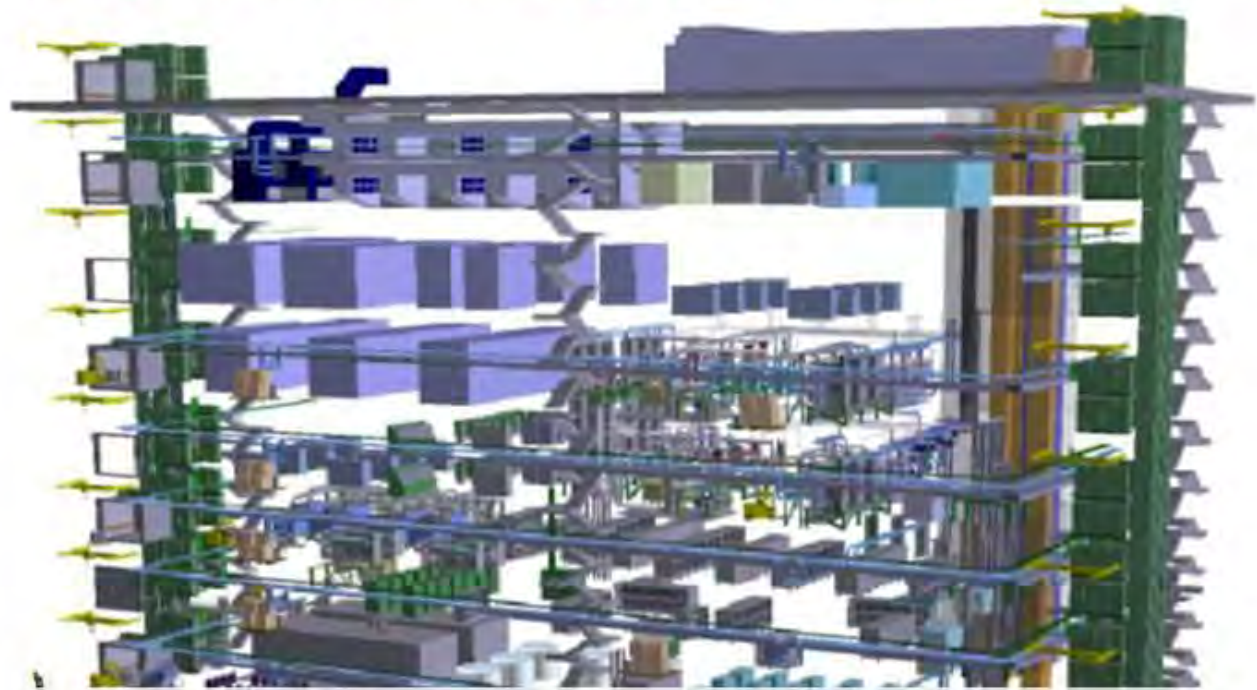
– using existing technologies but on a much larger scale (~factor 10)

7 floors
(2 below ground level)

L = 80 m

W = 25 m

H = 35 m

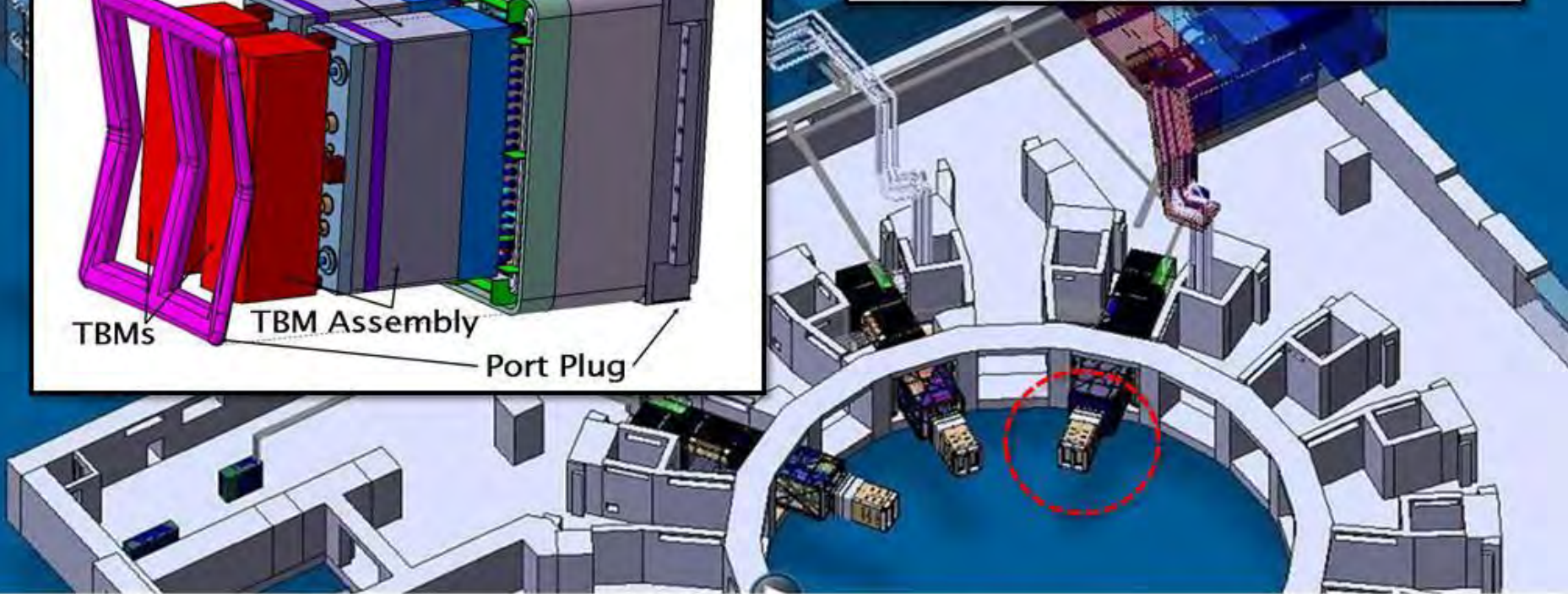
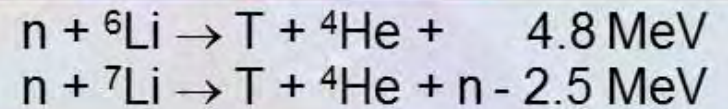
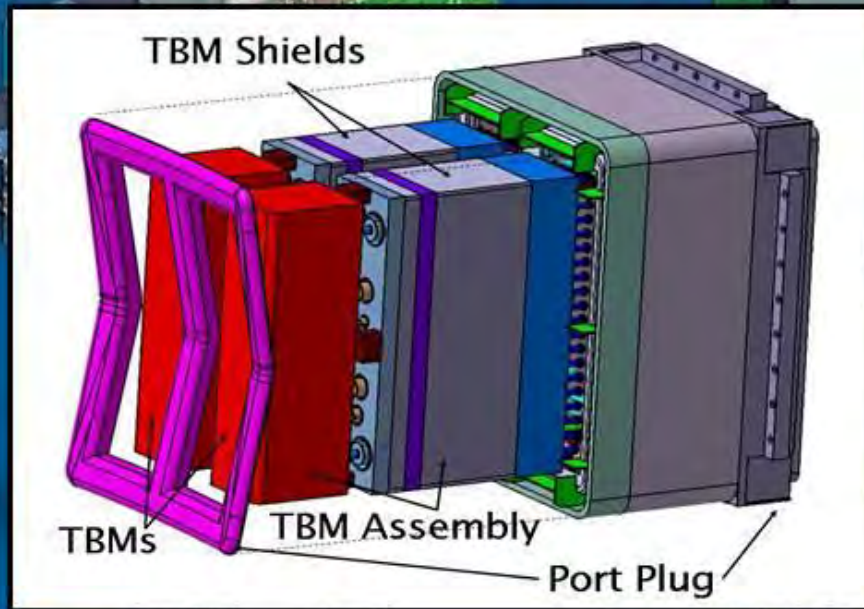


A maximum of 4 kg of tritium can be held on the ITER site → only about 20 kg of tritium anywhere on Earth at any one time

Nuclear operation: tritium breeding modules (TBMs)

Tritium fuel cycle is a major challenge for all DT fusion devices → ITER will test concepts

– 6 modules with different designs, all ITER parties involved



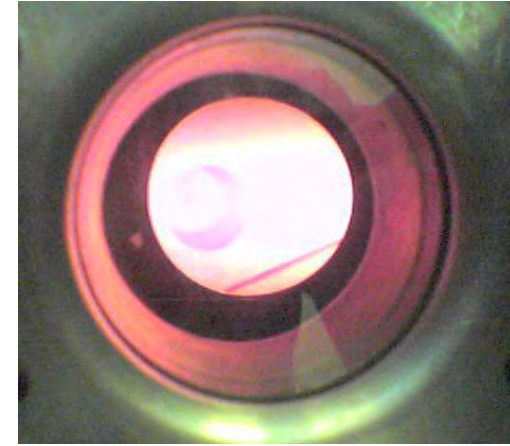
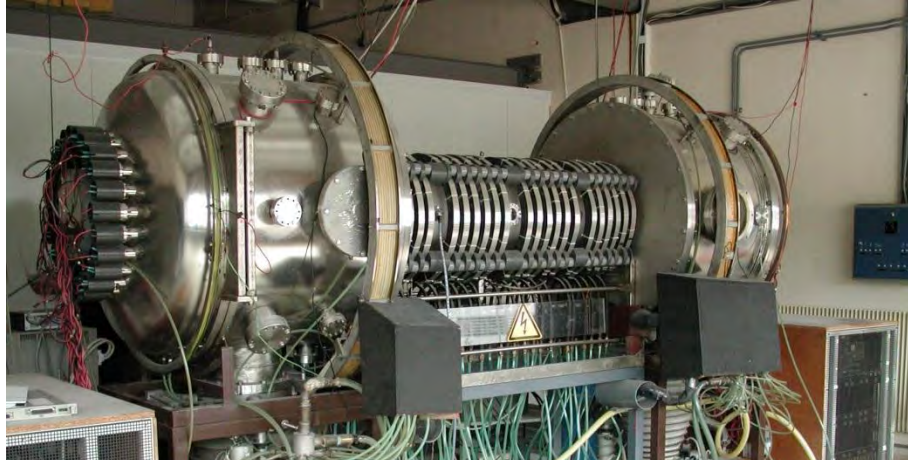
Development and validation of diagnostic tools for turbulent fluctuations and transport (probes, fast imaging,...)

- The Mirabelle device
- Drift waves and flutes modes – Dynamical states
- Turbulent transport → Probes
- Fast imaging of turbulent structures

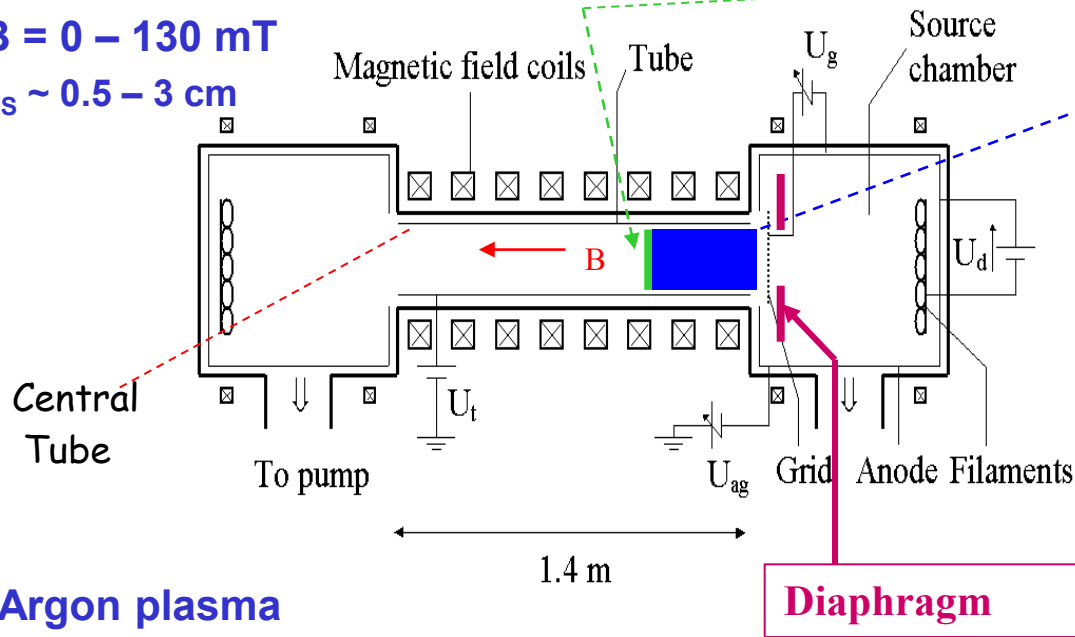
Characterization of turbulence and transport in the edge plasma

- Essential role played by intermittent and large scale structures ("blobs") in the cross-field energy and particle transport to the wall in the far Scrape-Off-Layer (SOL)
- From many experimental studies carried out in several machines (toroidal : Tore-Supra, W-7AS, Alcator-C, NSTX, D-III-D, ... and linear machines as well →
 - radially propagating "blobs" are responsible for ~50% of the transport
- Open questions:
 - Origin and formation of these "blobs" (core plasma, relation with ELMs?, near the separatrix, inverse cascade process?), propagation velocity, time and size scales,
 - need for improved or new diagnostics (probes arrays, **fast imaging**, ...), signal processing methods, comparison with numerical simulations,

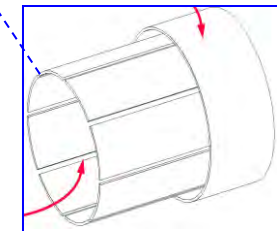
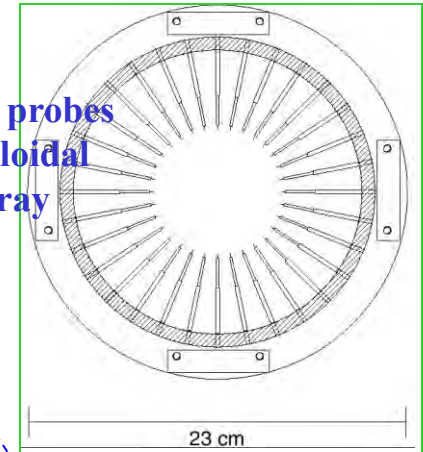
MIRABELLE: a linear, magnetized, low- β plasma device



$B = 0 - 130 \text{ mT}$
 $\rho_s \sim 0.5 - 3 \text{ cm}$



32 probes
 poloidal
 array



8 plates
 Exciter

Argon plasma

$P \sim 5 \cdot 10^{-5}$ à $5 \cdot 10^{-4}$ torrs; $T_e \sim 1 - 3 \text{ eV}$, $T_i \sim 0.02 \text{ eV}$; $n_e \sim 10^{15} - 10^{16} \text{ m}^{-3}$

Low frequency instabilities: Drift Waves

Magnetic Confinement → transverse gradients

→ 2 mechanisms: drift waves and rotation induced instabilities (Kelvin-Helmholtz, Rayleigh-Taylor)

1- Drift waves:

driven by a radial density gradient
 collective oscillations of electron and ion populations
 propagation: *mainly* azimuthal

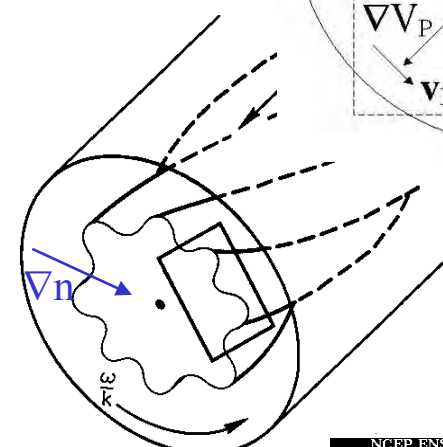
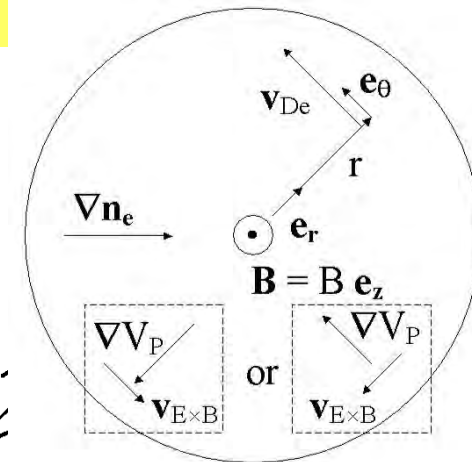
$$\omega = \frac{\omega^*}{1 + \rho_s^2 k_\theta^2} \text{ with } \omega^* = k_\theta V_{De}, k_\theta = \frac{m}{r}, \text{ and } \rho_s = c_s / \Omega_i$$

$$\rho_s = 0.5 - 3 \text{ cm}, f = 3 - 20 \text{ kHz}$$

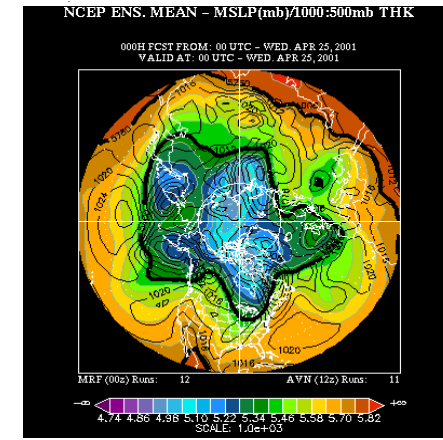
$$v_{dw} = v_{dia} / \sigma \pm E / B$$

close analogy with Rossby waves (F. Lorentz ⇔ F. Coriolis)

[M.V. Nezlin & E.N. Snezhkin, *Rossby vortices, spiral structures, solitons*, Springer-Verlag, 1992 p.43-66.]



$$V_{De} = -KT_e \frac{\left| \frac{\partial n_o}{\partial r} \right|}{qn_o B} e_\theta$$



Bilder: NOAA/ ForecastSystems Laboratory

LF instabilities: rotation induced instabilities

2- the Rayleigh-Taylor instability:

driven by a radial gradient of the plasma potential

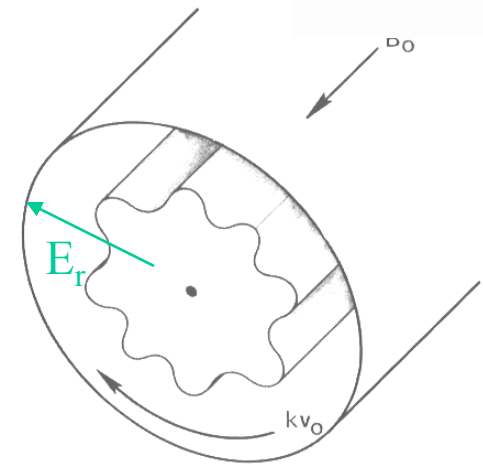
plasma rotation \rightarrow centrifugal force \sim effective gravity

purely azimuthal propagation \rightarrow flute modes

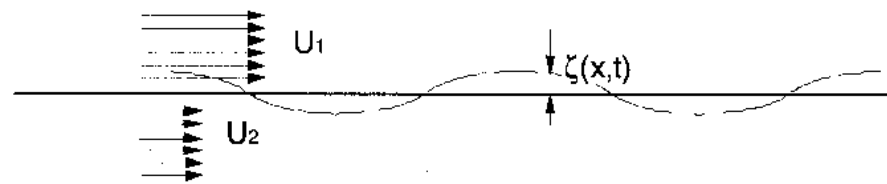
3- the Kelvin-Helmholtz instability:

driven by a poloidal velocity shear

purely azimuthal propagation \rightarrow flute modes

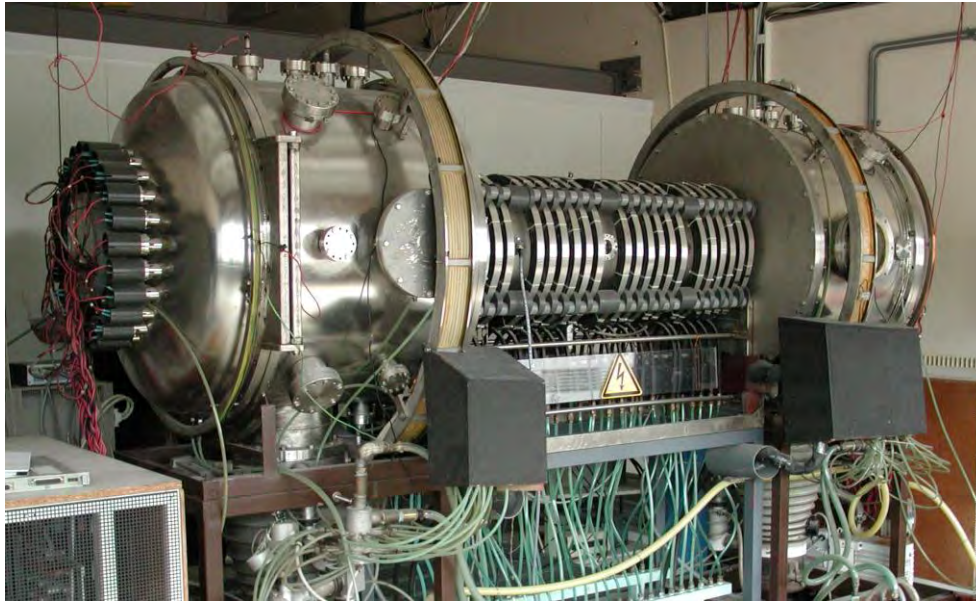


K-H: a typical hydrodynamic instability



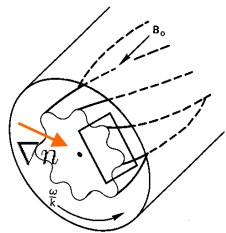
in Plasmas: Horton & Tajima, Phys. Fluids 30 (1987) 3485

Mirabelle device: a linear, magnetized, low- β plasma

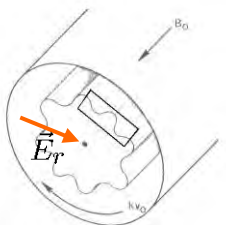


plasma density	$10^{15}-10^{16} \text{ m}^{-3}$
magnetic field	20–120 mT
electron temperature	1–5 eV
ion temperature	$< 0,05 \text{ eV}$
argon pressure	$(1-3) \cdot 10^{-4} \text{ mbar}$
Larmor radius ρ_s	0,5–3 cm
density gradient length	2–5 cm
instability frequency	3–15 kHz
ion cyclotron frequency	8–60 kHz
Collision frequencies ν_{in}, ν_{en}	$\sim 1 \text{ kHz}$

Possible plasma regimes:



Drift waves



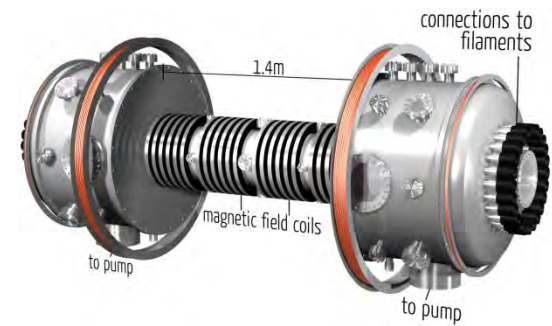
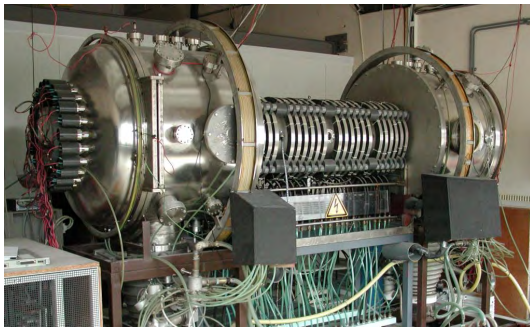
Flute modes

without control

controlled

Periodic
Periodic pulling
Intermittence
Weak turbulence

controlled
forced



Main findings and physics pictures

- 1 Characterising and selecting LF instabilities
- 2 Routes to spatio-temporal chaos and turbulence
- 3 Acting on LF modes
- 4 Cross-field transport
- 5 Characterisation of nonlinear mode couplings

Dynamics of LF Instabilities: Summary

- Characterization of the observed LF instabilities in the the low- β plasma column of the Mirabelle device \Rightarrow
 - without a limiter only drift waves are observed
 - by using a limiter, that creates a strong velocity shear at the edge at low magnetic field strength, a **transition from drift waves to the Kelvin-Helmholtz instability** is observed when B is decreased.
- As for drift waves the transition from regular state to spatio-temporal chaos and turbulence follows the quasi-periodicity (or Ruelle-Takens-Newhouse) route.
- Spatio-temporal open-loop synchronization was studied for each kind of low-frequency instability and turbulence as well.
 - **the efficiency of mode-selective control on the Kelvin-Helmholtz instability and turbulence was demonstrated** as previously for drift wave turbulence.
 - By using the same octupolar arrangement we also drive a regular state to a turbulent one.
 - The radial dependence was also studied

Transport measurements

$\langle \Gamma \rangle = \frac{1}{B} \langle \tilde{n} \cdot \tilde{E} \rangle$ Flux function of time and frequency:

$$\Gamma(f, t) = \frac{2}{B} |W_n(f, t)W_E^*(f, t)| \cos(\varphi[W_n(f, t)W_E^*(f, t)])$$

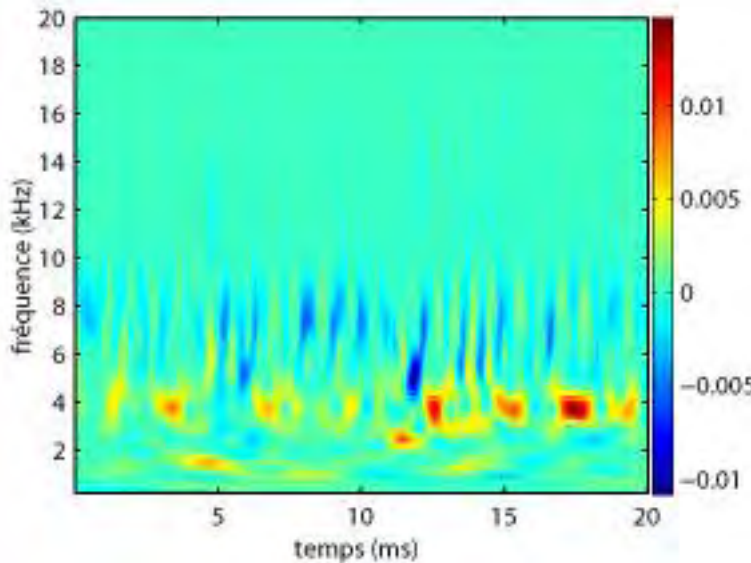
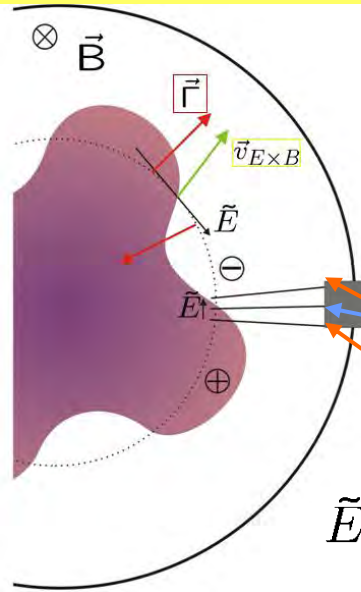
$\tilde{I}_{\text{sat}}(t) \propto \tilde{n}(t)$

cross-spectrum

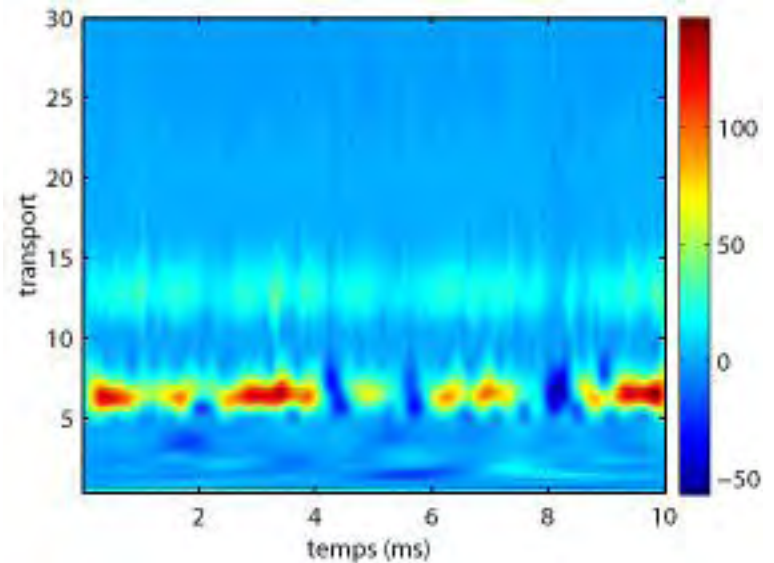
$\cos(\alpha_{nE}(f, t))$

Mean flux: $\langle \Gamma \rangle \propto |\tilde{n}| \cdot |\tilde{E}| \cdot \cos(\alpha_{nE})$

$$\tilde{E}(t) = \frac{V_3(t) - V_1(t)}{d}$$



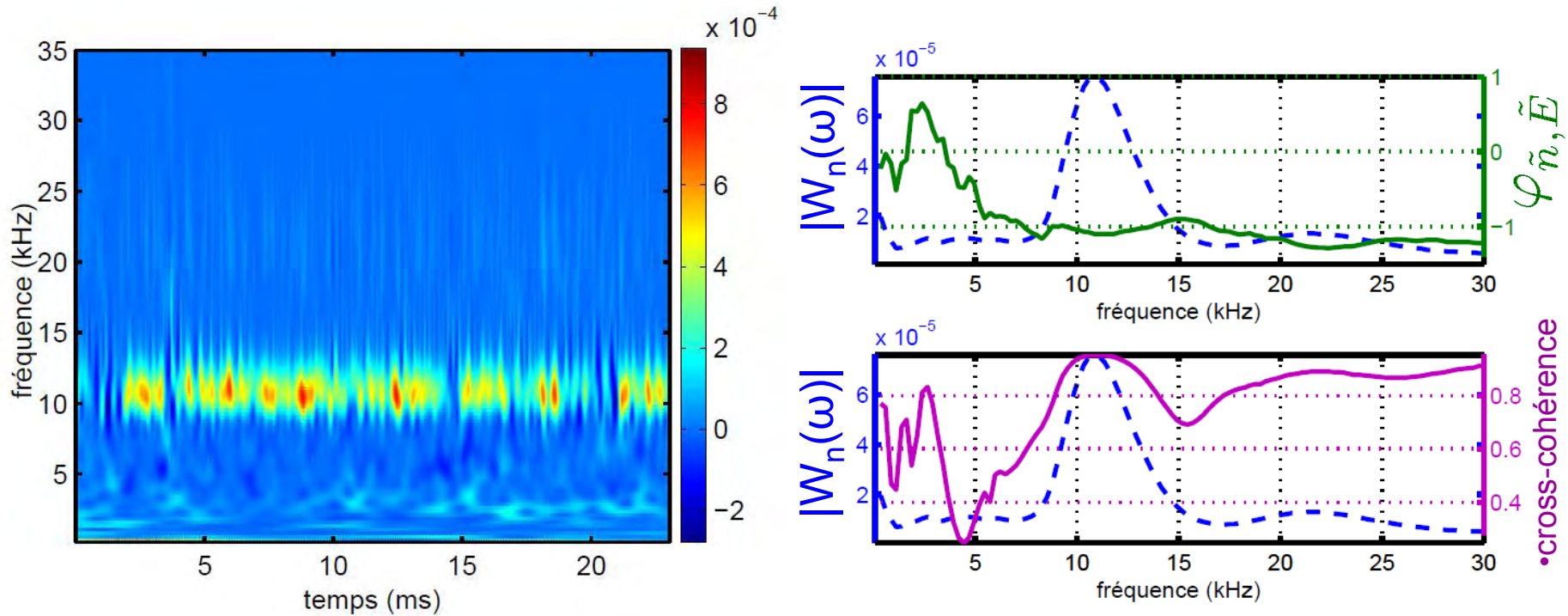
Drift waves (2 modes)



Flute mode

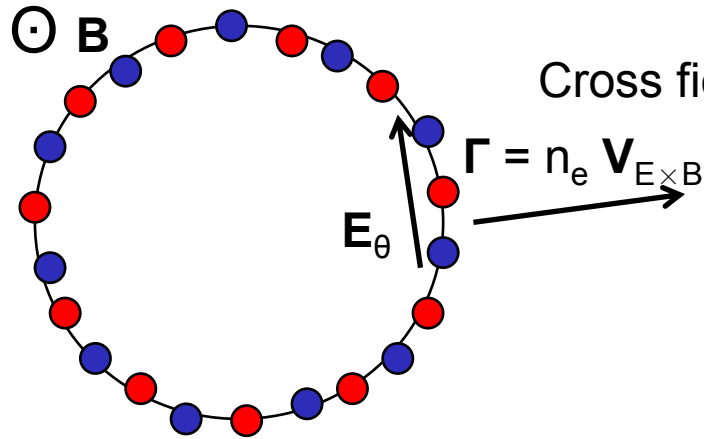
Transport measurements

Regular drift wave



Transport : outwards, one single frequency
with $\varphi_{\tilde{n}, \tilde{\phi}}$ close to 0.2π

Cross-field transport



- Floating probe
- Biased probe

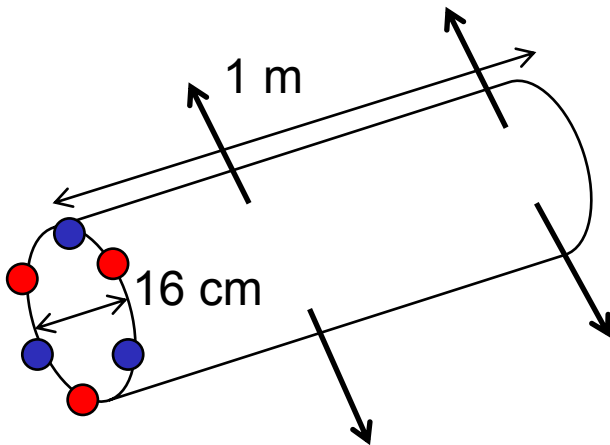
Mean flux measured with the probe array at $r = 8\text{cm}$: $\Gamma = 9.6 \cdot 10^{17} \text{ part. m}^2 \cdot \text{s}^{-1}$

Number of particles that are crossing the cylindrical surface: $4.8 \cdot 10^{17} \text{ part. s}^{-1}$

Total number of particles in the cylinder (using measured mean density): $2.6 \cdot 10^{14} \text{ part}$

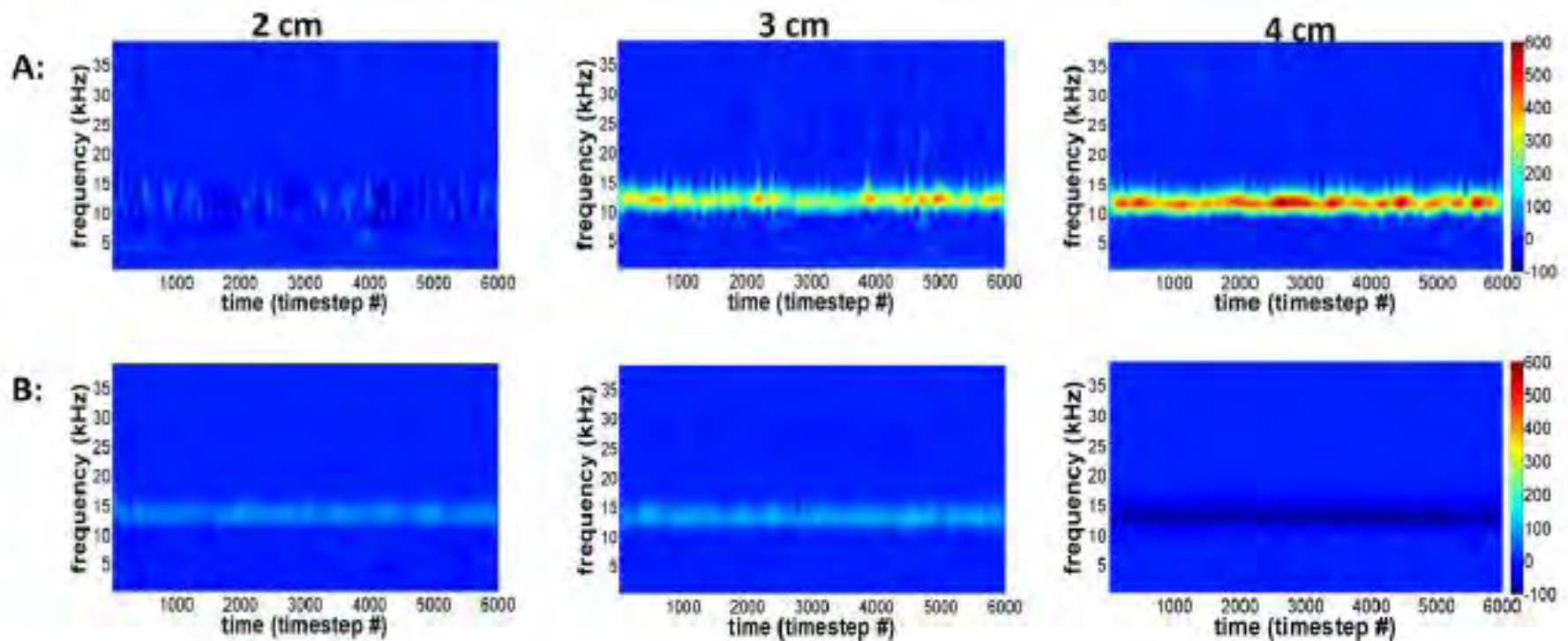
Time needed to empty the device $\approx 0.5 \text{ ms}$

Same order as the plasma decay time obtained by afterglow measurements

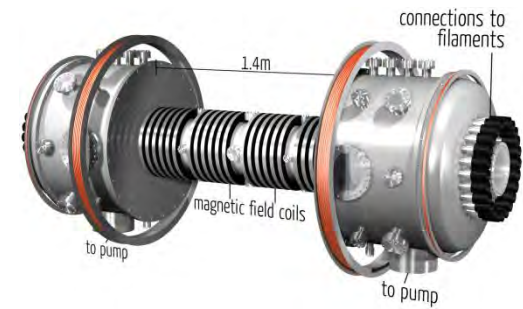
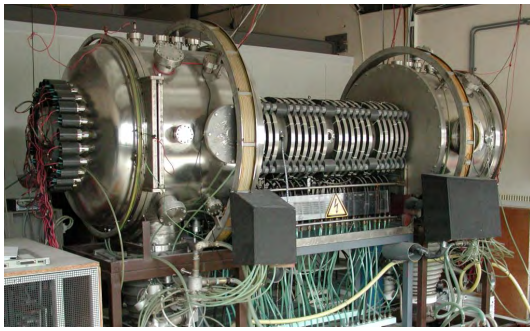


T. Pierre, G. Leclert, and F. Braun, Rev. Sci. Instrum, 58 (1), January 1987

Measurement of the cross-field transport



Cross-field transport measurements with emissive probes (A) and cold probes (B).



Future plans

short time prospects

Implementation of new diagnostic tools

- New probe array dedicated to transport measurement
- ball-pen probe
- Collective scattering

Comparison experiments / CYTO 3D simulations

Diagnosics tools for turbulence and transport

ANR SEDIBA -Tasks 3 (IJL)

**G. Bonhomme, S. Heuraux, N. Lemoine, F. Brochard, G.
Bousselin**

Institut Jean Lamour, CNRS – Université de Lorraine

Dpt p2M, Faculté des Sciences

BP 70239, 54506 Vandoeuvre-lès-Nancy

TASK 3: VALIDATION OF THE SYNTHETIC CAMERA DIAGNOSTIC

Objectives: This task aims at testing the validity of the synthetic camera diagnostic module to be implemented in the SOLEDGE3D code. It is divided into 2 sub-tasks.

- The first one will focus on experiments with fast cameras in a laboratory experiment, in order to refine the interpretation of the physical picture linking plasma fluctuations to light fluctuations, to be used in Tasks 1 and 2.
- The second one will be centered on the development and validation of analysis tools to be applied to experiments and simulations presented in Task 6.

WP 3.1 - Fast Camera testing in dedicated laboratory experiments



- Fast imaging with two cameras (located at both ends) in Mirabelle →

Makes it possible to follow simultaneously the spatio-temporal evolution of two species

- Photron Camera (non intensified) + interferential filters → neutrals atom. transitions (e.g. Ar, 420 nm et 765 nm)
- Intensified Camera (Phantom ?) → ion atom. transitions

Experiments in pure Ar or He plasmas, then with injected impurities

- Probe Measurements

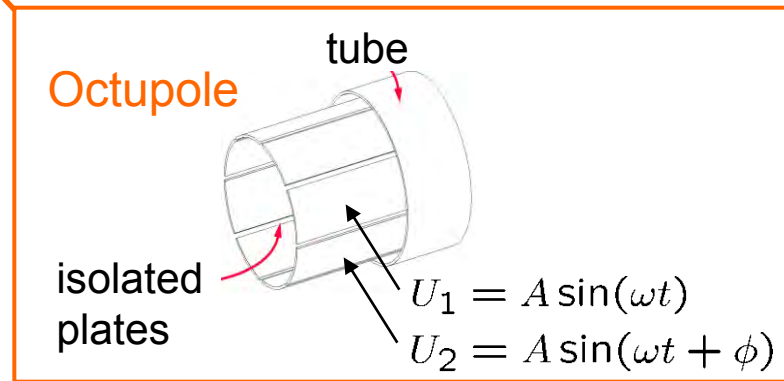
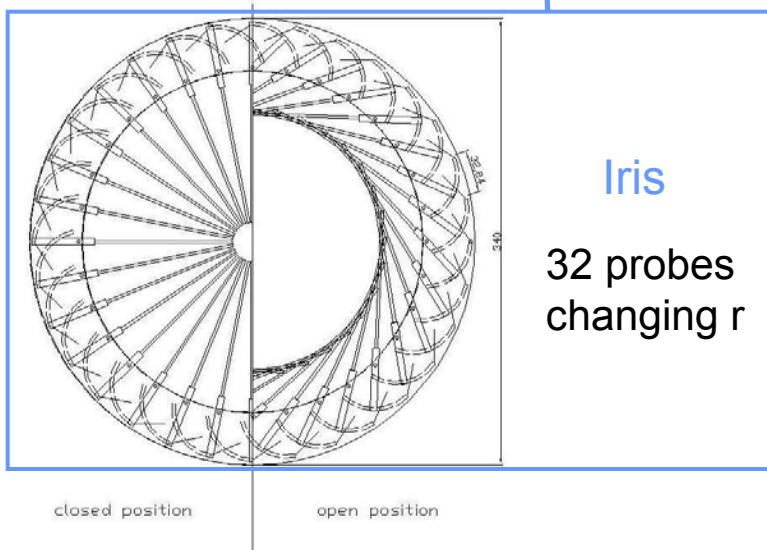
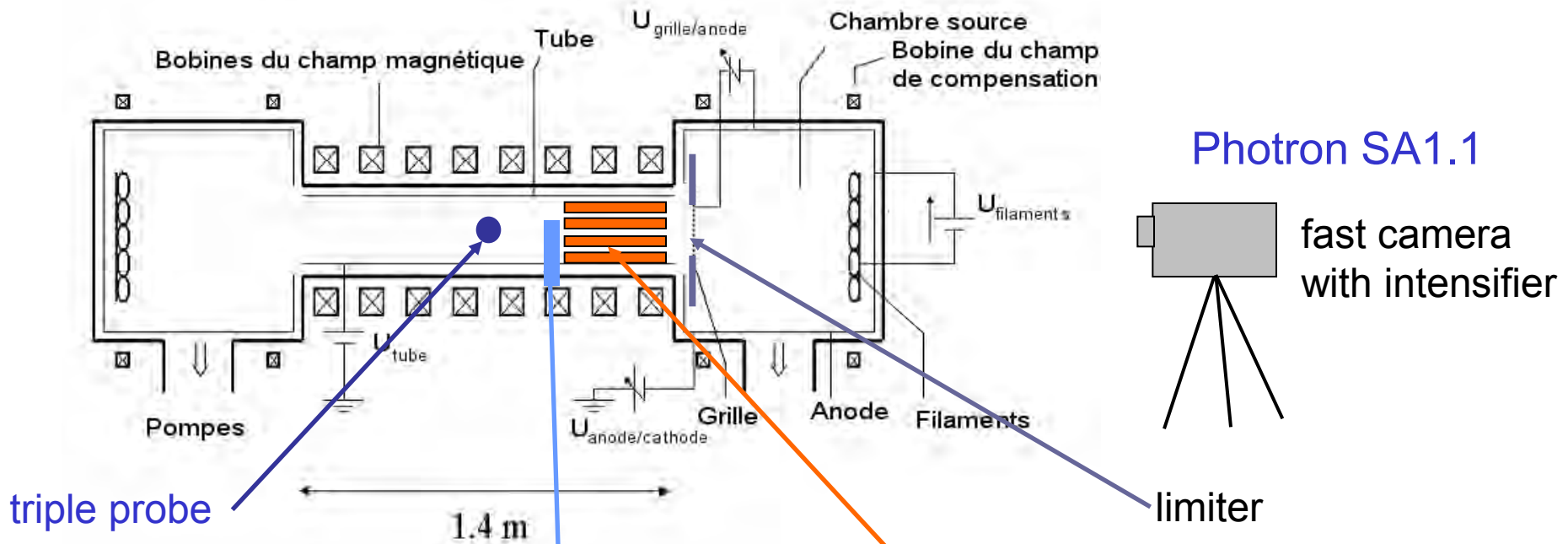
- New poloidal probes array IRIS, emissive probes, ball-pen, plane probes

→ Spatio-temporal dynamics, Turbulent transport measurement

→ Measurement of the radial parallel current profile

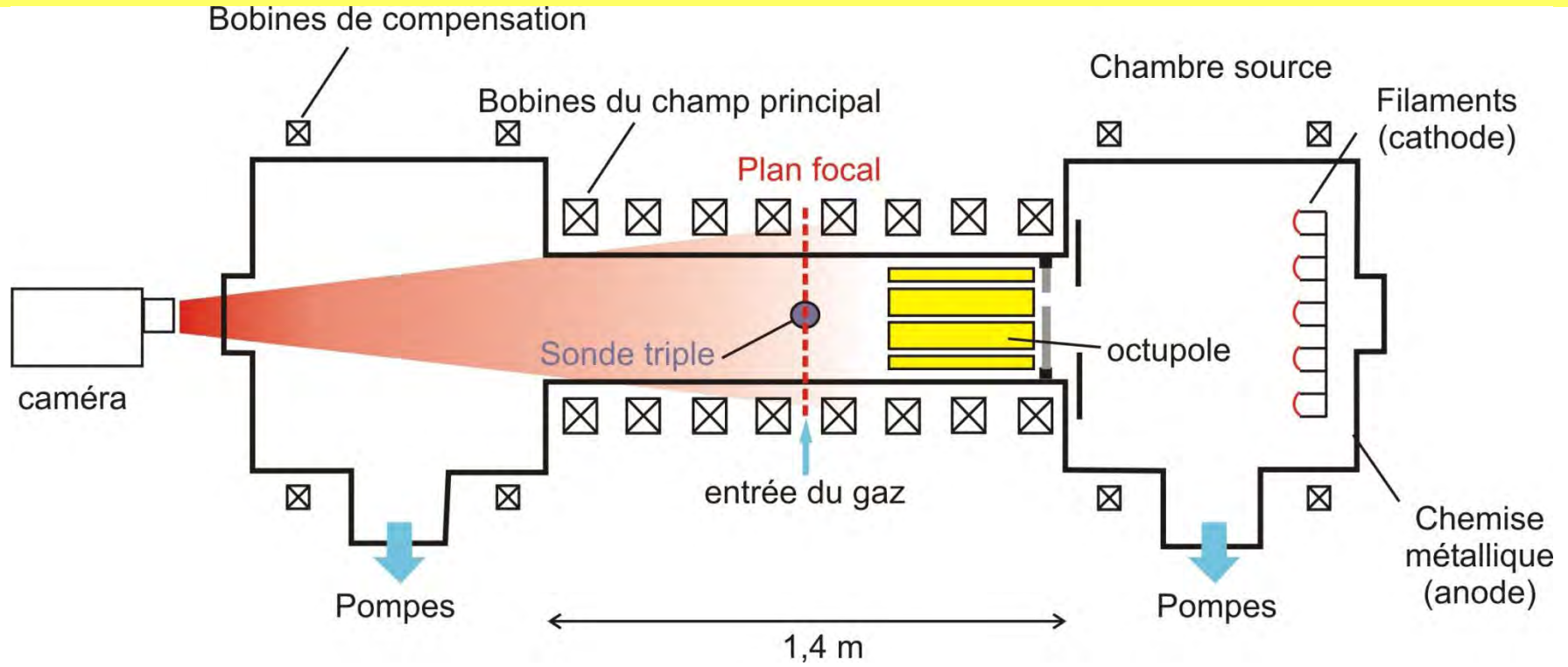
→ Excitation of blobs

Plasma control and diagnostics



Collective scattering (CO2 laser)
 Study of turbulence and transport
 (k_r and k_θ spectra)

Mirabelle: schematic view with diagnostics



Camera Photron SA1.1

Light intensifier Hamamatsu C10880

max efficiency wavelength 430 nm, gain ~1000
gating time 40 ns without filters, 8 μ s with filters

Interference filters: 420 nm, 765 nm (neutral Ar)
428 nm Ar⁺

200 mm, f=4. lens

Without the light intensifier

50 mm, f=1.2 lens

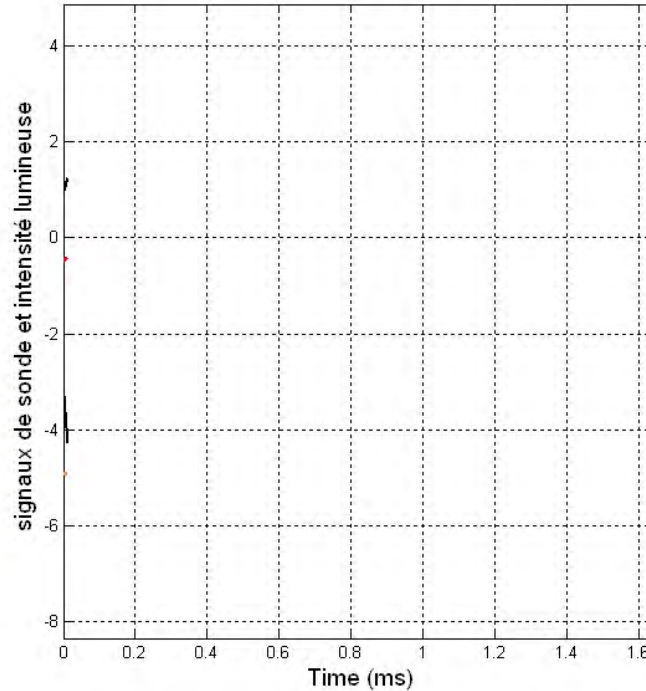
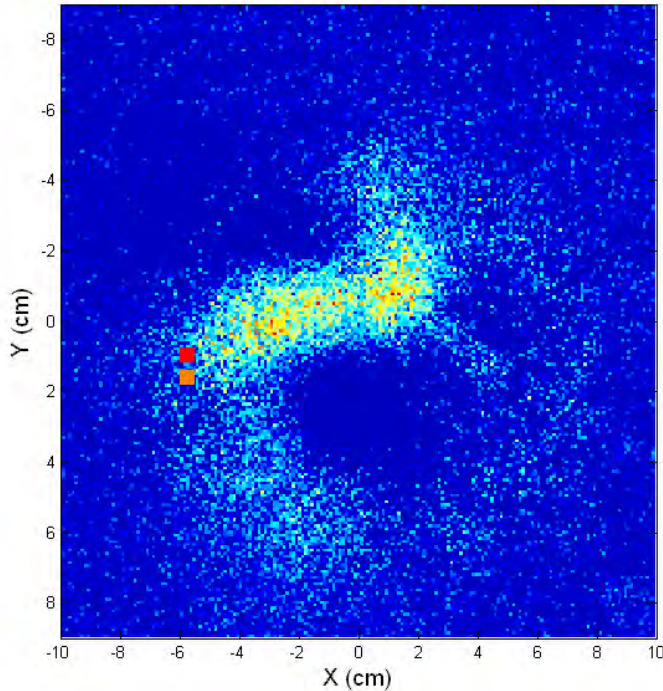
⇒ Field of depth ~ 5 cm

0.75 mm/pixel

Max radial shift due to
parallax error ~ 3 %

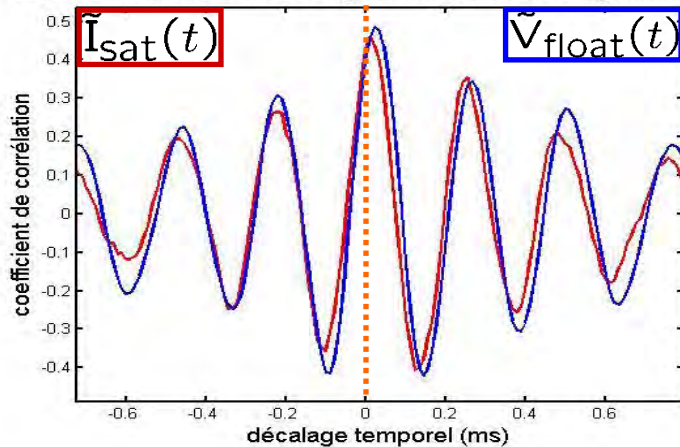
Direct comparison: Probe vs. Fast Imaging

t = 0 ms



- Lower probe
 $\tilde{I}_{\text{sat}}(t) \propto \tilde{n}(t)$
Light Intensity
- Upper probe
 $\tilde{V}_{\text{float}}(t)$
Light intensity

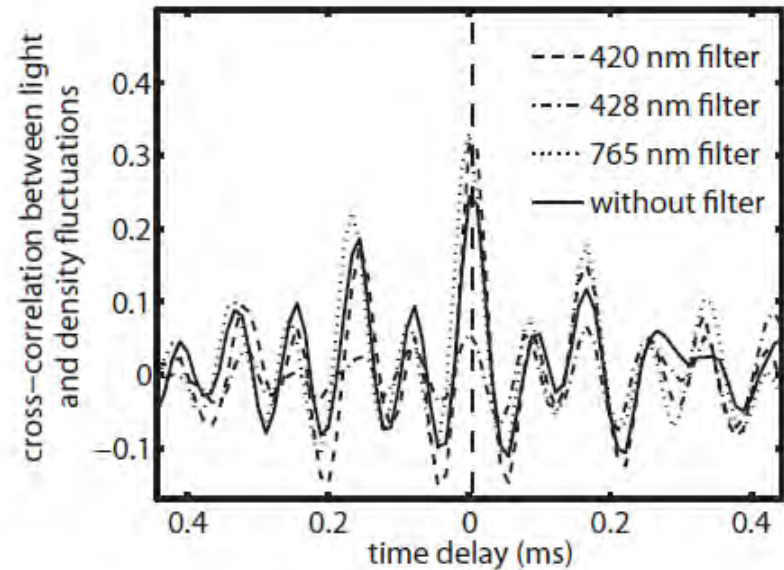
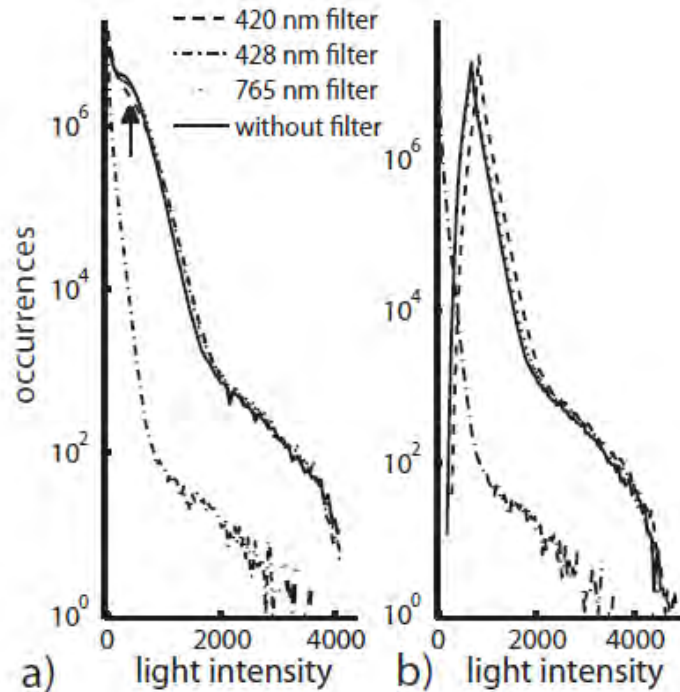
Cross-correlations entre les signaux de sonde et le signal lumineux



Plasma: irregular state

Good agreement between both diagnostics, especially for $\tilde{I}_{\text{sat}}(t)$ the recorded fluctuations of light intensity provide a visualization of the density fluctuation dynamics in the plasma column

Light fluctuations



Cross-correlation between the ion saturation current fluctuations and the light intensity fluctuations recorded without filter and with three different filters

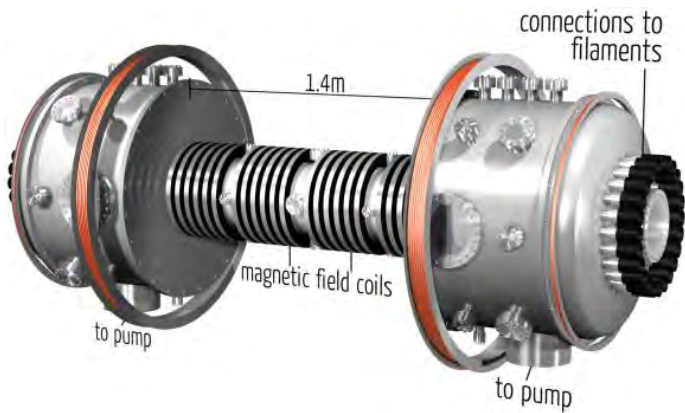
Histograms of light intensity.

a) Histograms computed from the original images.

b) Histograms computed after subtraction of the corresponding average image.

Spectroscopic interpretation and velocimetry analysis of fluctuations in a cylindrical plasma recorded by a fast camera, S. Oldenbürger et al., Rev. Sc. Instr. (2010)

Ongoing activities



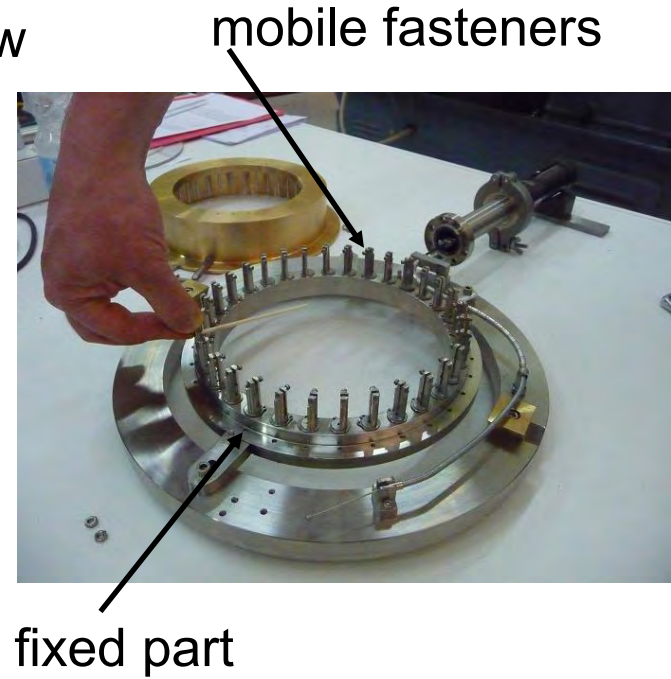
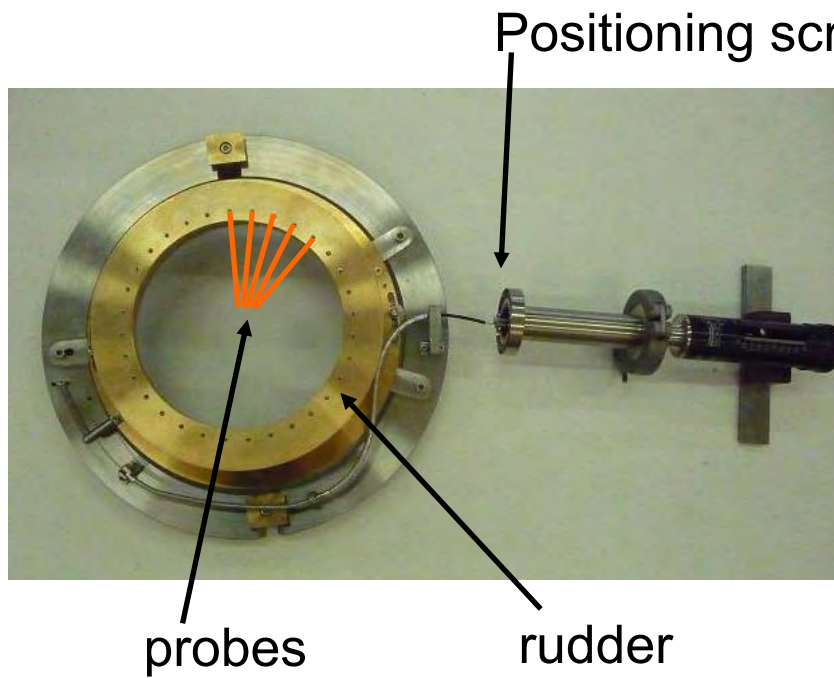
Implementation of new diagnostic tools

- Emissive probes
- Ball-pen probe
- New IRIS probe array dedicated to transport measurement

Implementation of a telescope instead of camera lens for fast imaging

Comparison experiments / CYTO 3D simulations

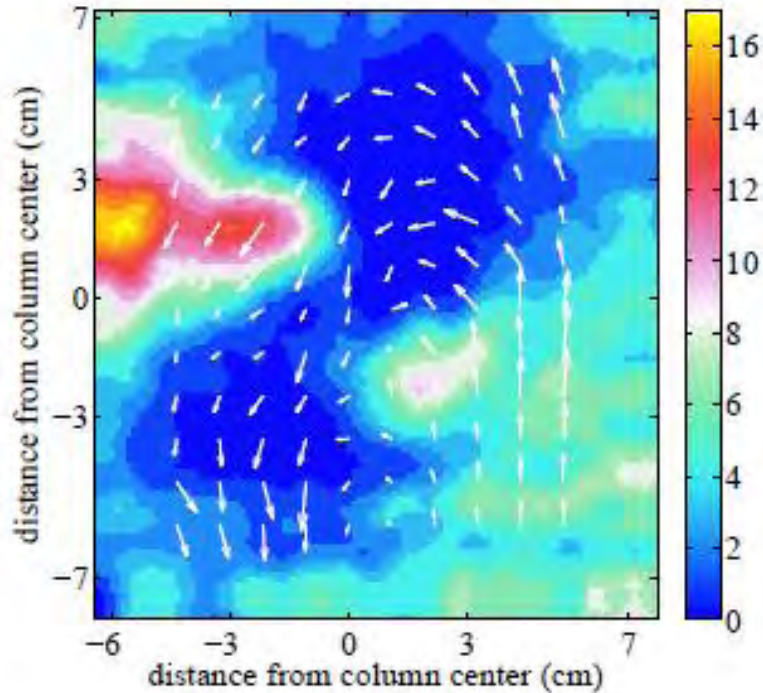
New poloidal probe array IRIS



WP 3.2 – Development and validation of analysis tools for the camera

- Developing data processing tools for characterizing and tracking of turbulent structures from fast imaging. (e.g. TIV)
- Addressing the tomographic reconstruction problem
 - The light collected by the camera is emitted by a volume extended source → currently underway: comparing the results obtained from a simple experiment with a ray-tracing code, seeking for the possible advantages brought by replacing the camera lens by a telescope?
 - In toroidal geometry a tomographic inversion is necessary to reconstruct the poloidal cross-section images → continuation of the task initiated by Romain N'guyen
- Testing the developed methods on numerical simulations results
 - CYTO 3D
 - SOLEDGE3D

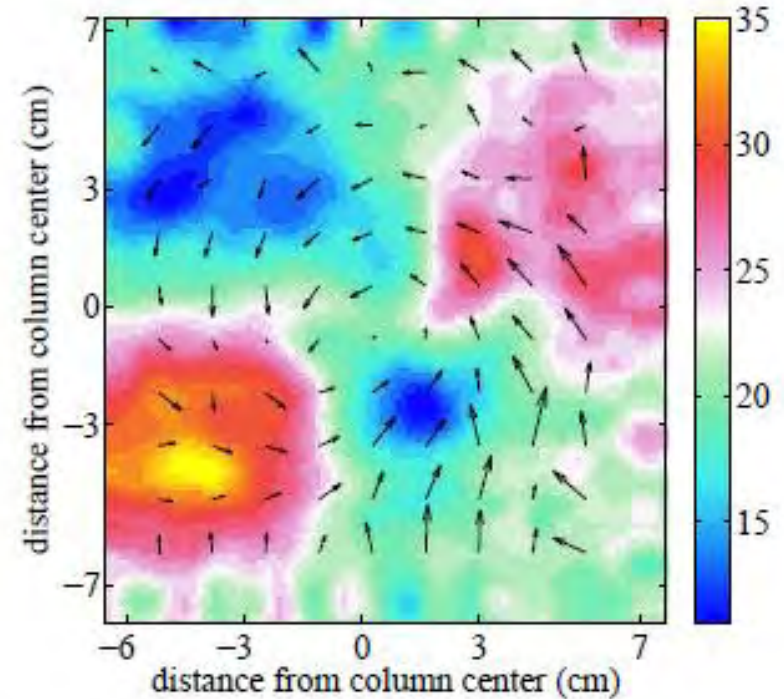
Application of the „TIV“ to Mirabelle



Velocimetry performed on a pair of fast camera frames. Superposition of the recorded light intensity and the quiver plot for the velocities

Photron SA 1.1, up to 90 000 - 180 000 frames/s, around 200x200 pixels

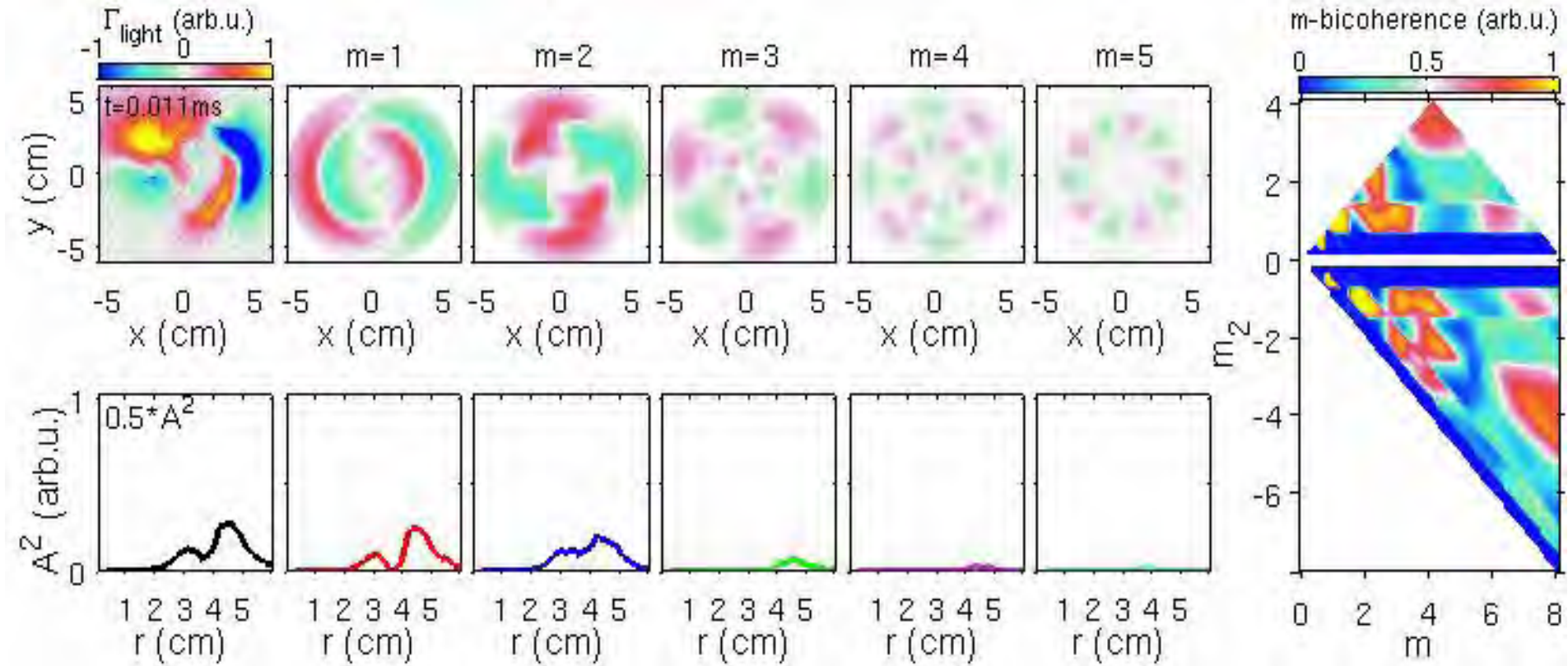
- pixel~ 0.8 x 0.8 mm²
- exposure time: 1 - 3 μ s



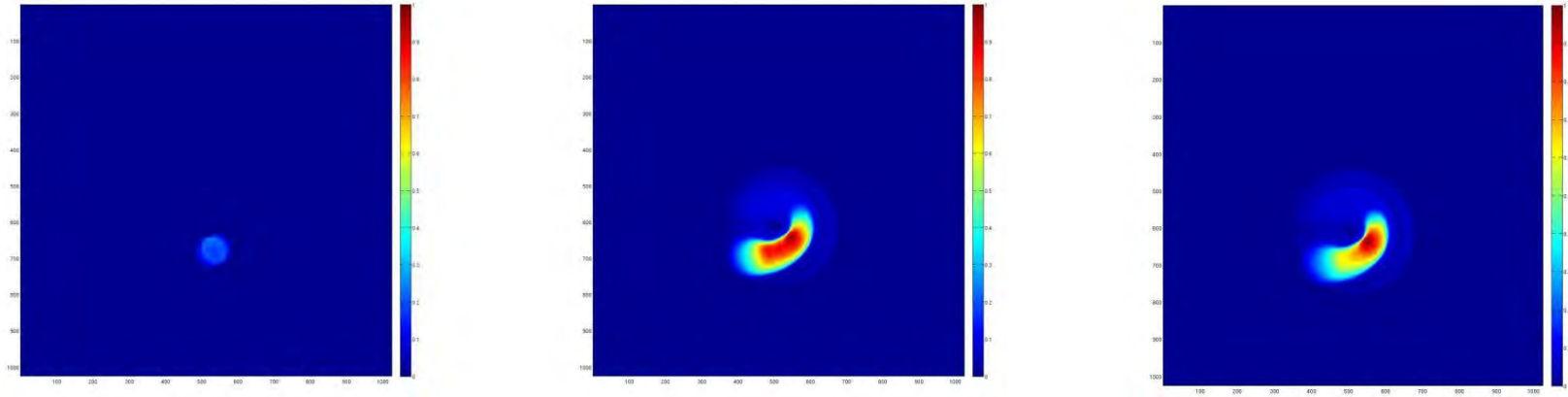
Average velocities obtained from 150 image pairs. Superposition of the first frame of the image sequence and the quiver plot for the velocities.

Stella Oldenburger, PhD thesis, (2010)

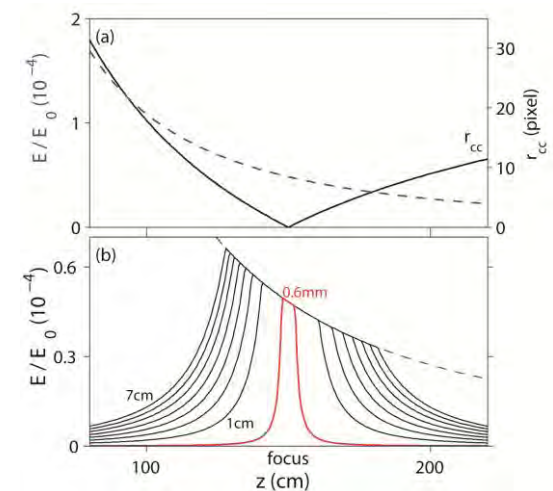
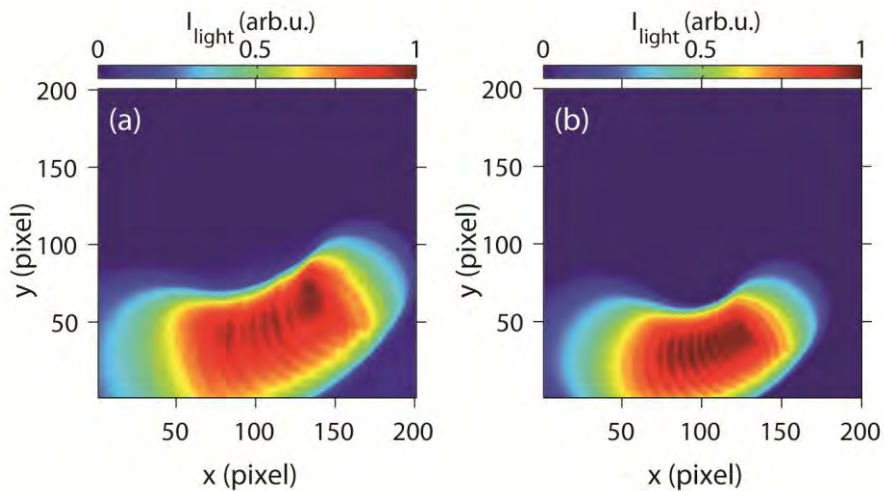
Decomposition of drift wave turbulence (in He)



Pb. Tomographic Reconstruction



Experiments (simulating a $m=1$ drift wave)

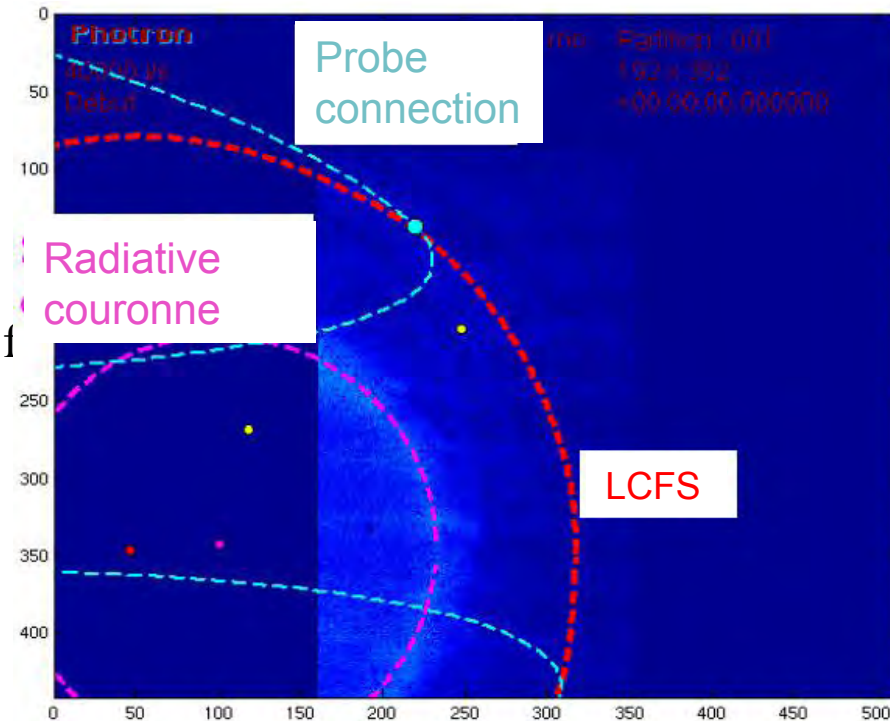
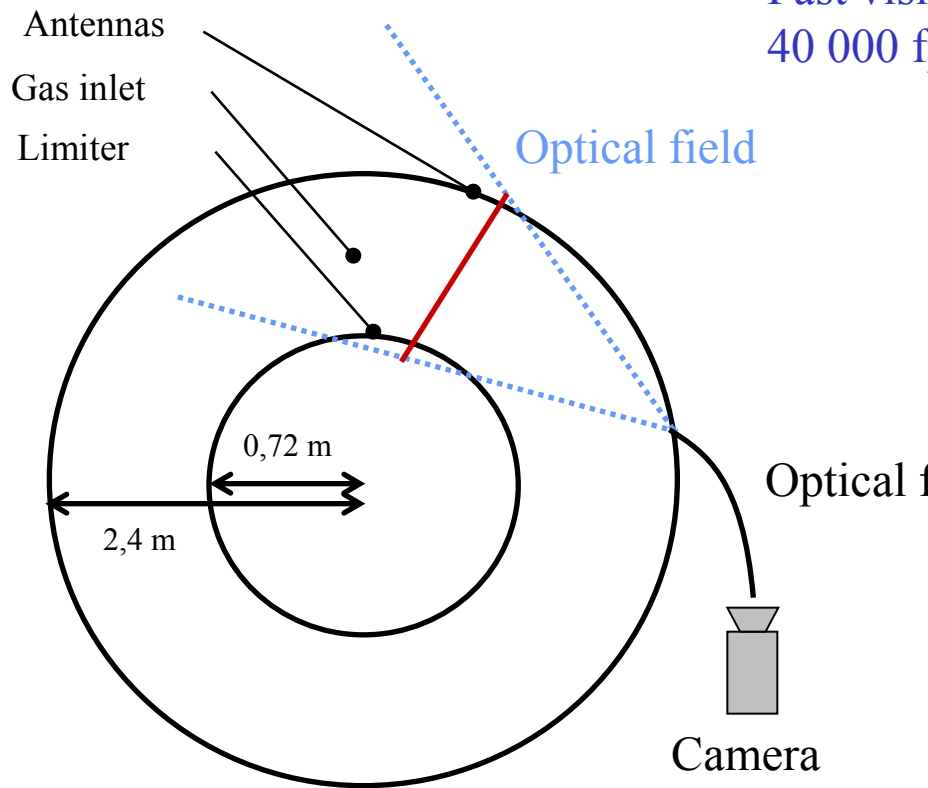


Ray-tracing Simulations

Experimental campaign on Tore-Supra

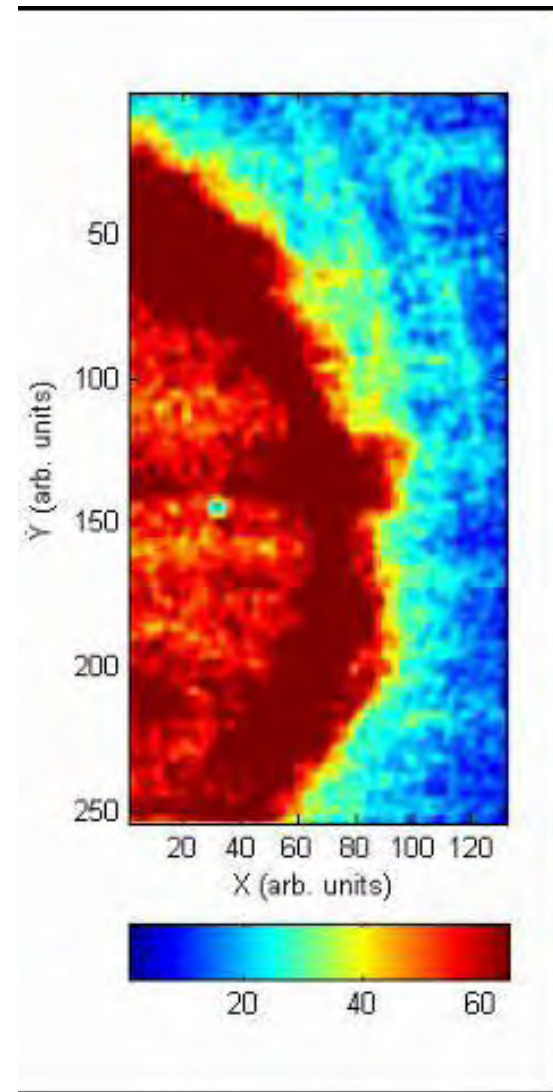
For the first time, synchronous measurements with:
poloidal array of probes
Doppler back-scattering and fast reflectometry
fast imaging

Fast visible commercial camera: Photron SA1.1
40 000 fps, Shutter $20 \mu\text{s}$

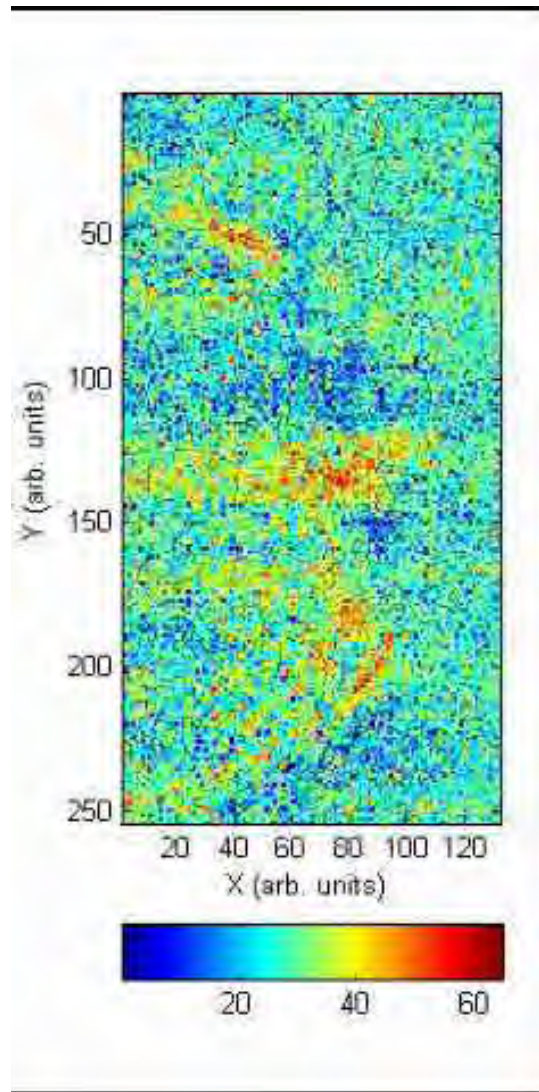


Video Processing (Shot #TS42967)

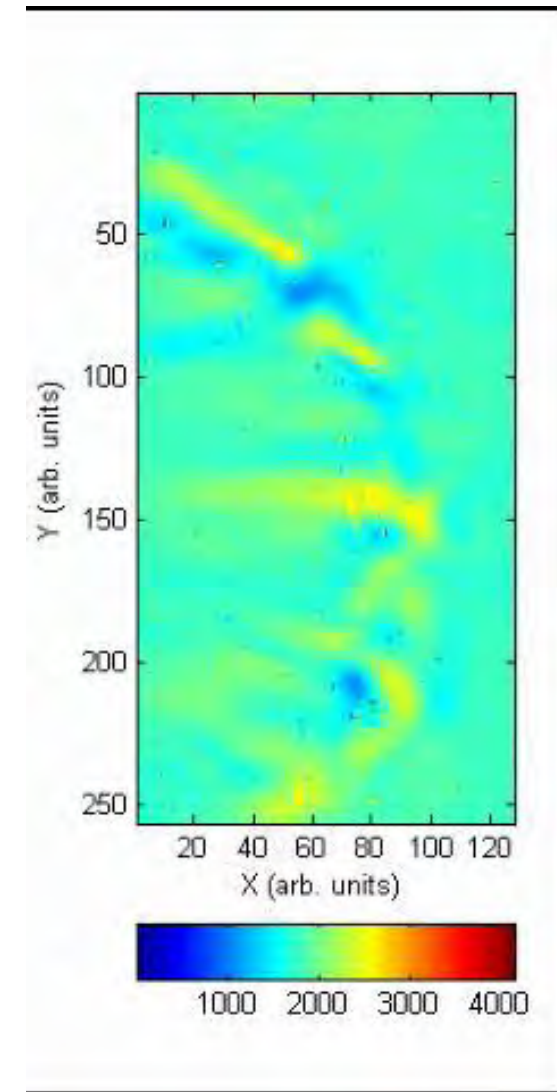
Raw movie



Fluctuations
(background removed)



After 2D wavelet denoising
(Kingsbury, NL thresholding)



Video Processing – « TIV »

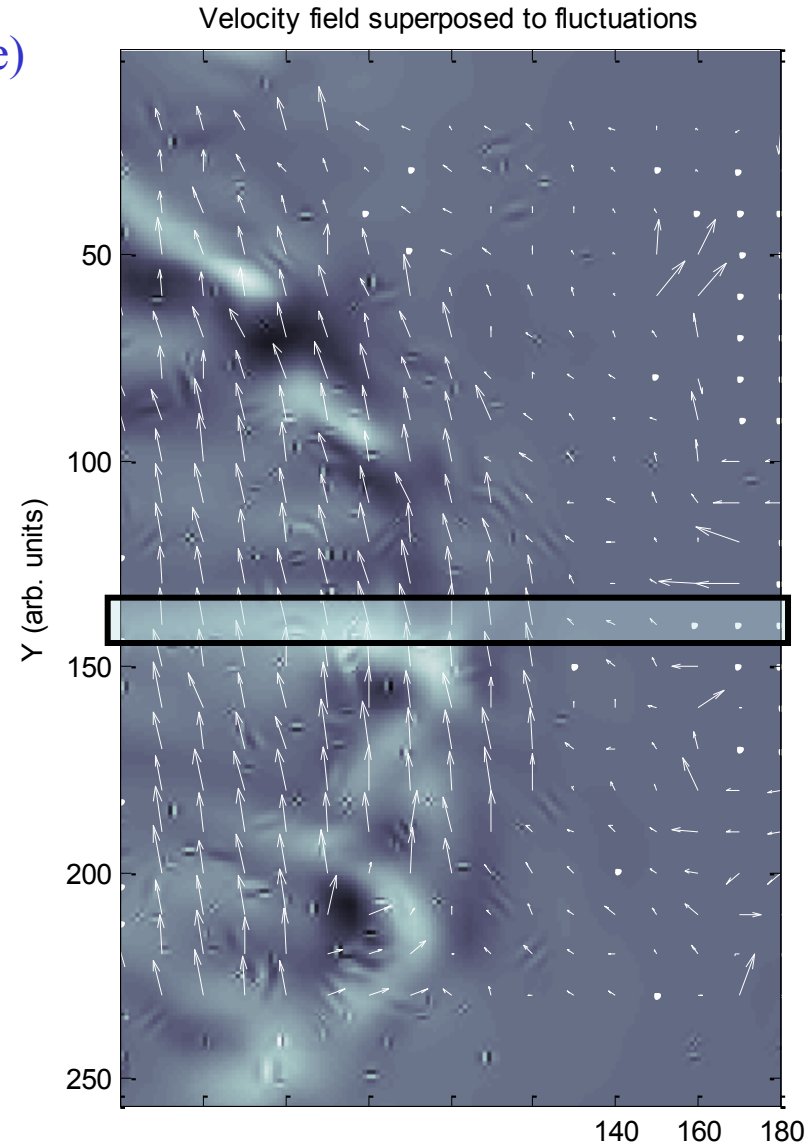
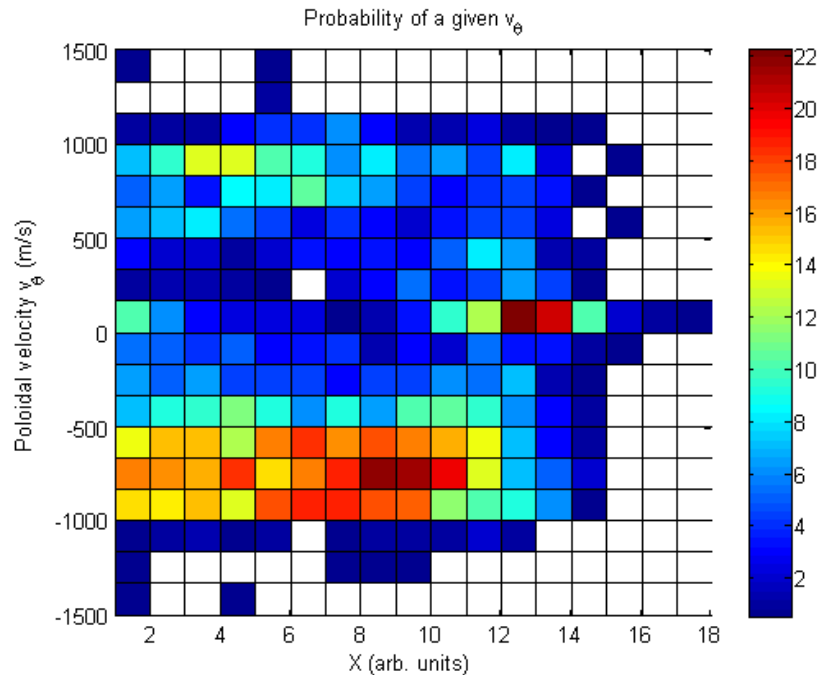
Principle of the MQD algorithm¹

MQD (Minimum Quadratic Distance) looks at the minimum of the squared difference between sub-windows

¹Sveen & Cowen

Spurious vectors

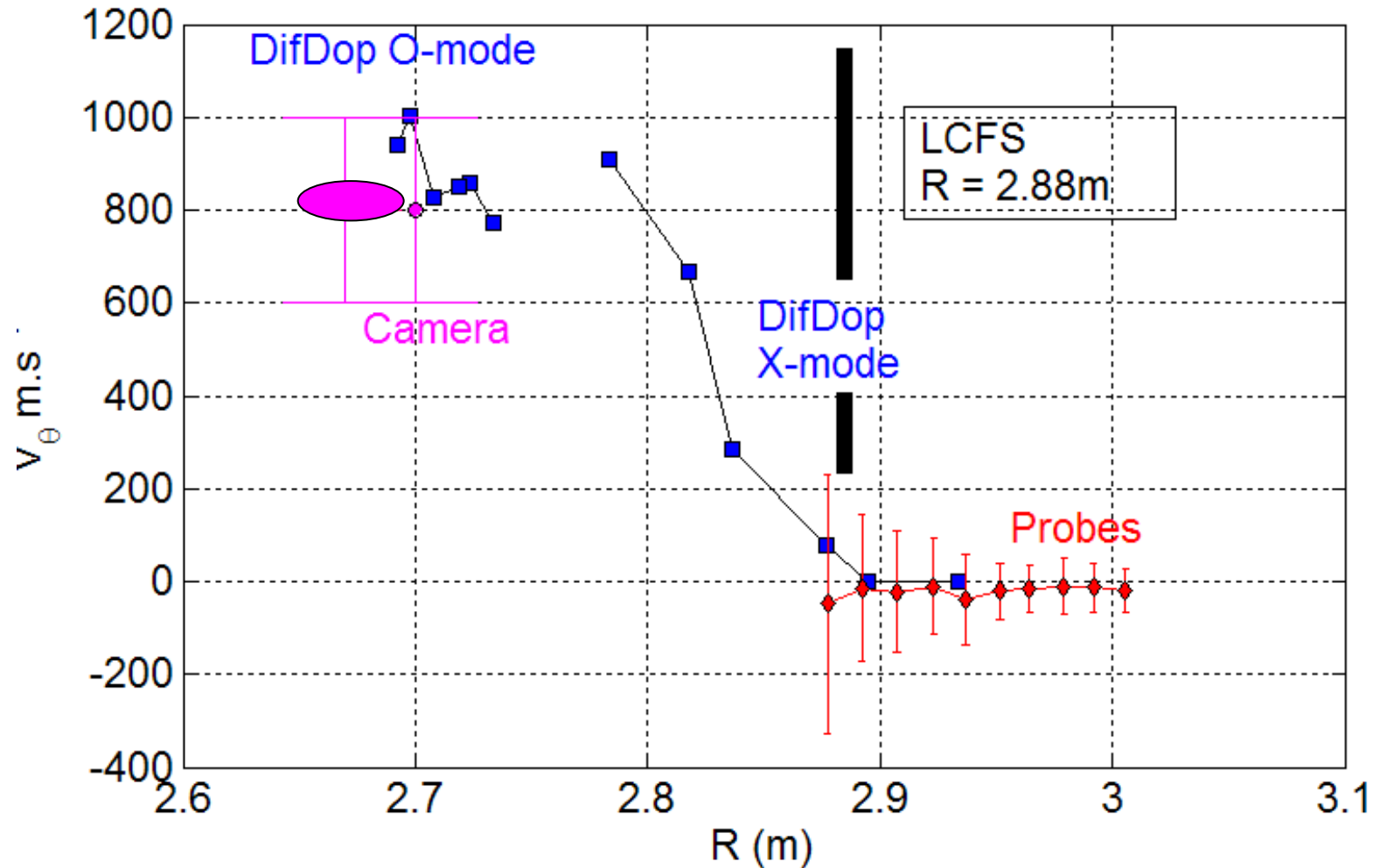
⇒ 200 pairs of frames (5 ms), Most likely velocity in PDF, in each sub-window



$$R(s, t) = \frac{1}{MN} \sum_{i=0}^{M-1} \sum_{j=0}^{N-1} [F'(i, j)^2 - 2F'(i, j)F''(i + s, j + t) + F''(i + s, j + t)^2]$$

Diagnosics comparison

Poloidal velocity profiles, detached plasma



Tomographic reconstruction of Tokamak edge light emission

R. Nguyen van
yen et al.,
Nuclear Fusion
52, 013005
(2012)

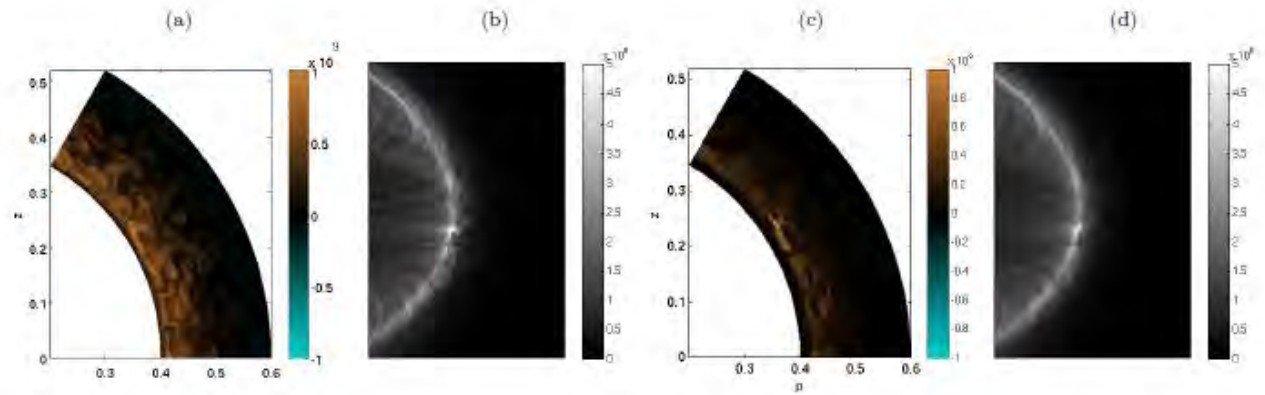


FIG. 7: Inversion test with artificial image generated from the TOKAM code. (a) Emissivity in the (r, θ) plane obtained from TOKAM run. (b) Artificial camera image obtained by stacking method. (c) WVD-inverted emissivity S_R . (d) Denoised image I_R obtained by applying K to S_R .

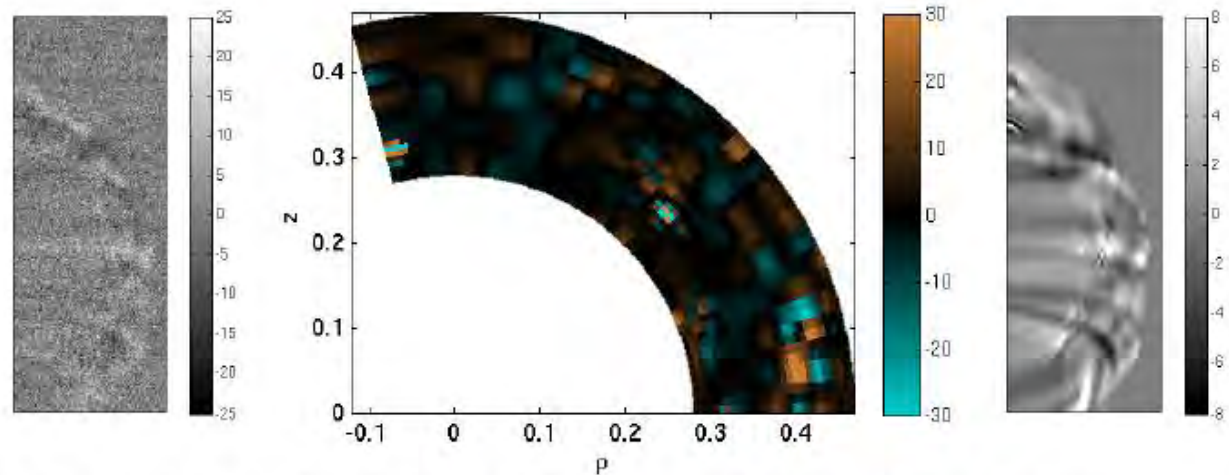


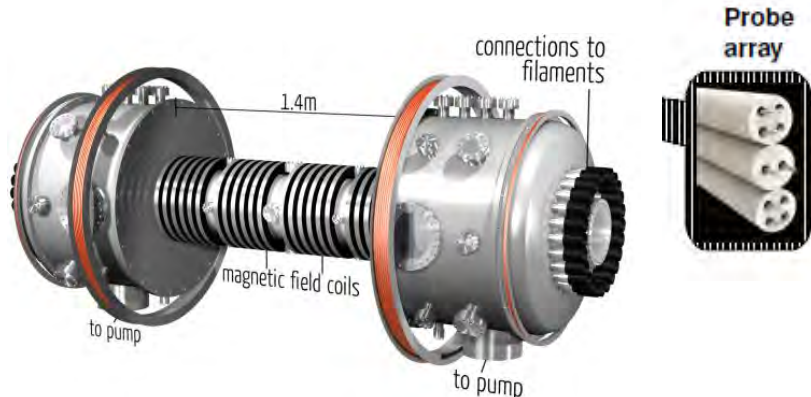
FIG. 8: Inversion test with experimental movie from Tore Supra shot 42967. Left: movie frame. Middle: WVD-reconstructed emissivity map S in (r, θ) plane. Right: denoised movie frame regenerated by applying K to S .

Comparison of ball-pen and emissive probe measurements in a low-temperature magnetized plasma

G. Bousselin, J. Cavalier, N. Lemoine, G. Bonhomme

Institut Jean Lamour, UMR CNRS 7198, Dpt P2M, University of Lorraine,
BP 70239, F-54506 Vandoeuvre-lès-Nancy, France
French Research Federation in Magnetic Fusion – ITER

Experiment



Radially movable probe array:

- Langmuir probe
- Emissive probes
- Ball-pen probe

- T_e, n_e, ϕ_p profiles
- n_e, ϕ_p fluctuations
- Crossfield transport

Experimental conditions:

- Helium and Argon plasma
- 3 working pressures:
 - $P_0 = 2 \times 10^{-4}$ mbar
 - $P_1 = 4 \times 10^{-4}$ mbar
 - $P_2 = 5 \times 10^{-4}$ mbar
- Magnetic field: 5-80 mT
- 3 probes with \neq diameters:
 $d=1\text{mm}, d=0.6\text{mm}, d=0.3\text{mm}$

Parameters	Helium	Argon
ρ_{ci}	0.4-6 mm	1-20 mm
ρ_{ce}	0.05-1 mm	0.05-1 mm
ω_{ce}	1-10 GHz	1-10 GHz
ω_{ci}	0.1-2 MHz	0.01-0.2 MHz
λ_D	50-700 μm	40-300 μm
$\nu_i = \nu_{ii} + \nu_{i0}$	0.3-30 MHz	0.3-20 MHz
$\nu_e = \nu_{ee} + \nu_{e0}$	0.3-2 MHz	0.5-2 MHz
$\lambda_i \sim \lambda_{ii}$	100-600 μm	50-500 μm
λ_e	1-3 m	5-20 m
$\beta_e = \frac{\Omega_{ce}}{\nu_e}$	$\gg 1$	$\gg 1$
$\beta_i = \frac{\Omega_{ci}}{\nu_i}$	< 1	$\ll 1$
$\sigma_{e,0}$	$7 \times 10^{-20} \text{ m}^2$	$1 \times 10^{-20} \text{ m}^2$
$\sigma_{i,0}$	$6.9 \times 10^{-19} \text{ m}^2$	$1.3 \times 10^{-18} \text{ m}^2$

Principle

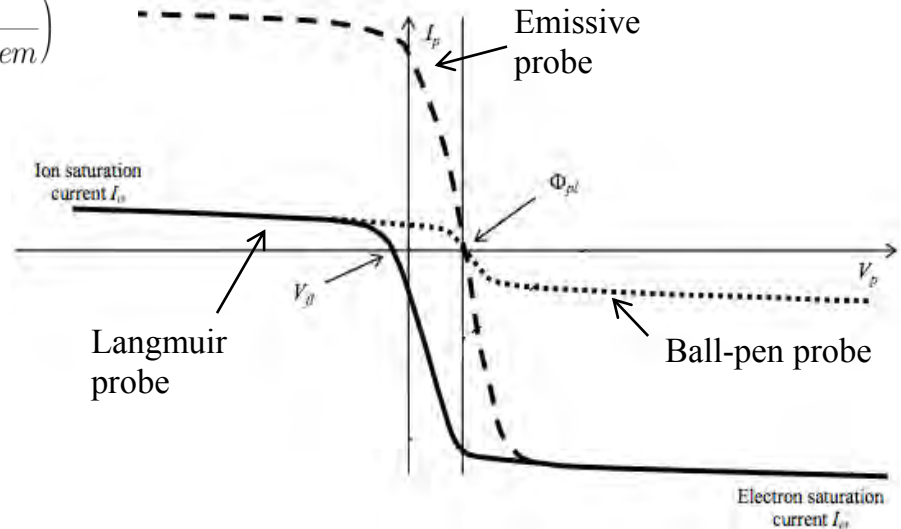
Langmuir probe theory:

$$\Delta = \frac{(\phi_p - V_{fl})}{T_e} = \ln \left(\frac{I_{es}}{I_{is}} \right) = \ln(R) \quad (1)$$

- Φ_p measured from 1st derivative of IV characteristics or calculated from Δ (knowing V_{fl} and T_e).

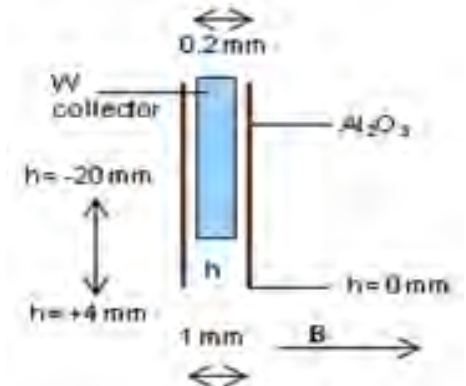
Emissive probe: $\Delta = \frac{(\phi_p - V_{fl})}{T_e} = \ln \left(\frac{I_{es}}{I_{is} + I_{em}} \right)$

- Emission current I_{em} adds to electron and ion currents from the plasma.
- Increasing I_{em} , the emissive probe floating potential approaches the plasma potential



Ball-pen probe:

- Consists of a movable Langmuir probe-like (metallic conductor placed inside an insulating tube).
- Probe axis oriented perpendicular to the magnetic field
- Utilizes the electron gyromotion to reduce I_{es} down to the level of I_{is} .
- The ratio $R = I_{sat}^- / I_{sat}^+$ can be adjusted to one.



Ball-pen probe design

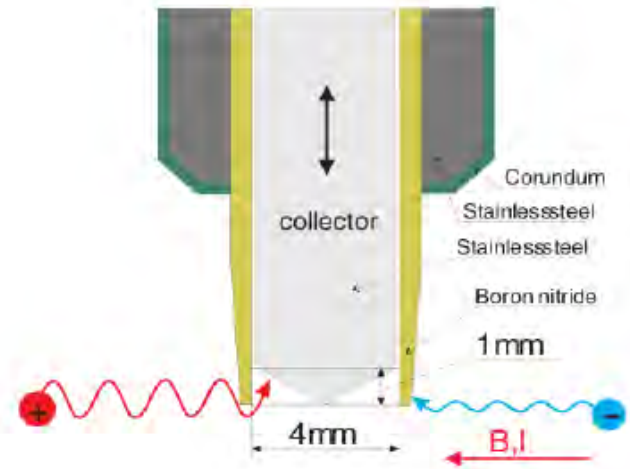
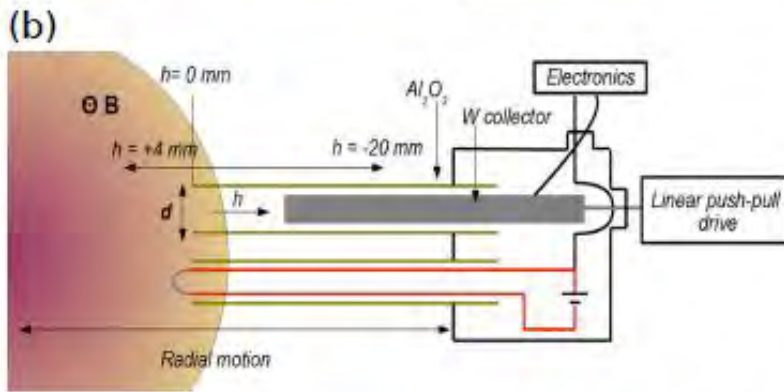
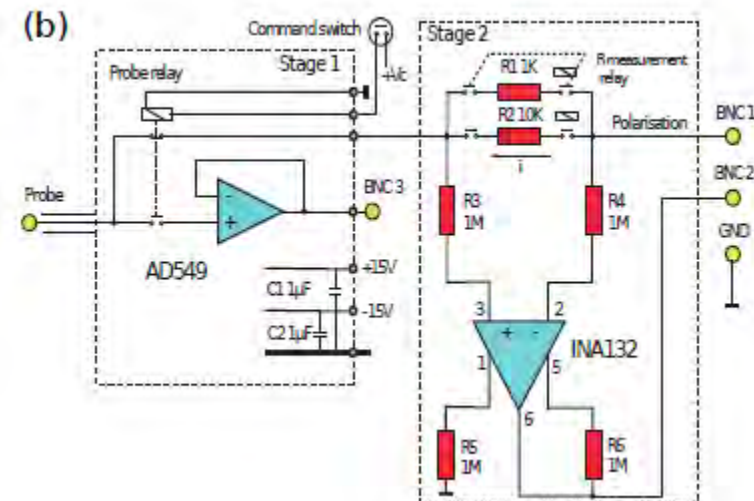
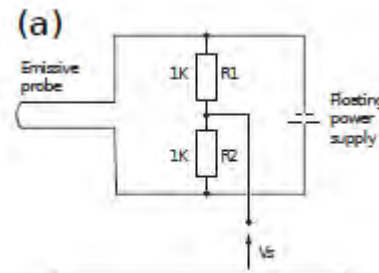


FIG. 2. (a) Photography of the radially movable probe array. (b) Scheme of the probe array constituted of one ball-pen probe (top) and one emissive probe (bottom).

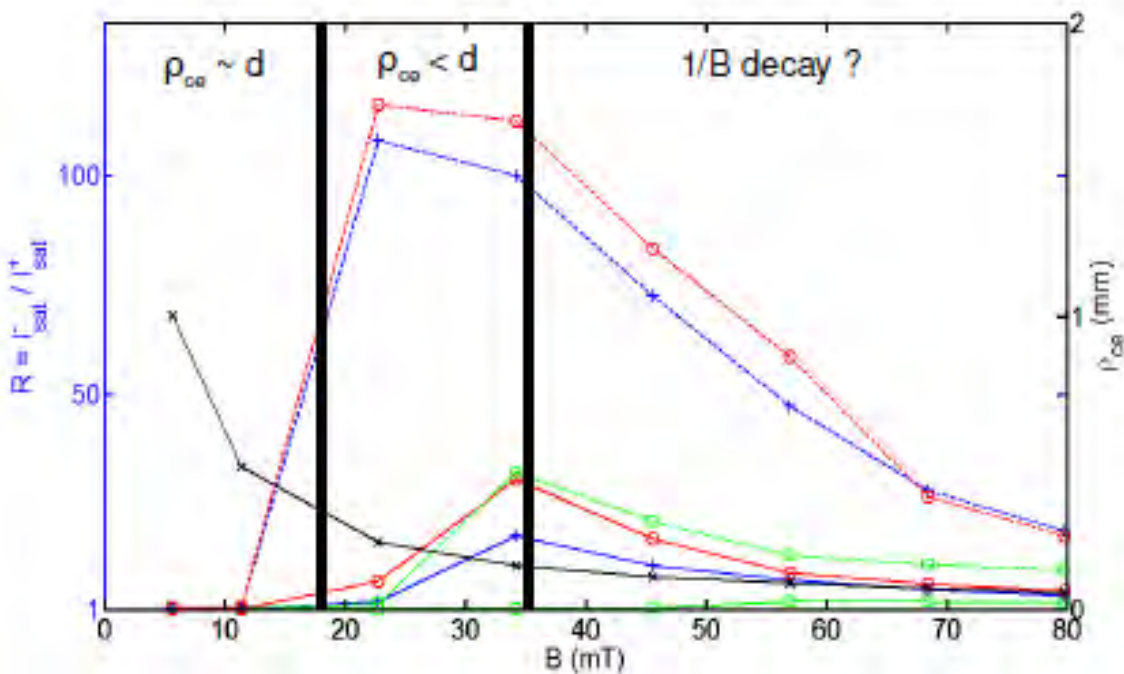


First results \rightarrow Design and validation of the ball-pen probe for measurements in a low-temperature magnetized plasma, G. Bouselin et al., submitted to RSI, (accepted 11.12.202)

Observations:

$\beta_e \gg 1 \rightarrow e^-$ magnetized \rightarrow transport driven by ExB drift.

$\beta_i < 1 \rightarrow$ transport driven by collisions.



3 regimes :

- $\rho_{ce} \sim d$

ExB drift limited by probe geometry and $\sigma_{e\perp} \sim \sigma_{i\perp}$

- $\rho_{ce} < d$

ExB shielding no longer effective and $\Gamma_e = n_e v_{ExB}$

- $1/B$ decay not yet understood, to be investigated

Ratio of the electron saturation current over the ion saturation current calculated from Eq. (1)

Ball-pen: Floating potential vs. h

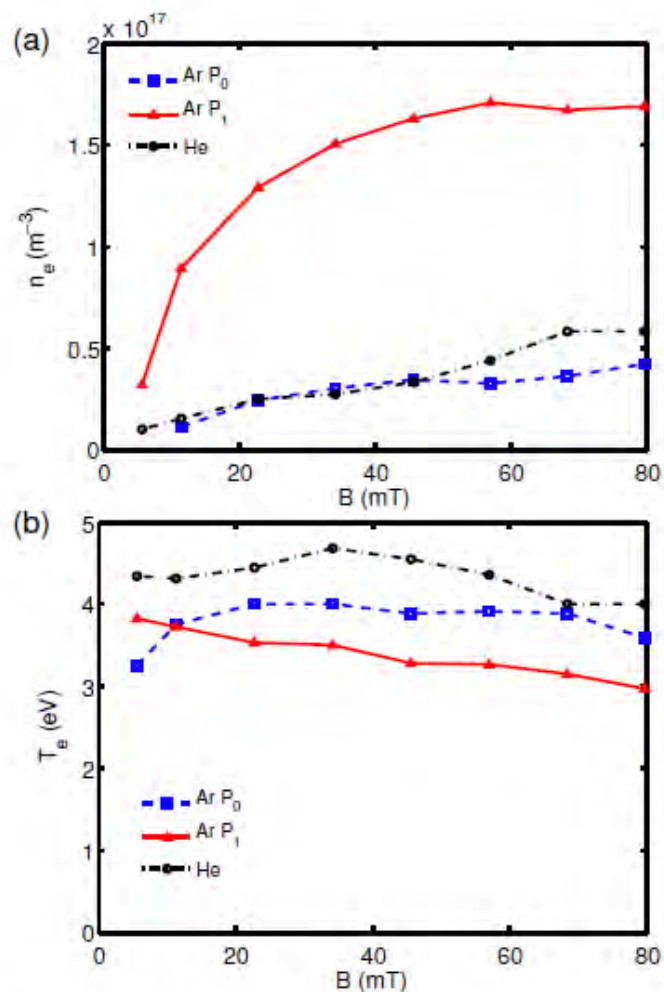


FIG. 4. (a) Electron densities obtained for the three different discharges (argon at $P_0 = 2 \times 10^{-4}$ mbar and $P_1 = 4 \times 10^{-4}$ mbar and helium with adjusted working pressure) with respect to the magnetic field. (b) Corresponding electron temperature.

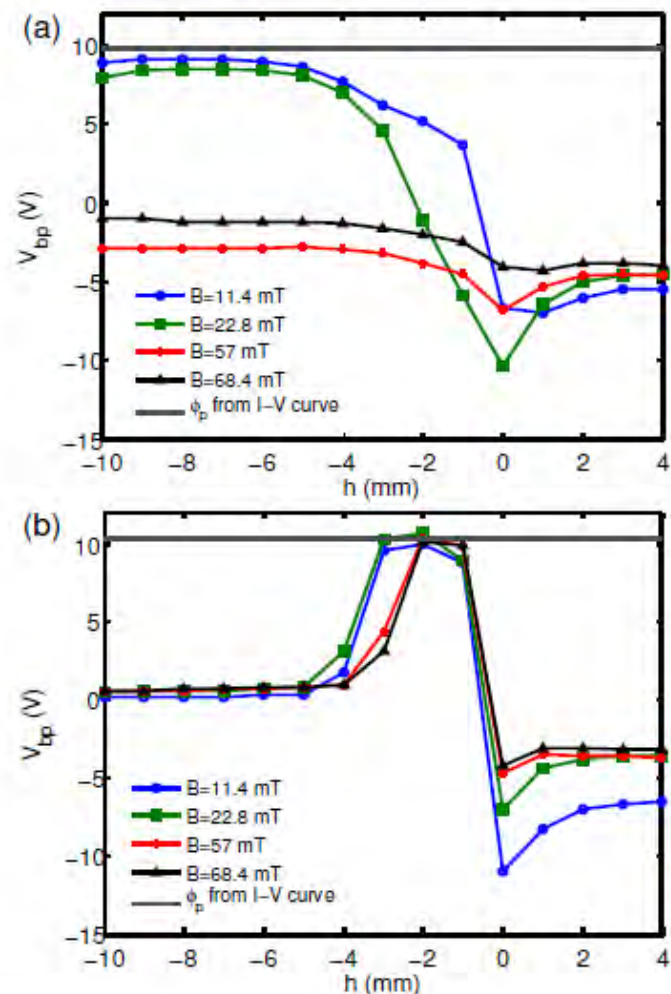


FIG. 5. Representative examples of ball-pen probe floating potential V_{bp} with respect to the depth of the collector h . Argon plasma at $P_0 = 2 \times 10^{-4}$ mbar. $V_{ac} = 8$ V, $V_g = 8.5$ V. (a) Tube diameter $d_1 = 1$ mm. (b) Tube diameter $d_3 = 0.3$ mm.

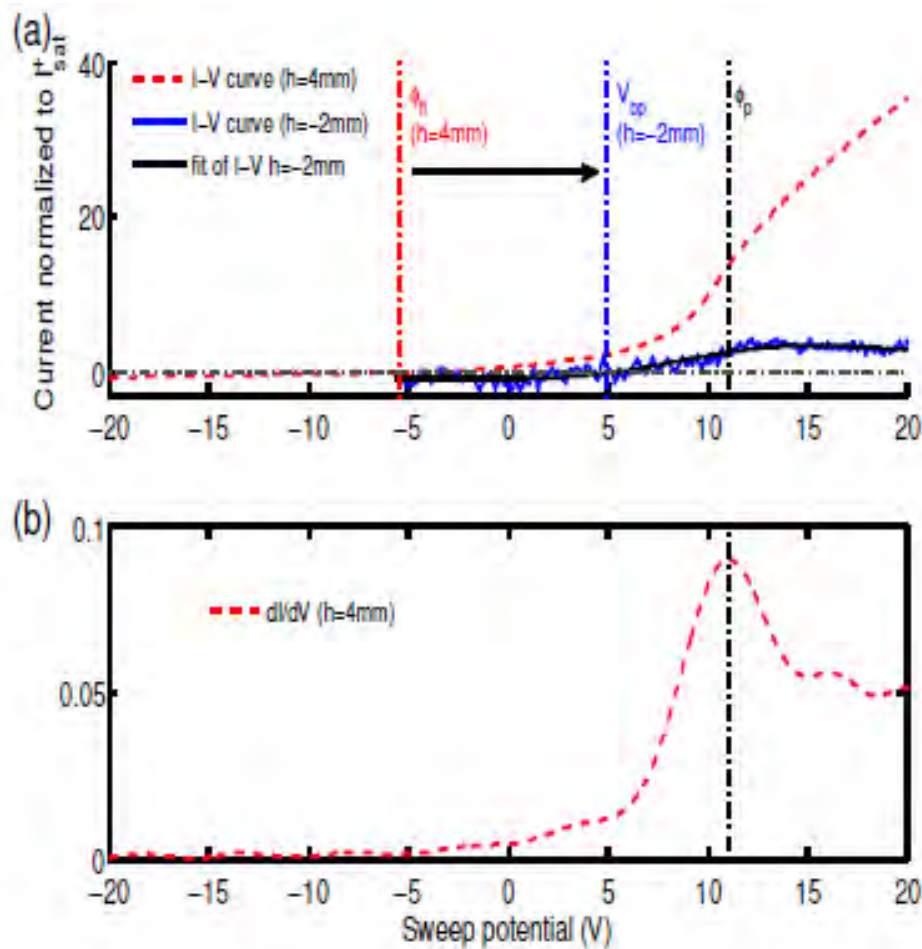


FIG. 6. (a) Normalized current-voltage characteristics recorded with the tube diameter d_1 at $h = 4$ mm and $h = -2$ mm. The discharge parameters are: argon plasma at $P_0 = 2 \times 10^{-4}$ mbar. $V_{ac} = 8$ V, $V_g = 8.5$ V, $B = 11.4$ mT. The shift of the floating potential of the ball-pen probe towards the plasma potential can be observed. (b) First derivative of the characteristic corresponding to $h = 4$ mm is also presented to show the determination of ϕ_p .

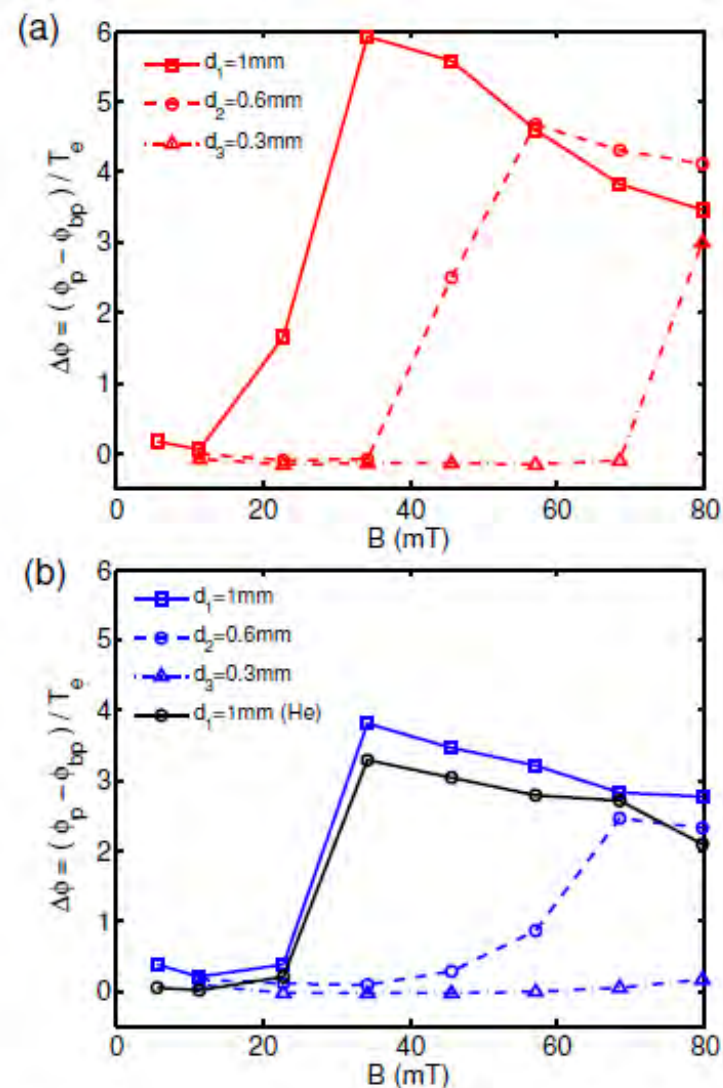


FIG. 7. Dependence of the normalized difference $\Delta\phi = (\phi_p - \phi_{bp})/T_e$ with the magnetic field B . (a) Argon plasma at $P_1 = 4 \times 10^{-4}$ mbar. (b) Argon plasma at $P_0 = 2 \times 10^{-4}$ mbar and helium plasma conditions corresponding to the same electron density than the argon case.

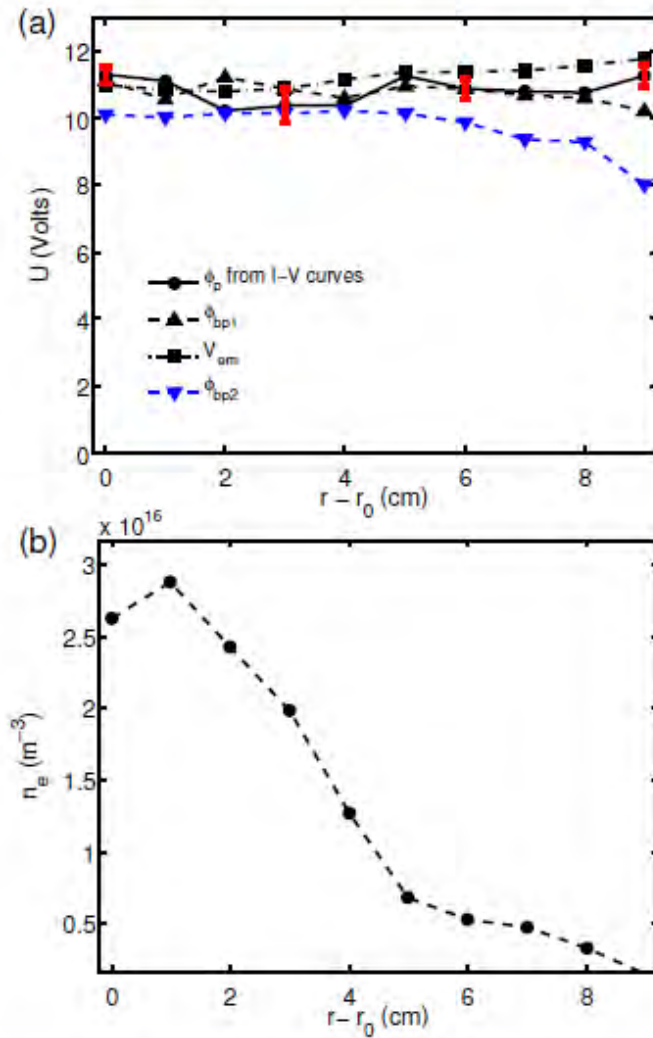


FIG. 8. (a) Radial profiles of two different ball-pen probe floating potentials (ϕ_{bp1} and ϕ_{bp2}), emissive probe floating potential (V_{em}) and plasma potential (ϕ_p) obtained from I - V characteristics in the following plasma regime: argon plasma at $P_0 = 2 \times 10^{-4}$ mbar, $V_{ac} = 8$ V, $V_g = 8.5$ V, $B = 34$ mT. (b) Corresponding electron density profile.

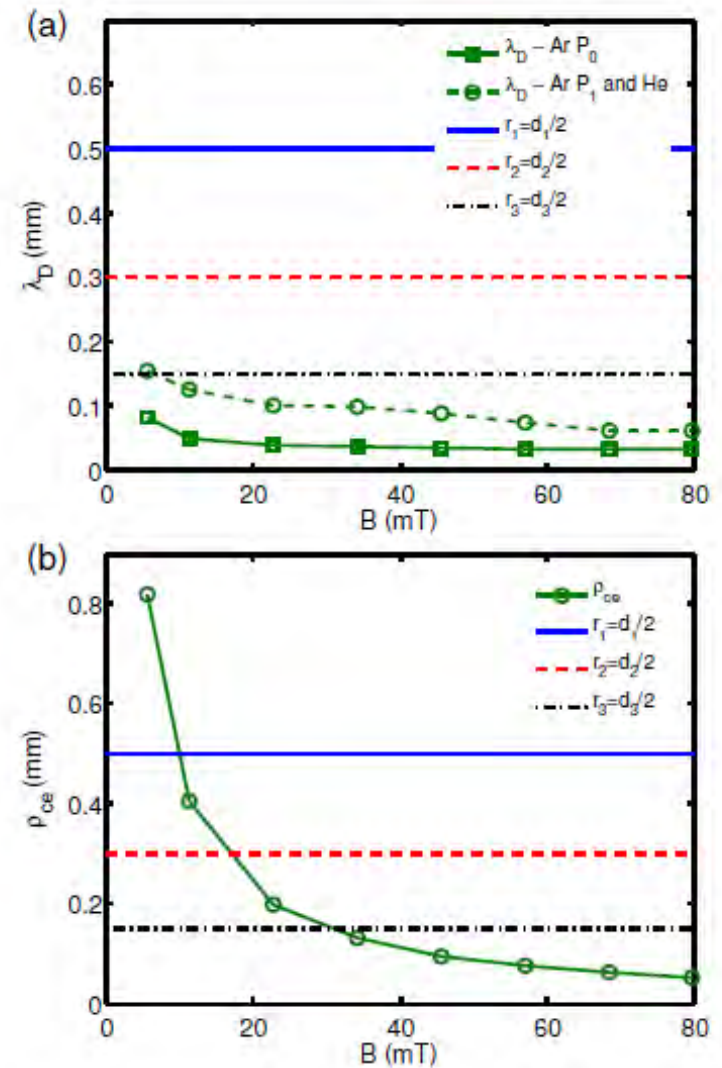


FIG. 9. Comparison of the characteristic lengths with the tubes radii. (a) Debye lengths corresponding to the different experimental conditions. (b) Electron Larmor radius corresponding to the argon plasma at $P_1 = 4 \times 10^{-4}$ mbar.

Ball-Pen probe: Conclusions – Prospects

- On the Mirabelle device, the plasma potential was successfully measured with the ball-pen probe at low pressure and for different gases.
- However, for high pressures the potential of the probe did not reach the plasma potential. The reason would be linked to the electron Larmor radius.
- At low plasma densities (high impedance) the design of the measurement circuit is also a very sensitive issue.
- In next experiments, the size of the probe has been modified to investigate geometry effects on the measurements.
- Through these systematic experiments a better understanding of the ball-pen behavior was achieved, but comparison with numerical simulations will be highly valuable.

Reflectometry and Antenna

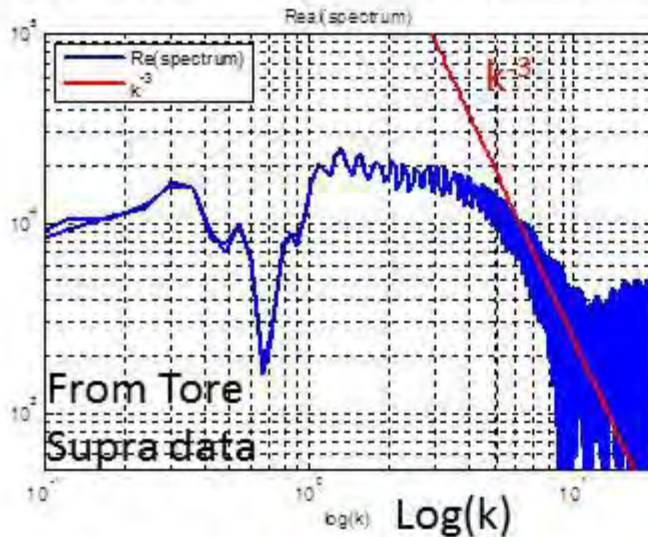
- Reflectometry modelling, S. Heuraux
- Antenna design and sheath, E. Faudot

Turbulence characterization using reflectometry: Developments of new diagnostics using EM waves

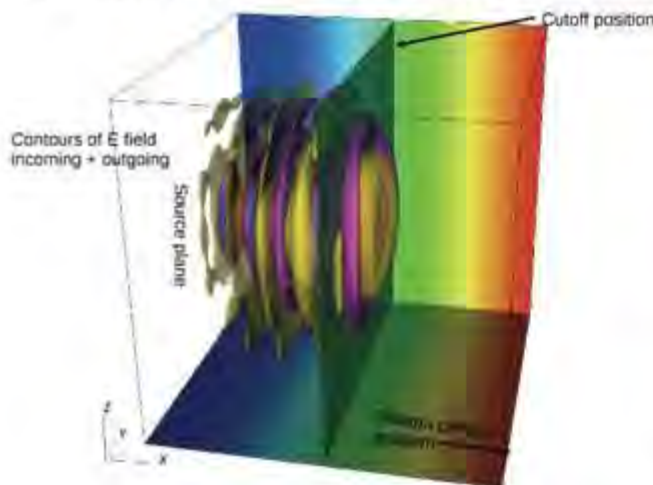
S. Heuraux, N. Kosolapova (PhD), E. Gusakov (Invited), A. Popov (Invited)

New concept

$S(k)$ using radial correlation reflectometer



1st results of the ERCC 3D code



Role of resonances (Basic Physics);,

NL Theory written for coherent dn $k_f = 2 k(x)$
and verified by simulations

In turbulent plasma with wide $S(k_f) \Rightarrow$

Electromagnetic flux \Leftrightarrow Born approximation

S. Heuraux et al *Contrib. Plasma Phys.* **51**, 126 (2011).

E. Gusakov et al *Physica Scripta* **84**, 04504 (2011).

New concepts (development of diagnostics)

Using radial correlation reflectometry

Applied to Tore Supra, FT_2, JET

Using hopping frequency reflectometer

N. Kosolapova et al *Plas. Phys. Cont. Fusion* **54**, 035008 (2012)

E. Gudakov *Plas. Phys. Cont. Fusion* **54**, 045008 (2012)

Coupling with turbulent code (synthetic diagnostics)

With GEMR, tokam_2D

Blob detection and dynamics of the turbulence

To be published in *Rev Sci Instrum.*

Code ERCC EFDA ITM_ERDG (new tool developments)

New Numerical scheme (unconditional) ERCC 3D Kernel

Reversible Near-Far field propagator to be published in *Fus.Sci.Tech*

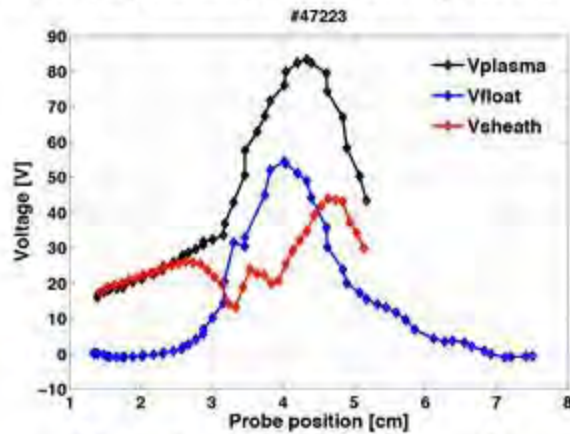
15 papers (2008-2012), Ioffé Institute St Petersburg,
IPFN IST Lisbon, IRFM CEA_Cadarache

Antenna-plasma Coupling RF sheath physics :

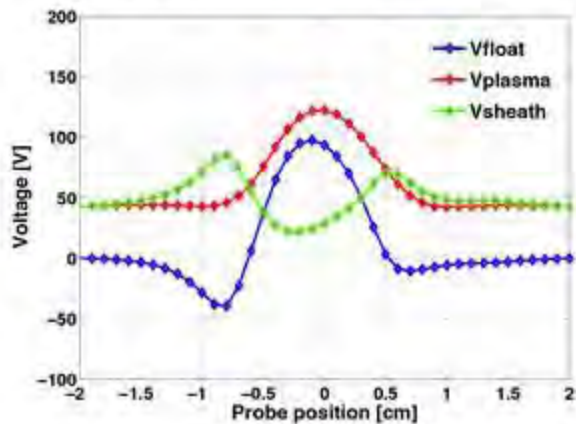
Generation of rectified potentials DC by RF - Measurements by Langmuir probes in RF

E. Faudot S.Heuraux

Tore supra Experiment (M. Kubic)



Simulations SEM on the probes measurements



$$U_{\perp} = 4 \text{ kms}^{-1}$$

$$\lambda_n = 3 \text{ cm}$$

* E. Faudot et al Phys of Plasmas **17**, 042503 (2010) **L. Colas et al Phys. of Plasmas **19**, 092505 (2012).

Fluid modeling and SEM code* : (theory and modeling)

including convection term U_d , conductivity σ_{\perp} , inertial current, anomalous viscous current, collisions ion-neutrals)
+ Coupling between rectified potential and density

ALINE Experiment on RF sheath (IJL Experiment)

RF sheath Physics (basics in magnetized plasma column)
Ionisation processes to take into account for $n > 0.5 \text{ MHz}$

SSWICH project (simulation european project)

Self-consistent Sheaths & Waves for IC Heating**

(IRFM, ERM Bruxelles, IJL, IPP-Garching) using
COMSOL multiphysics simulation models

PML description multi-modes in anisotropic plasma
Sheath boundary conditions
ITER and Tore Supra simulations

Role of DC anomalous perpendicular conductivity S_{\perp} (Basic)
 $V_{DC} + RF + \text{turbulence}$ Simulations PIC

Plasma-Wall Interaction

- Dust tracking, F. Brochard
- Plasma surface interaction (lab studies), L. De Poucques

Multi-machine investigation of dust mobilization, transport and impact on plasma performance

Joined research effort between Nancy University, IPP Garching and FZ Jülich: fast imaging of plasma-wall interactions in ASDEX Upgrade and TEXTOR tokamaks.

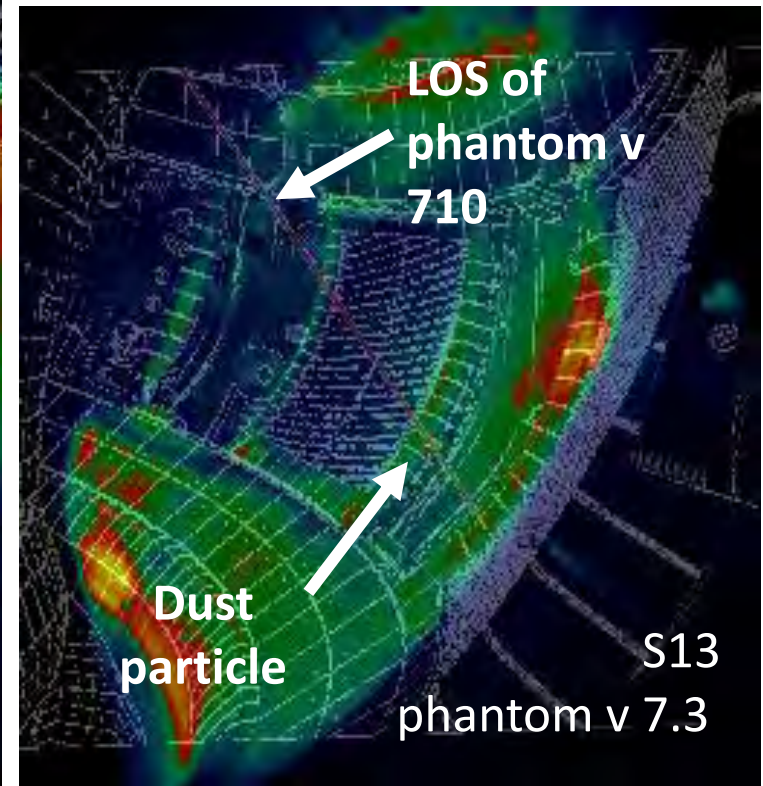
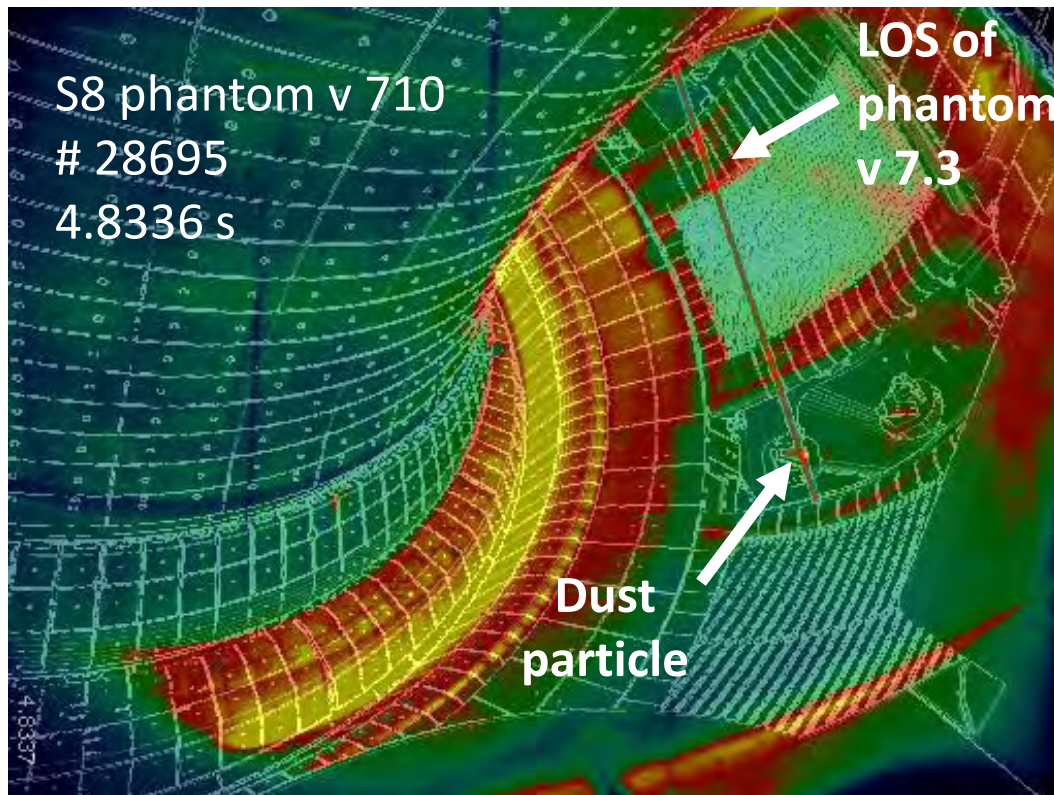
An algorithm, TRACE (Tracking and Classifying pinpoint Events), has been developed at Nancy University to analyze automatically the video data. TRACE able to characterize micrometer size dust (mobilization, trajectories), hot spots, unipolar arcs, (depending on frame rate), can also accurately detect disruptions and ELMs.

Fast imaging (typ. 10000fps) is routinely used on ASDEX Upgrade since 2008. 2268 shots have been analyzed with TRACE (~24 TB video data, 14370s plasma operation).

Main findings are:

- No decreasing of dust amount with plasma operation time, no significant impact of device opening on dust generation
- Dust mobilization only in specific discharge conditions: mainly disruption (especially when preceded by plasma vertical displacement), type I-ELMs, and inefficient coupling of heating power (NBI, ECRH).
- highest amount of dust observed at intermediate heating power ($3 \text{ MW} < P < 7 \text{ MW}$), and not at higher power

Multi-machine investigation of dust mobilization, transport and impact on plasma performance



Stereoscopic camera measurements enables to get 3D trajectories. Experiments since 2011 on ASDEX Upgrade (wide angle view, accuracy $\sim 9\text{mm}$).

Experiments were performed on TEXTOR in 2012 with injected calibrated dust (W spherical and C-flakes). Narrow view, accuracy $\sim \text{mm}$. Coupling with DUSTT simulations in 2013.

INPUT for modeling, ITER predictions.

Context and application

TOKAMAKS:

- ➔ Plasma interactions between hydrogen isotopes and first wall: beryllium, tungsten, **carbon**, etc.
- ➔ **Physical and chemical erosions (i.e. etching and re-deposition) of the carbon compound**
 - sputtering → dust formation and re-deposition
 - tritium retention
 - energy losses
- ➔ Phenomenon **unavoidable** but it could be **limited**

OBJECTIVE:

Improve the understanding of the carbon chemical erosion processes when facing the tokamak scrape-off-layer

LABORATORY PLASMAS:

- ➔ Allow to approach the conditions of the SOL⁽¹⁾:
 - $T_e < 5$ eV
 - $n_e \sim 10^{12}$ cm⁻³
 - low pressure p
 - incomplete ionization α
- ➔ Accessibility, low budget, diagnostic flexibility

OBJECTIVE:

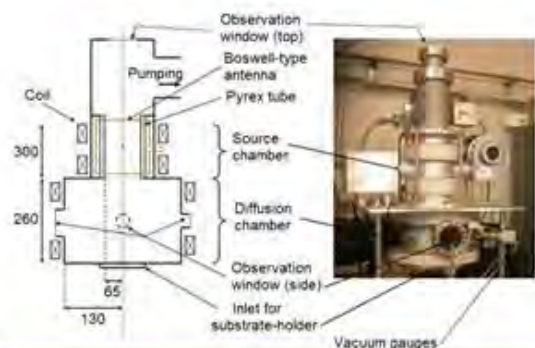
Obtain the **highest erosion rate i.e. the highest atomic hydrogen flux available**

- ➔ RF plasma reactor using a Boswell-type antenna
- ➔ Investigation of the different working parameters influence on the erosion rate

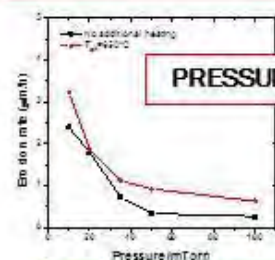
⁽¹⁾ J.P. Sharpe et al., *Fusion Engineering and Design* 63-64 :153, 2002.



Work overview



EXPERIMENTAL APPARATUS

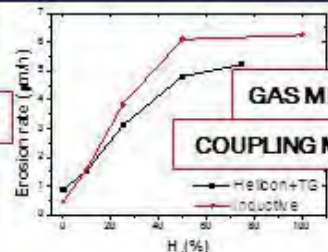


PRESSURE



Helicon+TG mode

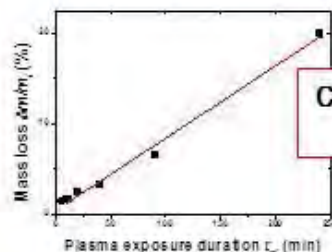
INFLUENCE OF THE WORKING PARAMETERS



GAS MIXTURE

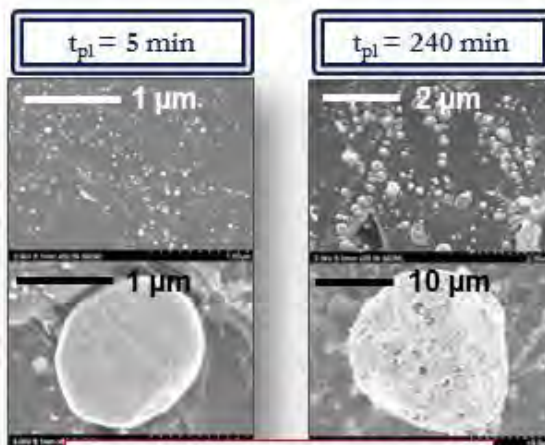
COUPLING MODES

Inductive mode



CONSTANT EROSION RATE: 6.0 µm/h

EROSION KINETICS



UP TO ϕ 20-30 µm DUST WITH A 4 cm² GRAPHITE SAMPLE (NO HYDROCARBON ADDITION)

PROSPECTS

High resolution micro-Raman spectroscopy, TEM, hydrogen retention.

High resolution OES, Langmuir probe, TALIF.

CORRELATIONS

Study of the plasma/wall interactions
In a H₂ plasma
(+He: byproduct of the D/T fusion)

THE AIM IS TO UNDERSTAND THESE INTERACTIONS IN AN ATTEMPT TO LIMIT THEM, AS WELL AS DUST TRANSPORT, IN FUSION PLASMA DEVICES.

(2) M. Richou et al., Carbon, 45 :2723, 2007.



Stellarators and our ESTELL project

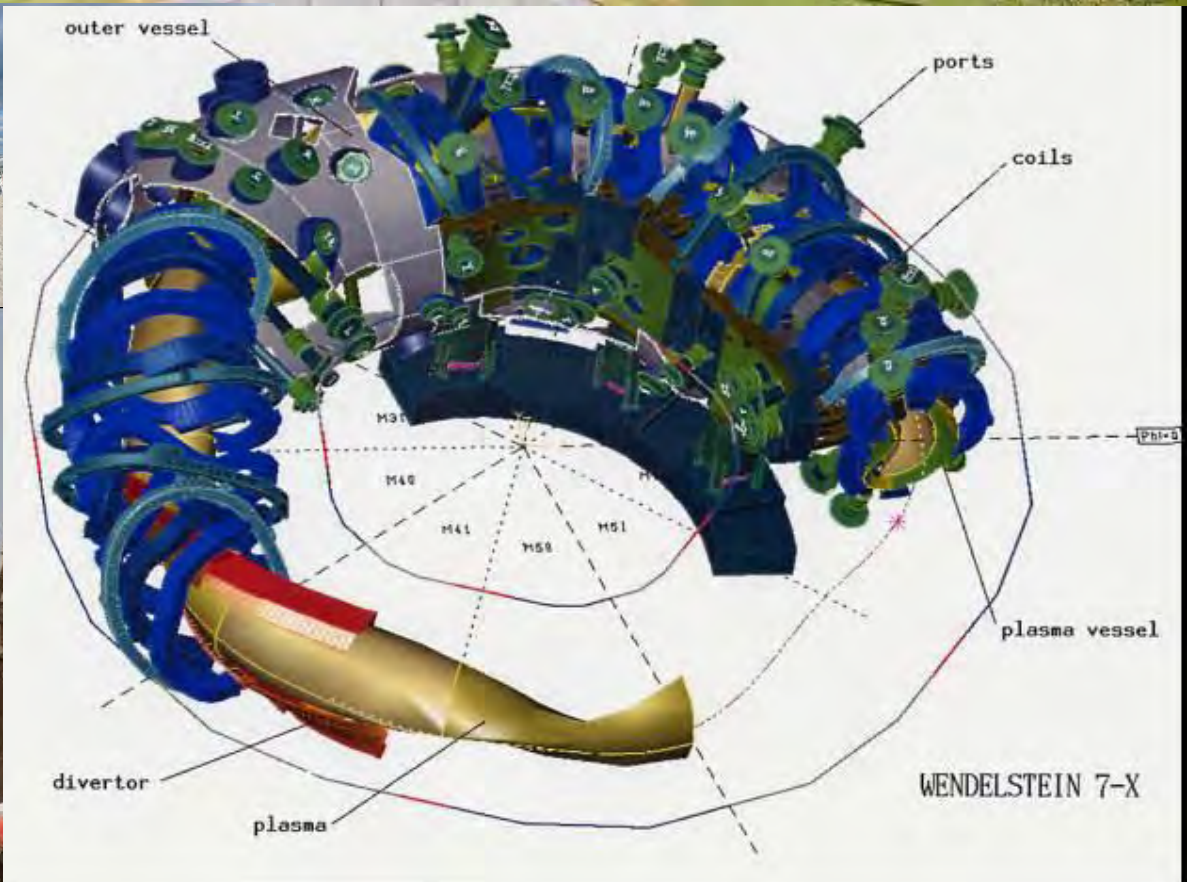
Stellarators vs. Tokamaks

- Three ways of producing a rotational transform:
 1. Driving a toroidal current → tokamaks, RFPs
 2. Elongating the flux surfaces and making them rotating poloidally as one moves around the torus
 3. Making the magnetic axis non planar
- Advantages and drawbacks of Stellarators:
 - Macroscopic equilibrium:
 - No current driven MHD instabilities that limit the performance
 - No disruptions
 - No Greenwald limit for the density
 - Higher β (pressure) limit than tokamaks
 - Neoclassical transport → a critical issue (advantage of symmetry)
 - Micro-instabilities and turbulence
 - Edge and divertor physics

P. Helander et al., PPCF, 54 (2012) 124009

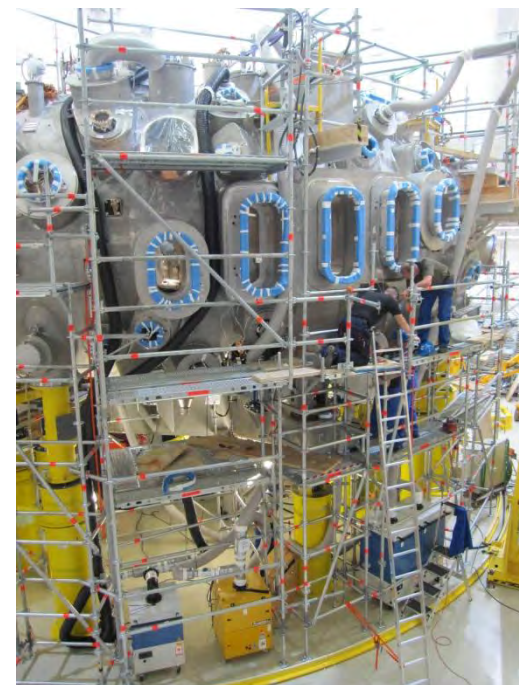
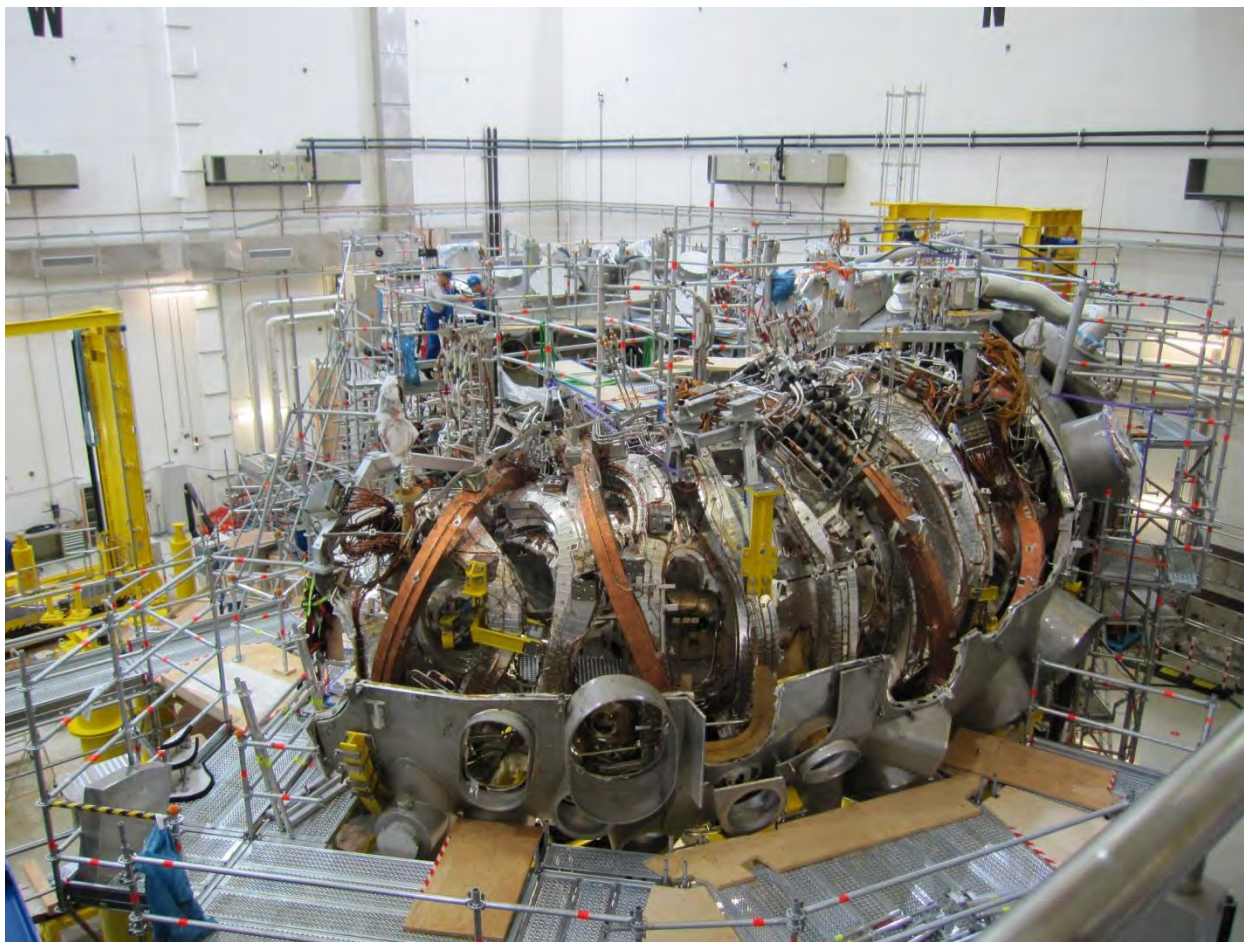
The Stellerator Wendelstein 7-X

Max-Planck-Institut für Plasmaphysik, Greifswald



The Stellerator Wendelstein 7-X *Max-Planck-Institut für Plasmaphysik, Greifswald*

Status in Oct. 2010



From ESTELL 1.0 to ESTELL 2.0

Simplest (technically) and cheapest solution: heliac configuration

Foreseen Parameters:

$R \sim 1.5 \text{ m}$

$D_{\text{plasma}} \sim 0.3 \text{ m}$

$B = 0.5 \text{ T}$ ($\rho^* \sim 10^{-2}$)

$P_{\text{ECR}} : 50\text{-}100 \text{ kW}$

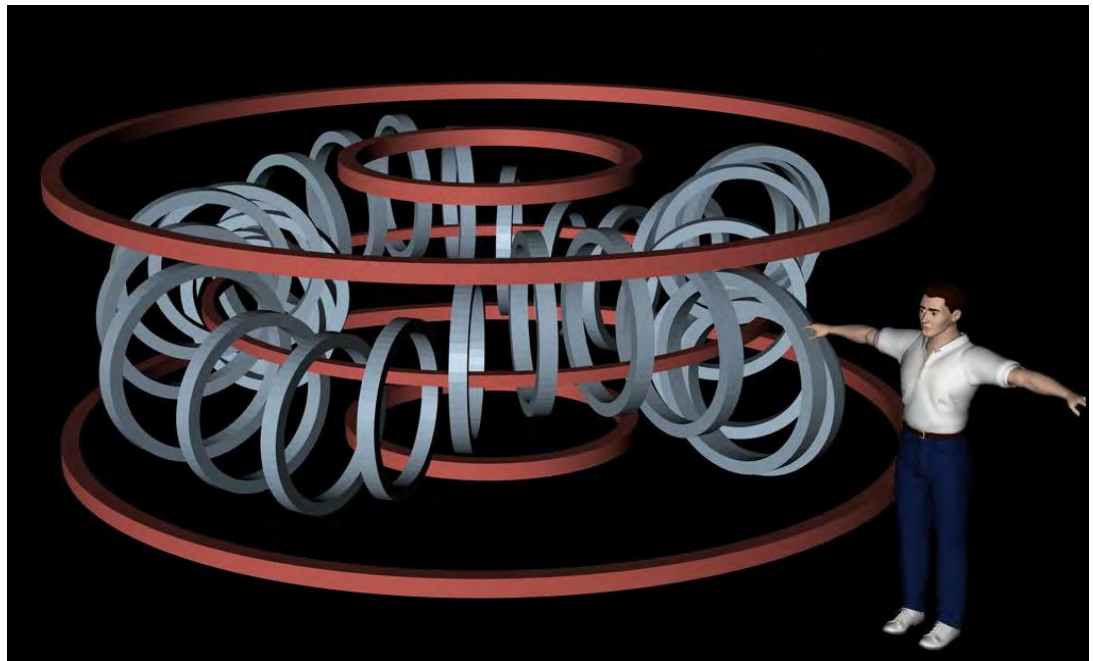
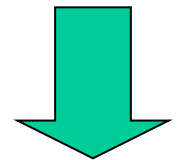
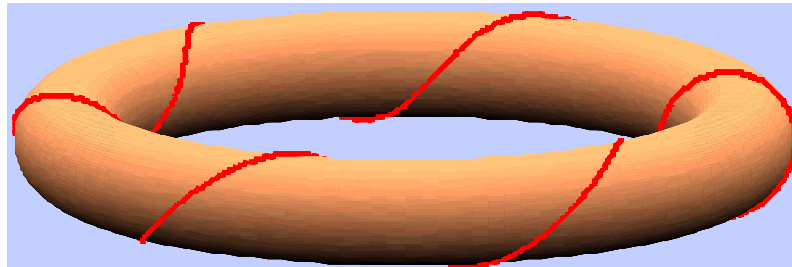
$P_{\text{RF}} : \sim 10 \text{ kW}$

Expected plasma parameters:

$T_e \sim 100 \text{ eV}$

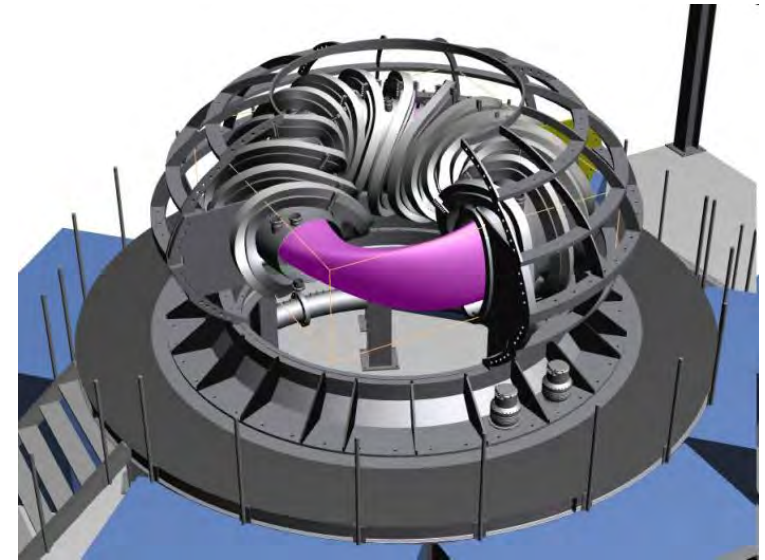
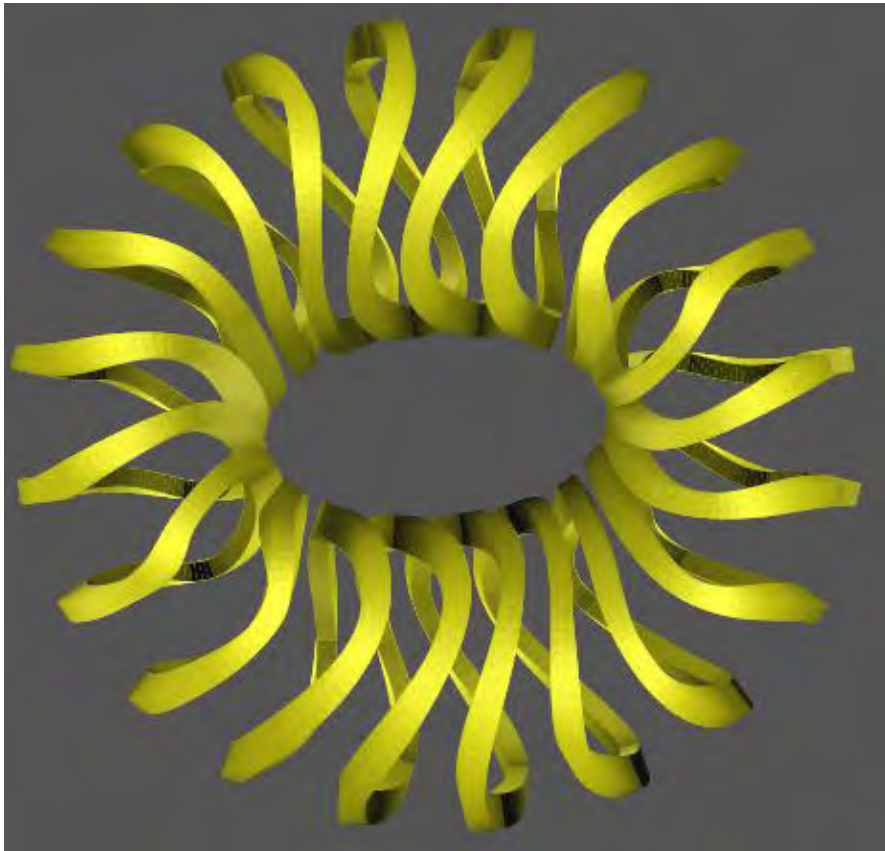
$T_i \sim 10 \text{ eV}$

n_e up to 10^{19} m^{-3}



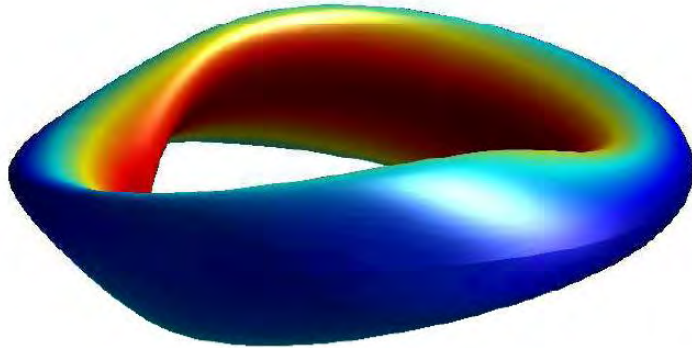
The *ESTELL* Project

*E*volutive
*STEL*larator
of *L*orraine



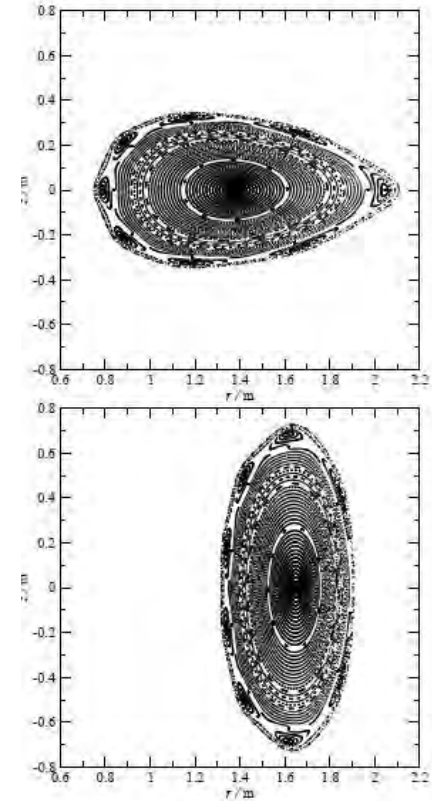
Magnetic configuration

- (1) M. Drevlak et al., *Design of a low-aspect-ratio, low-beta, quasi-axisymmetric stellarator, private comm.*

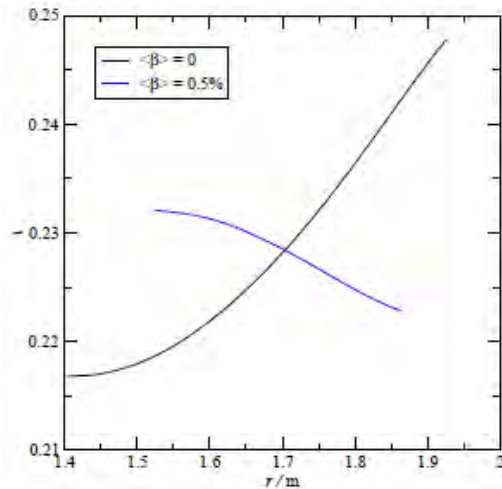


Plasma boundary with the strength of the magnetic field on it.

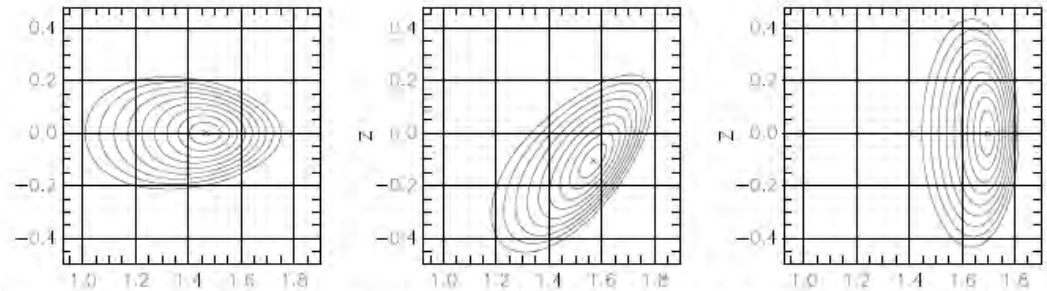
Poincaré cuts of the vacuum field produced by coil set with identical current.



Magnetic Configuration calculated at IPP Greifswald

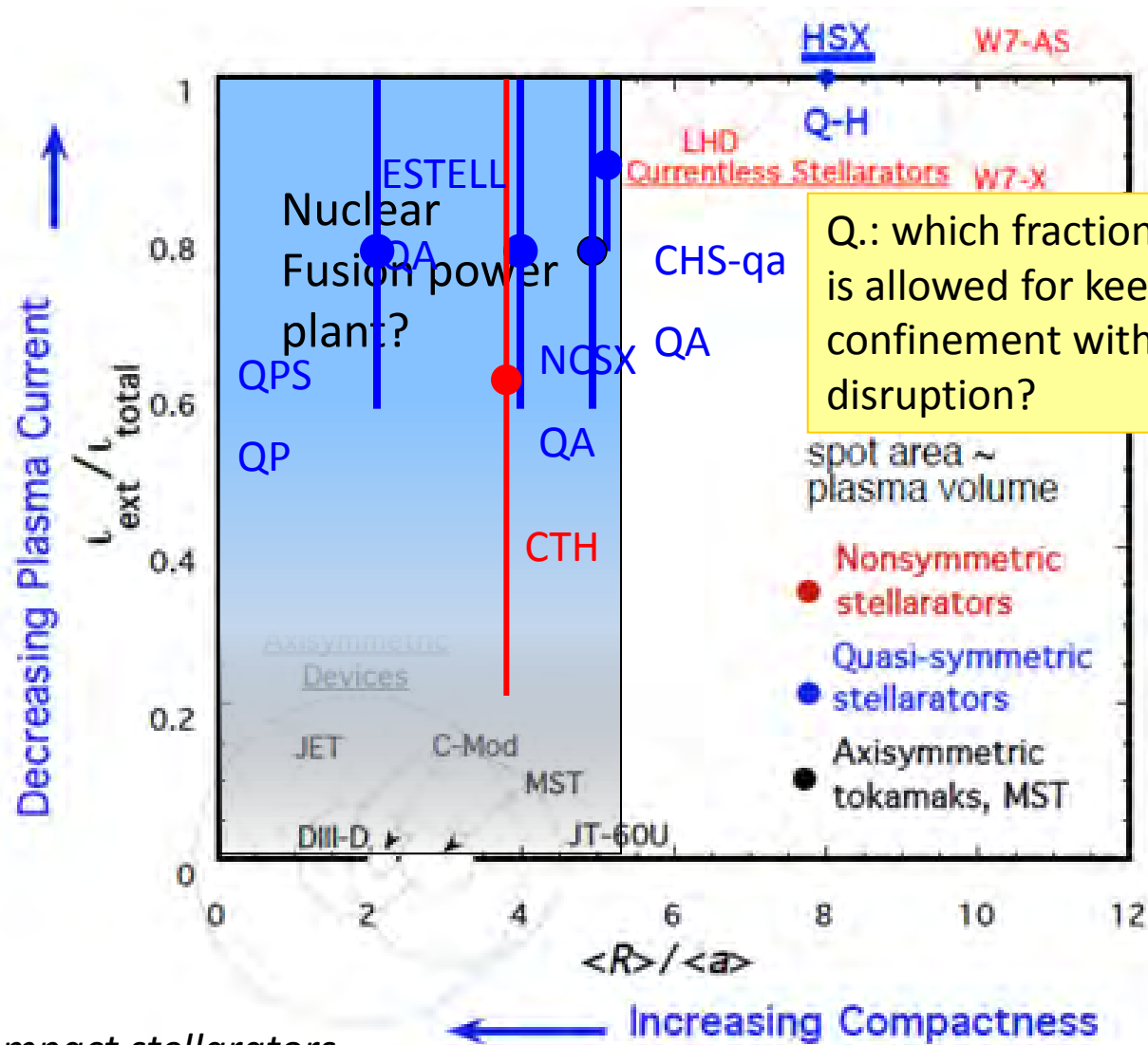


ι profiles at $\langle\beta\rangle = 0$ and $\langle\beta\rangle = 0.5\%$.



Fixed-boundary equilibrium at $\langle\beta\rangle = 0.5\%$.

International Context



Source : US compact stellarators programme

The ESTELL device parameters

Major Radius: 1.4 m

Average plasma minor radius: 0.28 m ($R/a = 5$)

Plasma Volume: 3 m³

Number of field period: 2

Rotational transform: 0.23

Number of modular coils: 20 (of 5 kinds; 5 power supplies to vary helical ripple)

Magnetic field strength: $B \leq 0.5$ T (1 T in pulsed mode?)

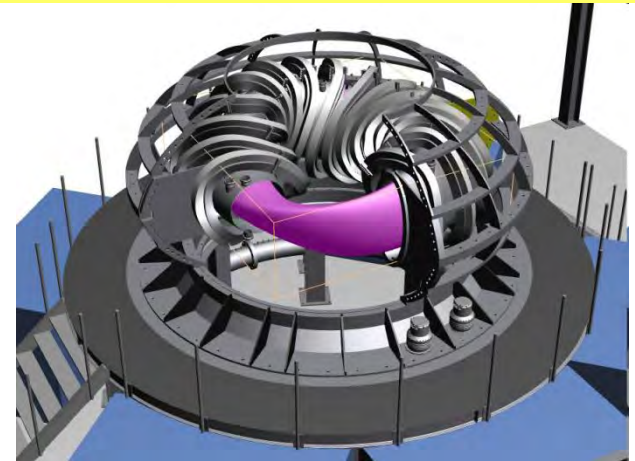
β (0.5 T, 200 kW ECRH): 0.5%

Pulse length: ~ 20 s / continuous

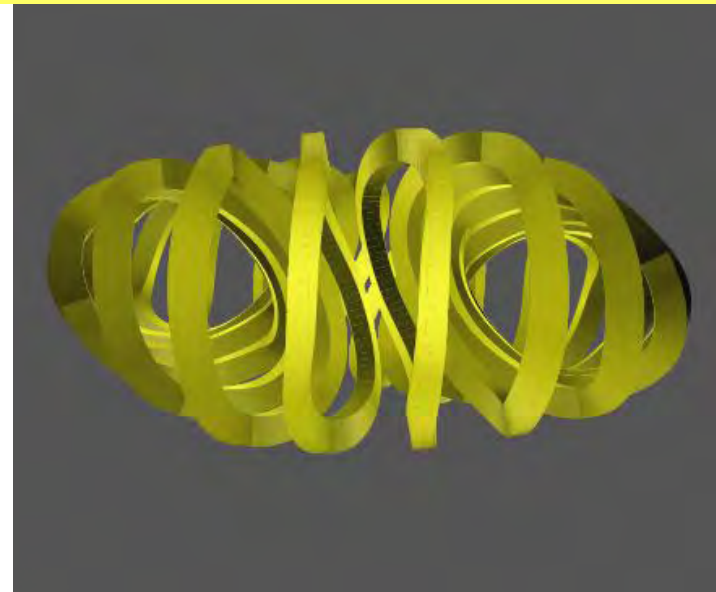
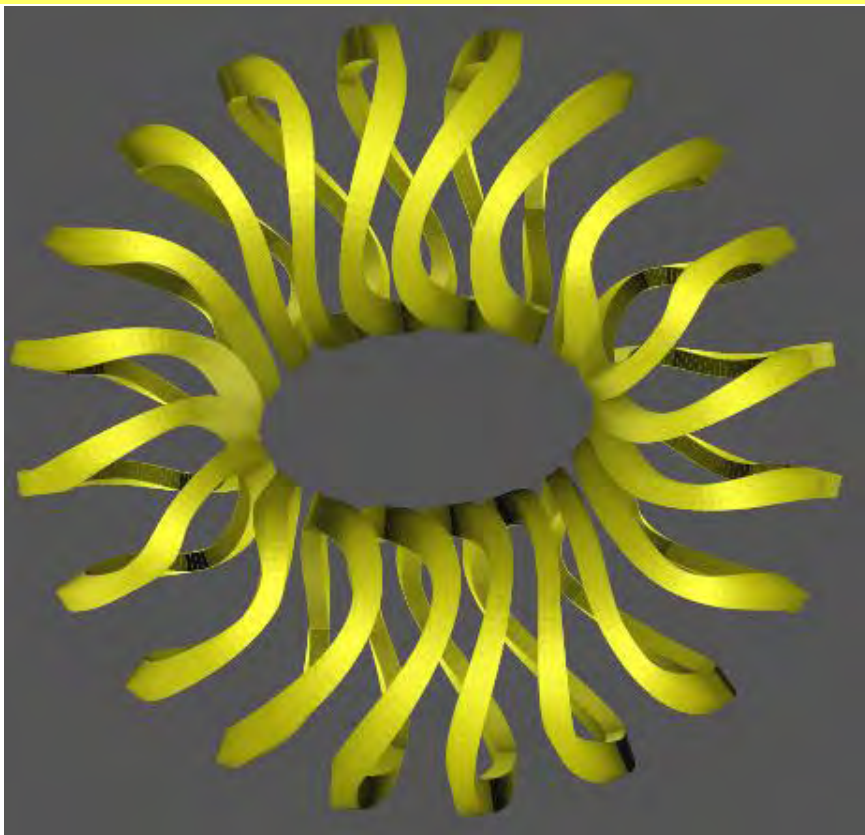
Heating power (ECRH, 28 GHz cw): 200 kW for starting (possibility of some LH and ICRH later)

Electron density: $\sim 5 \cdot 10^{18}$ m⁻³ (cut-off 10^{19} m⁻³) (a few 10^{19} m⁻³ if LH)

Central electron temperature: 1 keV (with a tail of the distribution at 1 MeV)



The *ESTELL* Project



- Coil set (20 modular coils of 5 different kinds, 10 coils/period), Flexibility enabled by 5 independent power supplies, in addition to LH and ECCD.
- Small rotational transform ($r \sim 0.2$) allowing: easy machining and coils winding, great accessibility for diagnostics (up to 80 cm between adjacent coils, mini 17 cm)

Scientific Motivations 1/2

CONFINEMENT: Demonstrate potential benefits of quasisymmetry in general, and specific properties of quasi axisymmetry (QA), for future fusion reactors.

- transport of suprathermal electrons according to the degree of QA
- explore stellarator/tokamak hybrid configuration, with finite but non negligible bootstrap current
- fill (partly) the hole left by the cancellations of NCSX (US) and CHS-qa (JP)
- compare relative properties of QA and Quasihelical symmetries (HSX)

PLASMA PHYSICS investigations:

- Edge plasma turbulence and transport in QA geometry
- RF heating and related RF sheath physics, including test-bed for ICRF alternative geometry antennas
- Plasma Wall Interaction (PWI)
- Diagnostics
- more generally, fill the gap between the physics in laboratory experiments and fusion devices

Scientific Motivations 2/2

EDUCATION: exceptional tool for educating young scientists and engineers (in Nancy: National Master <http://www.sciences-fusion.fr/> , Erasmus Mundus Master FUSION-EP www.em-master-fusion.org/ and Doctoral College FUSION-DC www.em-fusion-dc.org/ and FUSENET Association <http://www.fusenet.eu/>)
⇒ Opportunity to have a machine at top level with international visibility.

Astrophysics studies

Study of 3D magnetic reconnection: the ESTELL versatile coil power supply system makes it possible to shape magnetic islands. Then their dynamics and the reconnection process can be studied.

- ESTELL plasma parameters are relevant for astrophysics issues.
 - ESTELL magnetic field geometry gives the opportunity to study 3D reconnection with bent magnetic field lines.
- ⇒ ESTELL is also supported by several astrophysics institutes.

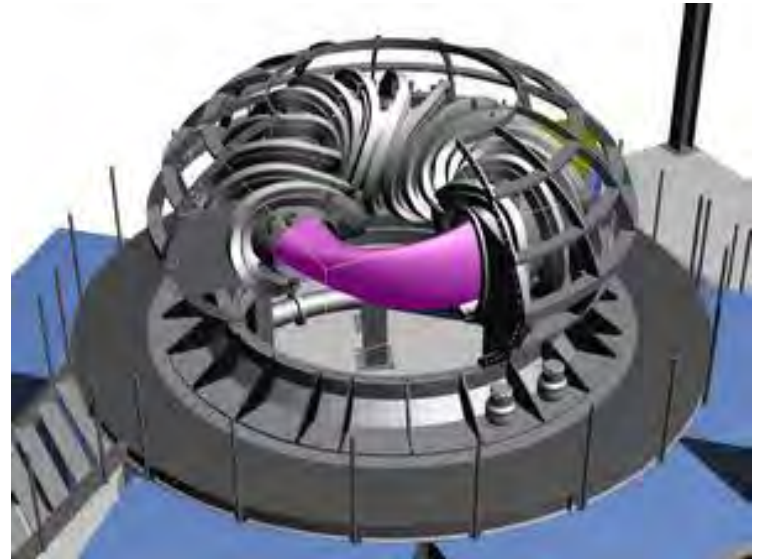
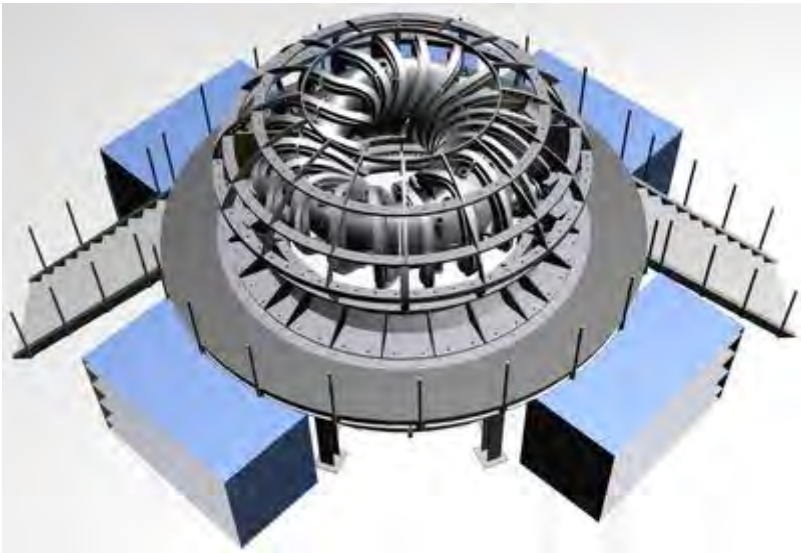
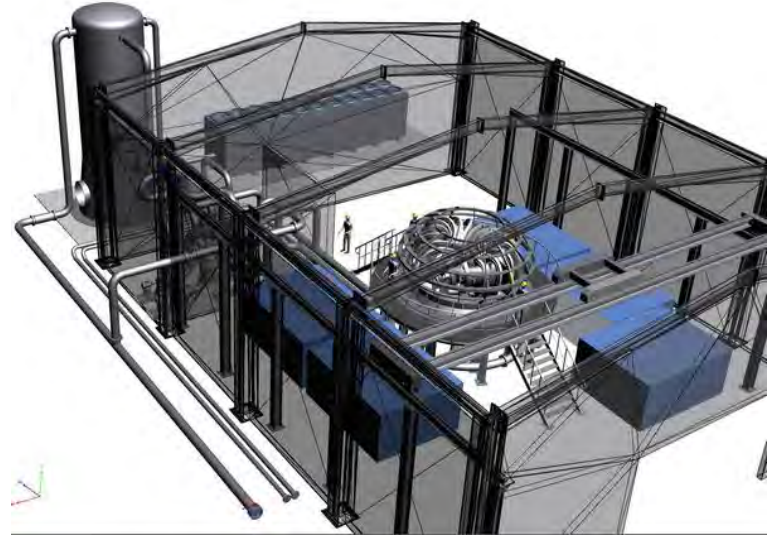
The ESTELL Project: Design issues

-A dedicated building on a new site in Nancy



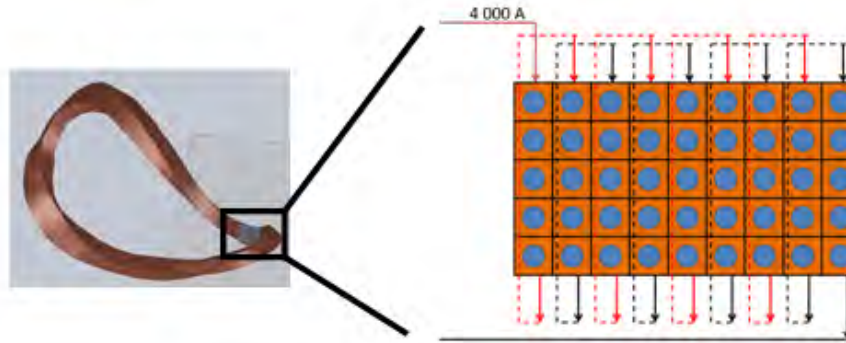
Sketch of ESTELL experimental Hall

- conceptual drawings of the ESTELL assembly



Main elements of the assembly

- 20 modular copper coils: similar as for W-7AS (~ 1.25 M€)



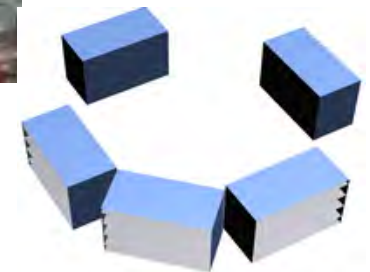
- Vacuum vessel with main coil supporting structure: (~ 2 M€)
 - The assembly is divided into quarters, connected with a flange, and can be easily disassembled.

- Heating systems: (~ 3 M€)

ECR heating: 2 long pulse (20 s) gyrotrons
100 or 200 kW each, frequency 28 GHz

- Power supplies: total power ~ 10 MW (~ 3 M€)

- Power converters from 20kV to 380 V
- Five 1.4 MVA bridge rectifiers (4 kA, 87 V for each coil)
- Two separate 200 kW bridge rectifiers for operating the gyrotrons



Main elements of the assembly

- Cooling system: (~ 1 M€)
 - two cooling groups of 1.25 MW each, 50 m³ water tank → will allow repetition of 40 sec discharges every 15 minutes.

- Supporting structure (~ 0.1 M€)



- Supervision and command control (~ 0.9 M€)

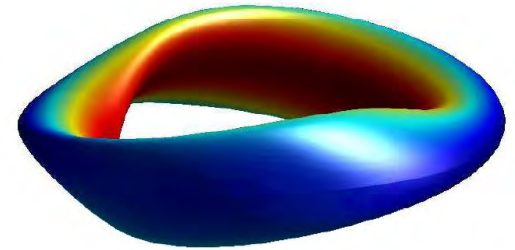
- Main diagnostics and accessories: (~ 2 M€)

- 40 Mirnov coils,
- Millimetric-wave interferometer (similar TCV),
- Reflectometer (as in Tore-Supra, X mode, 13.5 – 20 GHz and 20.25 – 30 GHz)
- ECA diagnostics for T_e and fast electrons,
- XUV camera, Fast visible camera & intensifier, IR fast camera, Probe systems,
- Precision manipulator with airlock (PWI studies),
- Data acquisition, Data storage

Soutiens internationaux et Collaborations

EUROPE

- Calculation of ESTELL magnetic configuration at **Max-Planck Institute Greifswald**. Participation of IPP-Greifswald as full partner of the Equipex project. ESTELL envisaged as satellite experiment of W7-X stellarator.



- Support of **CIEMAT** (Spain),
- **IFP** (Italy) : 3D magnetic reconnexion... (discussions)
- Support of European partners involved in Fusion Education (Fusion-DC, Fusion-EP).
- Scientific goals : objectives 3 & 4 of the EURATOM Fusion roadmap.

JAPAN

Collaborations with the **National Institute for Fusion Studies** (Nagoya) and **Kyushu University** : scientific participation to the research program, design of diagnostics dedicated to ESTELL, students internship & mobility.

Soutiens internationaux et Collaborations

USA

- Strong scientific and technical support of the **Princeton University**: magnetic reconstruction codes, possible participation in the operation costs (dedicated application to DOE) and in the device operation.
- Scientific collaboration with the **University of WISCONSIN** (joined scientific program with the HSX device).
- Support from **UCLA** (in particular regarding astrophysics studies)
- Students exchanges.

Summary: ESTELL, a worldwide open facility

- ESTELL to be built (?) at Nancy University, in a dedicated building nearby the Institut Jean Lamour (IJL). IJL laboratory is composed of 438 people, (researchers, professors and assistant-professors: 155, PhD students: 107, Post-docs: 23, technicians and engineers: 95). ESTELL will be essentially managed by a team gathering 18 plasma physicists and engineers and will benefit from the workshop of IJL (main ESTELL components designed and built by private companies).
- Magnetic configuration designed at IPP Greifswald.
- Advanced contacts for international collaborations with IPP Greifswald (theory), PPPL-Princeton (theory, equilibrium reconstruction, technical support), UCLA, Wisconsin-Madison (HSX), NIFS & Kyushu University (diagnostics, theory). [Other partners welcome!](#)
- Education: Nancy University part of the Erasmus Mundus Master Programme Fusion-EP and FUSENET (European Fusion Education Network), and coordinating the new European Doctoral Federation in Fusion Science and Engineering (EDF-FS). Also leading core partner of the International Erasmus mundus Doctoral College FUSION-DC which has just been selected (July 2011).

More infos...



<http://estell.blog.uhp-nancy.fr/>

Frederic.brochard@ijl.nancy-universite.fr

European initiatives in Fusion Education

Historical overview of the new initiatives in Fusion Science and Engineering Education

At Master level

- French national Master “en Sciences de la Fusion”, started in 2006
<http://www.sciences-fusion.fr/>
- European Master Erasmus mundus “Nuclear Fusion Science and Engineering Physics” FUSION-EP <http://www.em-master-fusion.org/> , started in 2006
Common Approach: Generic Master (Physics, Electrical Engineering, Material Science, ...) with Fusion accents through elective courses

Strong European coordination through the EURATOM programme

⇒ FUSion Education NETwork (FUSENET), started in 2008

Doctorate

- Joint Doctorate in Fusion Science and Engineering and European Doctoral Network, Padova-Lisbon-München
- European Doctoral Federation in Fusion Science FUSSION-EDF, started in 2010
- Erasmus mundus “Doctoral College in Fusion Science **and Engineering**”
FUSION-DC
accepted in 2011, starts September 2012 (enrollment of first PhD students)